National Library of Canada

Acquisitions and Bibliographic Services Branch

395 Wellington Street
Ottawa, Ontario
K1A 0N4

Bibliothèque nationale du Canada

Direction des acquisitions et des services bibliographiques

395, rue Wellington
Ottawa (Ontario)
K1A 0N4

Your file Votre référence

Our file Notre référence

NOTICE

The quality of this microform is heavily dependent upon the quality of the original thesis submitted for microfilming. Every effort has been made to ensure the highest quality of reproduction possible.

If pages are missing, contact the university which granted the degree.

Some pages may have indistinct print especially if the original pages were typed with a poor typewriter ribbon or if the university sent us an inferior photocopy.

Reproduction in full or in part of this microform is governed by the Canadian Copyright Act, R.S.C. 1970, c. C-30, and subsequent amendments.

AVIS

La qualité de cette microforme dépend grandement de la qualité de la thèse soumise au microfilmage. Nous avons tout fait pour assurer une qualité supérieure de reproduction.

S'il manque des pages, veuillez communiquer avec l'université qui a conféré le grade.

La qualité d'impression de certaines pages peut laisser à désirer, surtout si les pages originales ont été dactylographiées à l'aide d'un ruban usé ou si l'université nous a fait parvenir une photocopie de qualité inférieure.

La reproduction, même partielle, de cette microforme est soumise à la Loi canadienne sur le droit d'auteur, SRC 1970, c. C-30, et ses amendements subséquents.

Canada

UNIVERSITY OF ALBERTA

Microcomputer based dynamic simulator applied to a study of the control behaviour of an industrial grinding circuit

BY

Sreekanth Lalgudi

©

A THESIS

SUBMITTED TO THE FACULTY OF GRADUATE STUDIES AND RESEARCH

IN PARTIAL FULFILLMENT OF THE REQUIREMENTS FOR THE DEGREE

OF

Master of Science

Department of Chemical Engineering

EDMONTON, ALBERTA

Fall, 1992

National Library of Canada
Bibliothèque nationale du Canada

Canadian Theses Service
Service des thèses canadiennes

Ottawa, Canada
K1A 0N4

The author has granted an irrevocable non-exclusive licence allowing the National Library of Canada to reproduce, loan, distribute or sell copies of his/her thesis by any means and in any form or format, making this thesis available to interested persons.

L'auteur a accordé une licence irrévocable et non exclusive permettant à la Bibliothèque nationale du Canada de reproduire, prêter, distribuer ou vendre des copies de sa thèse de quelque manière et sous quelque forme que ce soit pour mettre des exemplaires de cette thèse à la disposition des personnes intéressées.

The author retains ownership of the copyright in his/her thesis. Neither the thesis nor substantial extracts from it may be printed or otherwise reproduced without his/her permission.

L'auteur conserve la propriété du droit d'auteur qui protège sa thèse. Ni la thèse ni des extraits substantiels de celle-ci ne doivent être imprimés ou autrement reproduits sans son autorisation.

ISBN 0-315-77087-2

Canada

UNIVERSITY OF ALBERTA

RELEASE FORM

NAME OF AUTHOR:	Sreekanth Lalgudi
TITLE OF THESIS:	Microcomputer based dynamic simulator applied to a study of the control behaviour of an industrial grinding circuit
DEGREE:	Master of Science
YEAR THIS DEGREE GRANTED:	1992

Permission is hereby granted to the University of Alberta Library to reproduce single copies of this thesis and to lend or sell such copies for private, scholarly or scientific purposes only.

The author reserves all other publication and other rights in association with the copyright in the thesis, and except as hereinbefore provided neither the thesis nor any substantial portion thereof may be printed or otherwise reproduced in any material form whatever without the author's prior written permission.

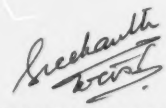

.....

PERMANENT ADDRESS:

21/B Balakrishna Road
Thiruvanmiyur
Valmiki Nagar
Madras, Tamil Nadu
India 600034

DATED: August 22, 1992

UNIVERSITY OF ALBERTA

FACULTY OF GRADUATE STUDIES AND RESEARCH

The undersigned certify that they have read, and recommend to the Faculty of Graduate Studies and Research for acceptance, a thesis entitled

Microcomputer based dynamic simulator applied to a study of the control behaviour of an industrial grinding circuit

submitted by Sreekanth Lalgudi in partial fulfillment of the requirements for the degree of Master of Science in Chemical Engineering.

.....
Professor R.K. Wood (Supervisor)

.....
Associate Prof. M. Rao

.....
Professor L.R. Plitt

Date: Aug. 21st 1992

To my parents

who have given so much and asked for so little

ABSTRACT

Dynamic simulators of mineral processes have gained popularity in the recent past since this makes the onerous task of designing control systems, elementary. However, to get the full benefit of such an exercise it must be ensured that such simulators represent the actual process accurately and one way to do it is to simulate an existing grinding circuit and compare the results. Once the validity of the simulator is established, it can be used to design and optimize control strategies.

A crucial factor in developing valid dynamic simulators is the selection of models to represent the unit operations in mineral processing. Dynamic models such as the one developed by Plitt to predict the classification performance of a hydrocyclone , must be able to faithfully represent the transient behaviour of the operating plant. As well, they must be easy to understand and convenient to program. The simulators using such models must be robust and user-friendly. In addition, if the coding is done in a commonly used language like FORTRAN, these simulators can be operated in any microcomputer with standard features.

The focus of this work was to develop a microcomputer based dynamic grinding circuit simulator that incorporated all the features described above. Its performance was validated using plant data from Hemlo Gold Mines Ltd. The salient features of this simulator include a modular approach to allow for easy modification of the simulator to meet individual requirements, and interactive features that allow the user to simulate various open-loop scenarios, effortlessly.

The conventional closed-loop Type I control strategy adopted in this work ma-

nipulated the fresh ore feed rate to control the product stream size to 90 percent less than 200 mesh. Secondary loops maintained the sump levels by adjusting the water flow rates. In spite of the high correlations, apparent in the open-loop studies, good control of the product stream was possible by using the Type I control configuration.

In view of the lack of reliability of on-line particle size monitors and the high costs associated with such devices, a particle size estimator to predict ore fineness in the hydrocyclone overflow stream using only measured values of other circuit variables was developed. However, due to the high correlation between the observed circuit parameters and the complexity of the circuit being simulated, the performance of the estimator during the transient operation of the circuit was not satisfactory. This endeavour, nevertheless, proved that developing particle size estimators for large circuits is non-trivial and that till such a time when general purpose estimators are developed, the Plitt model for the hydrocyclone performance is the best predictor available.

Acknowledgements

I would like to thank Dr. Reg Wood for his extreme patience while guiding me through the hurdles of my research. While acknowleding the financial and technical support of Brenda, I wish to extend my appreciation to Andre Vien for his timely help and suggestions. A big thanks to the department of Chemical Engineering for providing a congenial atmosphere for research.

I take this oppurtunity to thank all my colleagues who once again proved that most of the learning is beyond the confines of the classroom. I want to specially thank my fellow graduate students Natrajan Iyer, Lakshminarayanan Samavedam (Lax), Ravi Gudi, Pronob Bannerji (Dada) for their invaluable help and support. My appreciation goes to Christine Ho and Simarjit Dhaliwal (Sam) who were instrumental in making research work enjoyable. A heartfelt thankyou goes to Dr. Kun-Yu-Kwok without who this document may have been produced but would'nt have looked half as good. The lighter moments shared with Cindy Heisler at the general office will be remembered for a long time.

I would also like to extend my gratitude to all my friends outside the department who made this possible. In particular, I am indebted to all my past and present room-mates who sportingly put up with all my idiosyncrasies. My badminton buddies Ramesh and Siddu and musical inspiration Jayram deserve special thanks for helping me create a parallel world sans research.

Finally, I would like to thank my parents, sisters and brothers-in-law in India for their constant support and encouragement throughout all these years.

Contents

1 Introduction 1

2 Modelling, Simulation and Control in the Mineral Processing Industry 3

2.1 Introduction . . . 3

2.1.1 Models and Simulation . . . 4

2.1.2 General Applications of Dynamic Simulators . . . 5

2.2 Modelling In The Mineral Process Industry . . . 7

2.2.1 Dynamic Simulation of the Unit Operations . . . 7

2.3 Dynamic Simulation Software in Mineral Processing . . . 9

2.4 Mineral Processing Control . . . 11

2.4.1 Selection of the Control Strategy . . . 12

2.5 Grinding Circuit Simulation for Control System Evaluation at the University of Alberta . . . 17

3 Grinding Circuit Simulator Models 18

3.1 Introduction . . . 18

3.2 Grinding Circuit Representation . . . 19

3.3 Simulator Models . . . 20

3.4 Pump and Sump Model . . . 26

3.5 Conveyor and Pipeline Model . . . 29

3.6 Frictional Head Loss . . . 33

3.7 Disturbance Modelling . . . 36

4 Modelling and Characteristics of the Hydrocyclone 40

4.1 Introduction . . . 40

4.2 Operational Principles . . . 41

4.3 Effect of the Design and Operating Parameters on the Performance of the Hydrocyclone . . . 44

4.3.1 Design Variables 44
4.3.2 Operating Variables 49
4.4 Hydrocyclone Theories and Models 52
4.4.1 Physical Models 52
4.4.2 Mathematical Models 55
4.5 Description of the Hydrocyclone Model Used in this Work 58

5 The Grinding Circuit Simulator Structure 62
5.1 Introduction 62
5.2 The Grinding Circuit Simulator 63
5.2.1 The User Interface 64
5.2.2 The Shell 64
5.2.3 The Database 67
5.3 The Closed Loop Simulator 69
5.3.1 The Initialization Section 69
5.3.2 The Integration Section 73
5.3.3 The Termination Section 76
5.3.4 The DYFLO Subroutine Library 78
5.4 An Illustrative Example to Show the Flexibility of the Simulator . . . 79

6 Simulation of the Hemlo Grinding Circuit 83
6.1 Introduction 83
6.2 The Hemlo Circuit 85
6.3 Open Loop Simulations 91
6.3.1 Increase in the Fresh Ore Feed Rate (FOF) 93
6.3.2 Increase in the Sump Water Flow Rate (SWF) 99
6.3.3 Increase in the Fresh Ore Feed Hardness 103
6.3.4 Increase in Fresh Feed Ore Density 109
6.3.5 Increase in the Fresh Ore Hardness and Density 114

7 The Hemlo Circuit Feedback Control 118
7.1 Introduction 118
7.2 Design and Evaluation of Feedback Controllers 122
7.3 Type I Control Behaviour 124
7.3.1 Controlling a Step Change in Hardness 126
7.3.2 Controlling a Step Change in Density 132
7.3.3 Controlling a Simultaneous Disturbance of Hardness and Density 132
7.3.4 Controlling an Unusual Disturbance 135

7.3.5 Servo Control 138
7.4 Inferential Control of Grinding Circuits 141
7.5 The Estimator Model for the Hemlo Circuit 147

8 Conclusions and Recommendations **153**
8.1 Conclusions 153
8.2 Suggestions for Future Work 155

A DATA STRUCTURE **166**

B DYFLO Utilities **171**

C The Factorial Design of Experiments **176**
C.1 Introduction 176
C.2 A Single Observation Per treatment Combination in the 2^k design . . 178
C.3 A Factorial Design for the Hemlo Grinding Circuit 179

List of Tables

5.1 Process Subroutines and their Functions 77

6.1 First Column of Breakage Matrix for the Grinding Mills 88
6.2 Selection Function Associated with the Hemlo Circuit Grinding Mills 89
6.3 Steady State Particle Size Frequency Distribution for the Hemlo Circuit Grinding Mills' Feed and Product Streams 90
6.4 Physical Dimensions and Model Constants of the Hemlo Circuit Hydrocyclone Sets 91
6.5 Steady State Particle Size Frequency Distribution for the Hemlo Circuit Hydrocyclones' Feed and Product Streams 92

7.1 List of Possible Pairings of Controlled and Manipulated Variables . . 122
7.2 List of Possible Pairings of Controlled and Manipulated Variables for the Hemlo Circuit 123

C.1 Identification of Factors for the Hemlo Circuit 180
C.2 Order followed in changing the input variables 180
C.3 ANOVA table for the Cyclone Overflow Stream (COS) 182
C.4 ANOVA table for the Sump #1 Level (SMPL1) 182
C.5 ANOVA table for the Sump #2 Level (SMPL2) 183
C.6 ANOVA table for the Cyclone Feed Density (CFD) 183
C.7 ANOVA table for the Pressure at Cyclone Inlet (PR) 184

List of Figures

3.1 Schematic Diagram of a Typical Grinding Circuit Configuration . . . 21
3.2 Schematic Illustration of the Grinding Mills 22
3.3 Schematic Representation for Digital Computer Implementation of a Fixed Time Delay 30
3.4 Schematic Representation to Explain the Digital Computer Implementation of a Variable Time Delay 32

4.1 A Schematic Diagram of a Hydrocyclone Showing Vortex Formations 42
4.2 Typical Actual and Corrected Classification Partition Curves 43
4.3 Schematic Representation of a Hydrocyclone Showing the Principal Design Variables 46

5.1 Schematic Diagram of the Open Loop Simulator Structure 65
5.2 Schematic Diagram of the Closed Loop Simulator Structure 70
5.3 Schematic Diagram of the Subroutines Called by the CONFIG Subroutine 75
5.4 Illustration of the CONFIG Structure for Figure 3.1 81

6.1 Schematic Representation of the Hemlo Grinding Circuit 84
6.2 Schematic Representation of the CONFIG Subroutine for the Hemlo Grinding Circuit 86
6.3 Open Loop Response of the Hydrocyclone Overflows and Sump Levels to a 10% Step Increase in the Feed Ore Flow Rate 94
6.4 Open Loop Response of the Slurry Densities and Circulating Loads to a 10% Step Increase in the Feed Ore Flow Rate 95
6.5 Open Loop Response of the Hydrocyclone Overflows and Sump Levels to a 10% Step Decrease in the Feed Ore Flow Rate 97
6.6 Open Loop Response of the Slurry Densities and Circulating Loads to a 10% Step Decrease in the Feed Ore Flow Rate 98

6.7 Open Loop Response of the Hydrocyclone Overflows and Sump Levels to a 3% Step Increase in the Water Flow Rate to Sump #1 101
6.8 Open Loop Response of the Slurry Densities and Circulating Loads to a 3% Step Increase in the Water Flow Rate to Sump #1 102
6.9 Open Loop Response of the Hydrocyclone Overflows and Sump Levels to a 3% Step Decrease in the Water Flow Rate to Sump #1 104
6.10 Open Loop Response of the Slurry Densities and Circulating Loads to a 3% Step Decrease in the Water Flow Rate to Sump #1 105
6.11 Open Loop Response of the Hydrocyclone Overflows and Sump Levels to a Step Increase in the Fresh Ore Feed Hardness 107
6.12 Open Loop Response of the Slurry Densities and Circulating Loads to a Step Increase in the Fresh Ore Feed Hardness 108
6.13 Open Loop Response of the Hydrocyclone Overflows and Sump Levels to a Step Decrease in the Fresh Ore Feed Hardness 110
6.14 Open Loop Response of the Slurry Densities and Circulating Loads to a Step Decrease in the Fresh Ore Feed Hardness 111
6.15 Open Loop Response of the Hydrocyclone Overflows and Sump Levels to a Step Increase in the Fresh Ore Feed Density 112
6.16 Open Loop Response of the Slurry Densities and Circulating Loads to a Step Increase in the Fresh Ore Feed Density 113
6.17 Open Loop Response of the Hydrocyclone Overflows and Sump Levels to a Step Increase in the Fresh Ore Feed Density and Hardness 115
6.18 Open Loop Response of the Slurry Densities and Circulating Loads to a Step Increase in the Fresh Ore Feed Density and Hardness 116

7.1 Closed Loop Response of the Product Stream for an Increase in the Fresh Ore Feed Hardness 128
7.2 Closed Loop Response of the Circuit Variables for an Increase in the Fresh Ore Feed Hardness 129
7.3 Closed Loop Response of the Product Stream for a Decrease in the Fresh Ore Feed Hardness 130
7.4 Closed Loop Response of the Circuit Variables for a Decrease in the Fresh Ore Feed Hardness 131
7.5 Closed Loop Response of the Product Stream for an Increase in the Fresh Ore Feed Density 133
7.6 Closed Loop Response of the Circuit Variables for an Increase in the Fresh Ore Feed Density 134

7.7 Closed Loop Response of the Product Stream for a Simultaneous Change in the Fresh Ore Feed Density and Hardness 136
7.8 Closed Loop Response of the Circuit Variables for a Simultaneous Change in the Fresh Ore Feed Density and Hardness 137
7.9 Closed Loop Response of the Product Stream to a Step Water Input to Ball Mill #3 139
7.10 Closed Loop Response of the Product Stream to a Step Water Input to Ball Mill #3 140
7.11 Closed Loop Response of the Product Stream to a +3% Change in the COS Setpoint 142
7.12 Closed Loop Response of the Circuit Variables to a +3% Change in the COS Setpoint 143
7.13 Closed Loop Response of the Product Stream to a -3% Change in the COS Setpoint 144
7.14 Closed Loop Response of the Circuit Variables to a -3% Change in the COS Setpoint 145

List of Symbols

Technical Abbreviations

CFD	= cyclone feed density ($tonnes/m^3$)
COS	= hydrocyclone overflow size ($\% - 200mesh$)
CSSL	= continuous system simulation language
DMC	= dynamic matrix control
FH	= friction head
FOF	= fresh ore feed ($tonnes/h$)
FTD	= fixed time delay
HRD	= hardness of ore
IAE	= integral of absolute error
IMC	= internal model control
INA	= inverse nyquist array
MFO	= mass flow of ore to hydrocyclones ($tonnes/h$)
MFW	= mass flow of water to hydrocyclones ($tonnes/h$)
MIMO	= multiple input multiple output
MOCCA	= multivariable optimal constrained control algorithm
MPC	= multivariable predictive control
MRAS	= model reference adaptive control
P	= proportional controller
PH	= pressure head
PI	= proportional plus integral controller
PID	= proportional plus integral plus derivative controller
PR	= pressure at the hydrocyclone inlet
PSM	= particle size monitor
RDH	= resistance dynamic head
RLS	= recursive least square
SH	= static head

SISO = single input single output
SPL = sump level (m)
STR = self tuning regulator
SWF = sump water feed ($tonnes/h$)
TDH = total dynamic head
TW = total water flow into the circuit ($tonnes/h$)
VF = vortex finder
VTD = variable time delay

Variables

Uppercase

B = sub-diagonal matrix of breakage elements
D = diameter (cm)
F = mass flow rate of feed stream ($tonnes/h$)
H = mass holdup ($tonnes$)
I = attributes of variable time delay input stream
= or the identity matrix
K = arbitrary constant
= or controller gain
L = sump level measured from sump discharge (m)
M = sharpness of separation
N = number of blocks in the variable time delay
O = attributes of variable time delay output stream
P = pressure at hydrocyclone inlet (kPa)
= or mass flow rate of product stream ($tonnes/h$)
Q = volumetric flow rate of pulp (m^3/h)
S = total solids mass holdup of the sump ($tonnes$)
T = time constant
V = volumetric holdup (m^3)
W = mass flow of water ($tonnes/h$)
Z = static head from pump suction to pump discharge (m)

Lowercase

b = discretized breakage function

c = concentration ($tonnes/m^3$)

d = density ($tonnes/m^3$)

f = coefficient of friction

= fraction in the mill feed stream

$\underline{f}$ = vector of size fractions in the mill feed stream

g = acceleration due to gravity (m/sec^2)

h = vortex free height (cm)

k = number of components

p = mass frequency of particles in feed stream

$\underline{p}$ = vector of size fractions in the mill product stream

$\dot{\underline{p}}$ = derivative of $\underline{p}$ w.r.t time

q = volumetric flow rate (m^3/h)

s = selection function ($minutes^{-1}$)

t = time ($minutes$)

x = arbitrary variable

Superscripts

m = number of mixers in the mill model

α = breakage function distribution modulus

Subscripts

a = average

c = hydrocyclone diameter (cm)

= or controller gain

d = derivative

eq = equivalent

f = friction

i = particle belonging to the ith class size

= or inlet diameter (cm)

= integral

in = inches

j = particle belonging to the jth class size

k = particle belonging to the kth class size

m = maximum

o	= overflow diameter (cm)
p	= pulp
$PH1$	= pump head constant number 1
$PH2$	= pump head constant number 2
$PH3$	= pump head constant number 3
s	= solids
	= or steady state bias of controller
sp	= setpoint
u	= underflow diameter (cm)
$USGPM$	= gallons per minute (U.S.)
v	= specific volume
1,2	= first and second component
50c	= corrected equiprobable partition

Greek symbols

α	= sharpness of separation
Δ	= a small increment
ε	= error between setpoint and predicted output
μ	= microns
ρ	= density ($tonnes/m^3$)
τ	= time constant
	= or mean residence time in the mixer ($minutes$)
ϕ	= percent solids in the feed stream

Chapter 1

Introduction

The mathematical modelling of mineral processing operations dates back about three decades. As noted by Napier-Munn and Lynch (1992), until recently the technology has proceeded very slowly and has been, for the most part quite site-specific. The advent of powerful desk-top computers has provided the much needed shot in the arm for the modelling and simulation activity but as yet no commercial general purpose dynamic simulator is available. To address this situation, researchers at the University of Alberta have started developing a dynamic simulator that could serve both academia and industry for either training personnel or designing control systems. This work has been possible primarily due to the cooperation between the academic staff and graduate students in the Departments of Chemical Engineering and Petroleum, Mining and Metallurgical Engineering. Simulator development has now evolved to a stage where reliable grinding circuit models exist which can be used to track transient circuit behaviour and be employed to evaluate both continuous and digital control strategies. The main purpose of this work has been to develop a versatile microcomputer based based grinding mill simulator and validate simulated results by comparison with industrial data. In view of the recent developments in the field of mathematical modelling, there is a strong interest in employing different

types of models to enhance simulator performance.

Particle size monitors (PSM) used in the mineral industry are instruments that measure on-line particle size distribution of the product stream. These instruments have a high initial cost, are susceptible to frequent breakdowns and have high maintenance costs. A possible alternative is the use of a computer implemented estimator that can infer particle size distribution of the product stream from other measurable circuit variables. If a PSM is installed it could be used intermittently to calibrate the estimator. Such an approach thus involves designing an inferential control strategy that can be used for control of the grinding circuit. As is the norm, this strategy will be acceptable if the resulting simulator is able to maintain grinding objectives in the face of load disturbances and set point changes.

The thesis, concerned with further development of a the general purpose dynamic grinding mill simulator at the University of Alberta is organized in the following manner. In Chapter 2 a review of the work done in the recent past in the field of mineral grinding modelling, simulation, and control is presented. Chapter 3 describes the models used in the simulator. Chapter 4 gives a brief survey on the present status of hydrocyclone modelling and it is hoped that this will explain why the empirical models of hydrocyclone developed by Plitt is preferred. The simulator structure and features are outlined in Chapter 5. The open loop performance of the simulator is detailed in Chapter 6. Chapter 7 describes the Type I control strategy as applied to the three ball mill circuit of the Hemlo Mines Ltd. The estimator design is also elucidated in this chapter. The final chapter provides a review of the major results and includes recommendations for future work.

Chapter 2

Modelling, Simulation and Control in the Mineral Processing Industry

2.1 Introduction

Although the potential of using digital computers for simulation was realized in the late 1950's, hardware limitations made its realization physically impossible. As technology developed and as the mathematical modelling of processes became more and more exact, the viability of using a digital computer increased and by the late 1960's simulations were being done on the computer on a small but regular basis.

Later developments like easy access and availability of desk top computers and high level languages gave a definite impetus to the emerging trend. Ulsoy and Sastry (1981) in their review paper cite more than a hundred references which is indicative of the volume of work that had been done by the late 70's. Recent improvements in instrumentation and ready availability of distributed computer controlled systems has made it possible for plants to actually optimize their operation. Furthermore, reliable mathematical models of grinding circuits has also made it possible to develop circuit simulators to study plant operation before implementation.

2.1.1 Models and Simulation

Modelling in itself is a very general term. It could mean among other things, iconic (physical), visual or mathematical representation. For the purposes of simulating engineering processes, one is mainly concerned with mathematical models which are mathematical expressions that describe the operation of process units. Mathematical models can be further subdivided into different types. Fundamental or mechanistic models use the basic concepts of physics and chemistry to establish equations to describe the system, but often the values of the parameters must be known *a priori* in order to understand the underlying theory. These kind of models are usually quite general and arguably the most accurate. Phenomenological models are based on a theoretical understanding of the process but contain parameters which have to be obtained by experimentation on the process itself. The accuracy of these models are therefore subject to the reliability of the experiment. The third type of models are the 'black box' models or empirical models. Development of such models involves establishing a model entirely by observing changes in output(s) to changes in input(s). The parameters of such models are usually obtained by employing stochastic identification or possibly even by regression analysis. Most of the models used in mineral process industry fall into this category. This is due to the complexity involved in the physics of the mineral processing unit operations.

Simulation entails the implementation of a given set of mathematical models to describe the system of interest. Generally, such implementation is done by digital computers and therefore the terms mathematical simulation and computer simulation are often used interchangeably. Simulations can be either deterministic or stochastic. Deterministic simulation indicates that the output to input relationship is independent of time *i.e.* the repeatability is one hundred percent. On the other

hand stochastic simulation studies will yield varying outputs for a given set of inputs for each simulation (provided the seed for the noise generator is changed for each simulation). This type of simulation is usually performed to describe random process behaviour .

The models used by simulators can either be steady state or dynamic. Steady state simulators predict steady state behaviour of a system by solving iteratively a set of algebraic equations. The steady state solution is assumed to have been reached when the latest iteration falls within a specified tolerance level. When the transient behaviour of the system is of interest, one must use dynamic simulators. In dynamic modelling, time is the independent variable and the models are described by ordinary or partial, linear or non-linear differential equations. Dynamic simulators would be particularly useful for establishing start up and shutdown procedures but due to the lack of understanding of the operation of mineral processing equipment when not operating at full capacity, suitable models and/or simulators are not currently available.

2.1.2 General Applications of Dynamic Simulators

The most common application of dynamic simulation in the mineral industry is the off-line evaluation of process control strategies. Initially, in the study of classical control theory, this involved the analysis of single-input single-output systems, simulating open loop response to establish the PID controller constants. For example Stewart (1970) examined various feedback control schemes through computer simulation. However, implementation of classical control was rather difficult due to system interactions as a change in one of the inputs affected more than one output resulting in the detuning of one or more of the loops to achieve satisfactory control. Recent efforts have been directed to applying advanced control algorithms to mineral pro-

cessing circuits. Many of the algorithms employ model based strategies which require the use of a mathematical model of the system. Simulation allows the user to complement plant testing and in some cases may even eliminate the need for plant testing exercises.

The second major use of dynamic simulators is as a training tool for operators and a teaching tool for students. Although these simulations are not very sophisticated, they nevertheless, are useful in providing the operator the opportunity to react to unusual situations without disrupting the operating process. For a simulator to be really effective as a trainer, it must provide visual displays and allow for operator-machine interactions. The models describing the processes have to be sufficiently detailed, accurate and the simulation must run in real time. The design of a training simulator is consequently, quite involved and often requires a team of specialists ranging from the process engineer to computer hardware and software experts. Hence, these simulators tend to be quite expensive and usually unique to a given installation with limited transportability. A combination of these factors make such systems unattractive to the minerals industry at present.

As a teaching tool, dynamic simulators serve as excellent aids for learning and understanding circuit dynamics. A simulator provides the user means to scrutinize the process mechanisms more closely and an excellent opportunity to evaluate different control schemes for a wide variety of scenarios, some that rarely (or never) occur in an operating plant. Similarly, the effects of different kinds of disturbances can also be studied.

2.2 Modelling In The Mineral Process Industry

The mathematical models used in describing the dynamic behaviour of mineral processes have been constantly evolving for the last four decades. Wood (1975) has presented a good review of the literature concerned with the modelling of grinding circuits up until 1975. Researchers such as Herbst and Fuerstenau (1980) have used many of these models to create software which help in the design and sizing of grinding mills from laboratory data.

Significant work has been accomplished during the past fifteen years. Dynamic models developed by Lynch (1977) using the empirical (or regression) modelling method has been among the most notable. In fact, this has formed the basis for work done later by many researchers like Herbst and Rajamani (1979), Smith and Guerin (1980), Laguitton *et al.*(1983), Ford and King (1984) and Flintoff *et al.*(1985). The dynamic models are basically derived from their steady state counterparts. The phenomenological modelling approach is now gaining more popularity. Bloor (1987) and Hsieh and Rajamani (1988) are among those who recently have done distinguished work. The parameters associated with the phenomenological model can be estimated by various methods as described by Fournier and Smith (1972). Acceptance of dynamic models using other approaches such as models based on time series analysis of plant operating data as detailed by Romberg and Jacobs (1980) and the state space approach (Hinde *et al.*, 1977) has been slow.

2.2.1 Dynamic Simulation of the Unit Operations

In the development of a grinding circuit simulator, each mineral processing unit is modelled individually and the transfer of material from one unit to the next is represented by a time lag (representing conveyors, pipes *etc.*). Herbst and Mular (1979)

present a good introductory review of the process of modelling and simulation of unit operations. Sastry and Adel (1984) show that almost all unit operations have dynamic and steady state models. Some of these models have been reviewed by Niemi (1983) with discussions on the applications of some of these models. Noteworthy work has been done by researchers like Kelsall and Stewart (Kelsall *et al.*, 1968 and Stewart *et al.*, 1977) in the area of grinding mill modelling. Workers like Flintoff *et al.*(1985), to complement existing mill models, have presented models for circuit holdups *e.g.* sumps, bins; pipes and conveyors (modelled as variable and fixed time delays respectively) and a pump model based on pump manufacturer's head-capacity curves. As this work deals mainly with the simulation of grinding circuits, operations of the mineral processing plant like crushing, floatation, dewatering *etc.* will not be discussed in any detail.

Given the number of papers that have been published in the area of modelling and simulation of grinding circuits, it would be impossible to list all of them. Austin (1972) presents a good account of some of the earlier work done in this area and the book of Lynch (1977), is maybe one of the most referenced books on this subject. With few exceptions, all grinding circuits in operation today are of the closed circuit type, typically employing a hydrocyclone for classification. Consequently, the modelling of the hydrocyclone is a key to building any good simulator. Extensive research has been done on hydrocyclone modelling by Lynch and Rao (1975) who developed empirical equations from a large number of plant databases on the performance of hydrocyclones of different sizes. Plitt (1971,1976) formulated another empirical correlation based on data gathered from experiments with the hydrocyclone and data supplied by Lynch and Rao. Apling *et al.*(1980), in their attempt to use both the Lynch-Rao and Plitt models report that there are advantages and disadvantages for the use of either model.

For two data sets, although the Lynch-Rao model fit the data adequately, it was not possible to extrapolate from one data set to another. The Plitt model with its published constants could not be fit to either data set but upon modifications of the constants, this model provided a good fit and allowed extrapolation over a wide range of operating conditions. Most of the recent studies of the hydrocyclone use either the Lynch Rao model (Smith and Guerin, 1980) or the Plitt model (Laguitton, 1984). A good review of the present technology in hydrocyclone modelling is presented by Flintoff *et al.*(1987).

2.3 Dynamic Simulation Software in Mineral - Processing

The mid-60's marked the begining of the use of computers for analyzing mineral processing operations. Initial use of the digital computers was for calculating steady state material balances on specific unit operations. The steady evolution of modelling coupled with improvements in the computer technology has helped build general purpose steady state simulators. On inspection, one can discern the existence of two distinct groups in the area of developing dynamic plant simulators. One group makes use of the continuous system simulation languages (CSSLs) and the other uses high level procedural languages like BASIC and FORTRAN. The main advantage in using a CSSL is that a framework for solving the differential and algebraic equations is built-in and hence requires a minimal amount of programming. Simulators falling in the second group, however, require that either the builder or the user design specific subroutines to do the mathematical tasks. As a result, simulators using a high level language like FORTRAN are more difficult to develop and, are frequently, intended for a particular installation. A major drawback of simulators using a CSSL is the

difficulty experienced when handling multi-attribute streams as noted by Wood and Flintoff (1982). As well, the CSSL software systems are quite expensive when compared with a FORTRAN based simulator which requires only a FORTRAN compiler. Furthermore, apart from the cost of the CSSL software, which in itself is more expensive than a FORTRAN compiler, the CSSL's require a FORTRAN compiler as a separate software item.

Richardson (1983) and Sastry and Adel (1984) have reviewed the development and state of simulation software in the mineral industry. Both surveys report a lack of general, multipurpose, dynamic simulators. Most of the dynamic simulators reported hitherto have been for specific circuit configurations. Of particular note are simulators built by Herbst and Rajamani (1979), Finlayson and Hulbert (1980), Smith and Guerin (1980), Bascur and Herbst (1985) and Laguitton (1984). Reluctance of the developers to release details of the dynamic simulators seems to be universal.

DYNAMILL, developed by Herbst and Rajamani (1979), is one of the few simulators which takes into account auxiliary equipment like pumps *etc.* but its inability to cater to more than three standard circuit configurations is a major limitation. Bascur and Herbst (1985) have announced the development of DYNAMILL II and DYNAFLOAT II written in BASIC and recommend it be used for training of personnel due to its 'user friendliness'. Work by Wood and Flintoff (1982), Wong (1984), and Flintoff *et al.*(1985) is based on the DYFLO system (Franks, 1982), a collection of FORTRAN subroutines intended for dynamic simulation in the chemical industry. The simulator as such, is capable of handling only grinding circuits, but is very appropriate for studying process control applications. The approach of simulating each unit operation as a subroutine is similar to that of Herbst and Rajamani (1979) and Adel and Sastry (1982). However, it is superior to these simulators in that it

can handle any grinding circuit configuration. As suggested by Flintoff *et al.*(1985) any circuit can be simulated by calling appropriate subroutines in the correct order. Hence this simulator can be expanded to include all operations normally associated with a mineral processing plant.

2.4 Mineral Processing Control

Given the fact that grinding is a cost intensive process, it is logical that improved milling efficiencies can lead to substantial savings with usually even larger financial gains being obtained through the beneficial effects of better milling on downstream processes. However, it is difficult to improve efficiency and maintain optimum conditions on account of the random and inevitable disturbances that occur in this process. Thus, one major reason for employing process control to grinding circuits is to achieve stable operation at high efficiency in the presence of unavoidable disturbances.

Developments in the process control in the mineral processing industry over the last two decades have been greatly influenced by advances in instrumentation, innovations in computer technology and newer control strategies. Wood (1975) gives a very detailed account of the control techniques practiced in the mineral industry during the late 60's and early 70's. Ulsoy and Sastry (1981) identify numerous instances where computer control has been used to achieve desired performance. In fact, they contend that all mineral plants in existence use control of some form or the other. However as Herbst and Bascur (1984) report, the majority of control schemes in use at that time were classical control strategies where the feedback control law involved only proportional and integral actions. The use of advanced control strategies is increasing and as Hulbert (1989) suggests, virtually all modern control approaches like optimal, adaptive, model based predictive schemes *etc.* are finding application

with selected grinding circuits.

The nature of the grinding process being so prone to natural disturbances, requires effective control but on-line instrumentation is not available to measure the typical input disturbance of ore hardness, density and composition. Furthermore, although possible instrumentation to measure particle size is available, for many operations the cost is prohibitive. The standard practice to circumvent this lack of measurements is to use mechanistic models of the process. Even so, far fewer measurements exist on most grinding circuits than would be necessary for a complete on-line estimation of all the variables and states of a comprehensive model of the circuit. This shortcoming has spurred the growth of applications of model based control techniques. In some cases, a Kalman filter has been used to estimate the ore hardness disturbance (Herbst *et al.* 1980, Herbst and Alba 1985).

2.4.1 Selection of the Control Strategy

Techniques applied to the control of grinding circuits range from single input-single output (SISO) system to different types of modern advanced methods. In a typical grinding circuit, a conventional control strategy would involve single loop controllers for each variable that needs to be controlled. Most circuits employ ratio control (*e.g.* feedwater to ore ratio), and some utilize cascade control for their operations. The numerous examples of discussion in the published literature indicate the popularity of this technique. Lynch (1977) has reported on the systems used at the Mt. Isa Mines and at Silver Bell unit of Asarco Inc. Bradburn *et al.*(1977) have described the use of a similar strategy at Brenda Mines. As well, Deister (1986) describes the use of a multiple single-loop control scheme employed on the grinding circuit at Buick including a mention of the effect of the resultant interactions. Apart from being very easy to understand and implement, the principle reason for the popularity of

single loop proportional-integral (PI) and the proportional-integral-derivative (PID) feedback controllers is their availability at low cost as well as insensitivity to minor nonlinearities or multivariable interactions. The multiloop SISO control scheme, although simple and inexpensive to realize can sometimes result in highly undesirable interaction between the controllers. Multiloop interactions could be due to one or more of the following reasons. Lack of information regarding the magnitude of controlled variable response to manipulated changes in another input variable either due to an inexact model or due to limited knowledge of process dynamic behaviour. The nonlinear nature of the majority of the mineral processing unit operations and noisy instrument signals aggravate the problem even further. The steady wear *e.g.* rods and balls in the mills also contribute to the difficulty of satisfactory control. Frequently, these problems are simply handled by detuning one or more of the control loops so it is unlikely that optimum performance is achieved. Another method employed to reduce interactions while using single loop controllers for multivariable systems is the use of decouplers. With the decouplers in place, each single controller loop behaves independently with no affect of other control loops. It is common practice to make use of the Inverse Nyquist Array (INA) technique, introduced by Rosenbrock (1975), to design multivariable controllers that incorporate either static or dynamic decouplers. INA techniques have been successfully applied to many milling circuits as documented by Niemi *et al.*(1982), and Hulbert and others (1980). McDougall *et al.*(1986) show that dynamic compensators perform better than static decouplers.

In the selection of classical feedback controller parameters it is assumed that the direction of change in a manipulated variable required for correction of a control variable is known and that a set of controller gains can be determined that will be suitable for all circumstances. However, the varying nature of the milling process makes

it extremely difficult, if not impossible, to determine this unique set of constants and often controller gains, appropriate under one condition cause instability under another. An alternate approach is to use a model based control strategy which involves building a model that contains the missing information about the process. Then, by incorporating an on-line model in the control strategy, appropriate responses can be achieved to obtain an 'optimal' control performance. The components of this strategy include an empirical or phenomenological model, an estimator which is usually a Kalman filter, an optimizer to calculate the optimal control strategy and a controller to carry out the control action. When the control algorithm is derived by the use of a dynamic model of the plant and includes an optimization, possibly subject to some constraint(s), of a single index of performance, such a strategy is usually considered to be optimal control. Typically, measurement data from the process is used for the deduction of all relevant 'states' by an 'observer'. In contrast to feedback control, the optimal control approach determines the output of one controller from a combination of errors in all controlled variables rather than just one. As well, the control action over the 'control horizon' is calculated in such a way as to minimize the error. One popular approach in optimal control is to use linear state space equations with constant coefficients for the model and a quadratic performance index that depends on the states of the process and the control actions. Optimal control with a quadratic performance index has been applied successfully to grinding circuits (Herbst and Bascur, 1984). Niemi *et al.*(1982) studied a milling circuit at Vuonos, and found that its performance under a control system designed by INA technique was similar to that under an optimal control strategy. An excellent article on optimal control of wet ball mill grinding circuits is given by Rajamani and Herbst (1991). Optimal control gives the optimum control strategy for a process if the full control problem

can be expressed sufficiently accurately in the manner required, if the solution can be computed precisely, and if the practical implementation of the control is feasible.

When a control strategy uses empirical models to predict the output value over a specific time (prediction horizon) into the future, such strategies fall under the category of multivariable predictive control (MPC). Under this classification there are many different control strategies like the dynamic matrix control (DMC), internal model control (IMC), inferential control *etc.* One of the attractive features of the MPC methods is their conceptual simplicity and as such is easily understood and implemented by the plant engineer. Vien *et al.*(1991) have implemented a MPC based algorithm called multivariable optimal constrained control algorithm (MOCCA) for the circuit considered in this work. Lanthier and coworkers (1989) reporting on the use of IMC as an alternate approach to classical control contend that such model based techniques are to be preferred because the random behaviour of the circuit is taken into account.

Control technique where changes in the dynamic characteristics of the process are taken into account each time the controller gains are established is termed as adaptive control. These changes may be due to variations in the region of operation of a nonlinear process, or to characteristics of the process that are time varying. Four schemes have been suggested by Rajamani and Hales (1987) for the application of adaptive control: gain scheduling, model reference adaptive control, self-tuning regulator and optimal adaptive controllers. In gain scheduling, feedback (or feedforward) controllers are used in conventional way, except that the gains (and sometimes other parameters as well) are altered in accordance with auxiliary process variables that correlate well with changes in the process dynamics. In model-reference adaptive system (MRAS), a reference model is specified by the desired response of the process

to the set point(s). The controller parameters are adjusted accordingly to the difference between the behaviour of the reference model and that of the actual process plus its controller. The values of the process inputs and outputs can also be used in the calculation of the adjustments. A self-tuning regulator (STR) involves the on-line application of any controller design method in conjunction with on-line identification. When the STR uses a single model expression for process model as well as control calculation and where the controller parameters are estimated directly, it is termed as an 'implicit STR' (Rajamani, 1985). In an 'explicit STR' the parameters for a process model are estimated from on-line measurements and the design of the controller is updated using the model parameters. In the optimal adaptive control scheme, a state space representation of the process model is used with the information provided by the process instrumentation used in the parameter estimation scheme. The estimation scheme is usually a recursive least square (RLS) algorithm (Kalman filter) which takes into account unknown stochastic disturbances in the process as well as noise in the measurements with the control vector calculated on the basis of minimized weighted sums of squares of process errors and control effort. One of the advantages of adaptive control is that it can be installed for the control of a process without the requirement for periodic retuning to compensate for changes in operating conditions during subsequent months or years of operation. Rajamani and Hales (1987) provide a good account of the developments in adaptive control and its potential in the mineral industry.

In spite of the numerous different types of control algorithms that might be employed for a computer based control system, there is no general consensus and the choice of which algorithm will be most satisfactory will likely continue to depend on specific conditions, resources, skills and opinions. However there is a tendency

of simple SISO control schemes being replaced by multivariable control strategies wherever deemed necessary.

2.5 Grinding Circuit Simulation for Control System Evaluation at the University of Alberta

There is a long history of model development for mineral industry at the University of Alberta. As will be presented in Section 4.5, the steady state modelling of the hydrocyclone was started by Plitt in the early 70's (Plitt, 1971, 1976). However, the dynamic modelling work was initiated by Wood and Flintoff (1982) who were also responsible for starting the work towards developing a dynamic simulator for the grinding circuit suitable to carry out various control strategies. Initially, the work was based largely on Franks (1982) DYFLO subroutines, but subsequently, specific subroutines were developed to simulate individual unit operations. Wong (1984) successfully used these and the DYFLO subroutines to study various single-input single-output schemes at the Lake Dufault grinding circuit. McDougall (1987) developed a dynamic simulation package based on the work of Wong (1984) incorporating advanced control schemes such as multivariable time delay compensation and noninteracting control. An IBM PC version of the grinding circuit simulator created by McDougall (1987) has been developed by Neale (1987).

Chapter 3

Grinding Circuit Simulator Models

3.1 Introduction

The reliable mathematical modelling of unit operations has come a long way in the last two decades starting from early attempts by researchers to produce empirical models from plant operating data. Very few of these early models were general so although the models were effective for specific plants, operated within a narrow range of operating conditions, their acceptance was not very widespread. Subsequently, other methods of modelling gained popularity and were suitably refined so that now there are models for most of the common unit operations which are valid over a wide range of operating conditions. In fact, with the advent of computers, digital simulation using these mathematical models is now common.

This chapter is mainly devoted to describing the dynamic models used in the grinding circuit simulator developed at the University of Alberta. As noted in Chapter 2, research in this area was initiated by Wood and Flintoff (1982) and then developed further by Wong (1984), McDougall (1987) and Neale (1987). The mathematical models used in the simulator for the major unit operations followed, for

most part, those outlined by Smith and Guerin (1980). The prime reason of choosing these models were their simplicity which ensured clear understanding and eased the computational load. Furthermore, these models had been successfully applied to model existing grinding circuits. As the simulator is modular in structure, if desired, other unit modules can be substituted in place or added to the existing models. The next section describes the general purpose mineral grinding circuit components. Section 3.3 discusses the components of the grinding circuit that are modelled followed by detailed explanation of each of the models. Also included is a section on disturbance modelling.

3.2 Grinding Circuit Representation

Although types of grinding mills and their configurations in individual flow sheets vary, most of the conventional rod mill - ball mill grinding circuits consist of a combination of these process units :

1. Grinding Mills *Crushing and Milling*
2. Pump and Pump Box *Transport and Storage*
3. Conveyors and Pipelines *Transport*
4. Hydrocyclones *Classification*

In order to develop a detailed dynamic simulator of comminution operation it is essential to have mathematical models of each of the components in the system. Fortunately, considerable work has been done in this area of modelling and numerous mathematical models are available for each item of process equipment. However, to be consistent with previous studies at the University of Alberta, mathematical models

used by McDougall (1987) and Neale (1987) for mills, pump-sump and conveyors-pipeline have been adopted. These models are based on the work of Smith and Guerin (1980). The mathematical model for the hydrocyclone has been taken from the work of Plitt (1976) and will be discussed in detail in the next chapter. One of the most common general grinding circuit configuration known as *Reverse Closed Circuit* is shown in Figure. 3.1. A configuration similar to the one shown in Figure. 3.1 will be used in in this work involving both closed and open loop simulations. The next section of this chapter gives details of the grinding mill employed in this simulator. The mill model used in the simulator has been shown to be effective in modelling both the rod mill and ball mill. The form of the models follow those outlined by Austin (1972) and are called continuous time, discrete size interval models. This form of grinding equation is quite popular as it has been found to be effective for a wide range of grinding mills.

3.3 Simulator Models

Rod mill and ball mills, shown schematically in Figure. 3.2 are employed in various combinations in wet grinding operations. The mechanism is as follows - the coarse feed slurry, consisting of water and solids, enters both types of mills through a scoop box or chute. From there, the slurry is gravity fed into a rotating mill where it is ground with either steel rods or balls. Rod mills are used to grind coarse feed ranging from 80% passing 20 mm to 80% passing 4 mm into a product size ranging from 80% passing 2 mm to 80% passing 0.5 mm. Ball mills are used to produce product particle sizes ranging from 80% passing 0.5 mm to finer than 80% passing 75 micrometres.

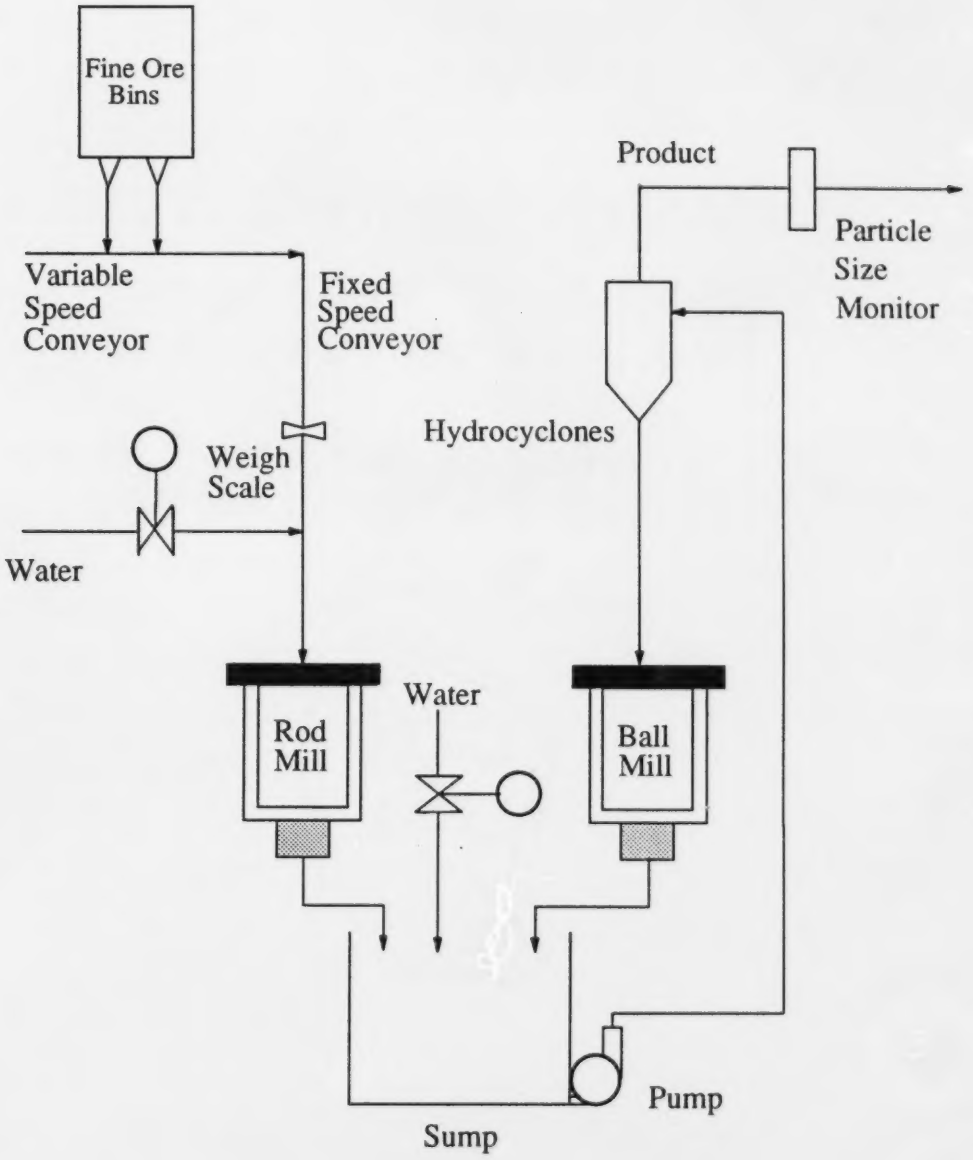

Figure 3.1: Schematic Diagram of a Typical Grinding Circuit Configuration

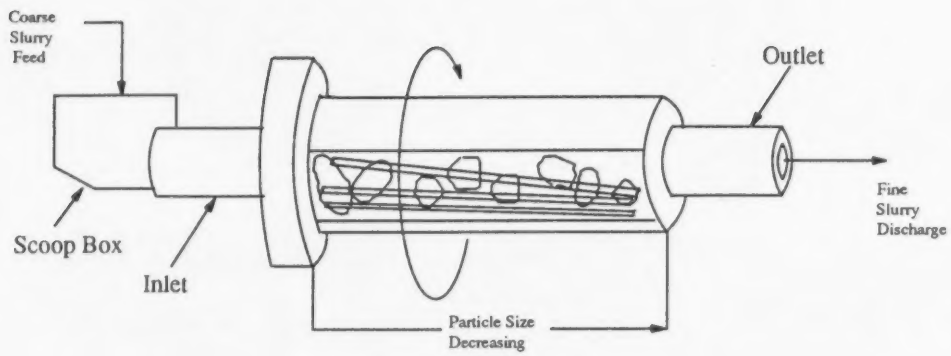

ROD MILL

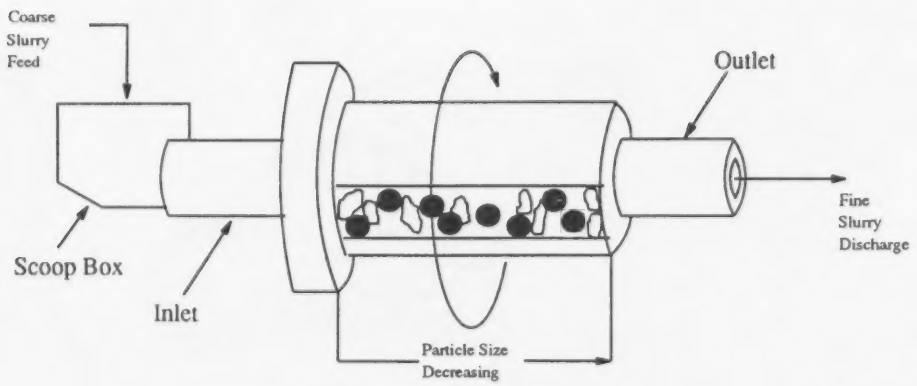

BALL MILL

Figure 3.2: Schematic Illustration of the Grinding Mills

Grinding Mill Model

The basic form of the mill model that can be used for both rod mill and ball mill is attributed to Kelsall *et al.*(1968). In matrix notation it can be written as

$$\dot{\underline{p}} = \left[(B - I)\,S - \frac{1}{\tau} I\right] \underline{p} + \frac{1}{\tau}\,\underline{f} \tag{3.1}$$

The model is based on a perfect mixer transport model with first order breakage rate. This model can be improved by considering that the ore is composed of two components *i.e.* a low density hard component and a high density soft component, each having unique breakage and selection functions and size distributions Neale (1987). Stewart and Weller (1977) have indicated that it is more appropriate to model grinding mills as up to three perfect mixers in series. Starting from an unsteady state material balance, Equation. 3.1 can be expanded in a way so as to make it suitable for computer implementation.

Since

$$Accumulation = Input - Output + Generation$$

it follows that,

$$\frac{d\,(H_s p_i)}{dt} = F_s f_i - P_s p_i - H_s s_i p_i + \sum_{j=1}^{i-1} b_{ij} s_j p_j H_s \tag{3.2}$$

Now, with $F_s = q\rho_s F_v$; $P_s = q\rho_s P_v$ and $H_s = V\rho_s$

substitution for F_s, P_s, and H_s yields

$$\frac{d\,(V\rho_s p_i)}{dt} = q\rho_s F f_i - q\rho_s P p_i - V\rho_s s_i p_i + \sum_{j=1}^{i-1} b_{ij} s_j p_j V\rho_s \tag{3.3}$$

Extending this material balance to a situation where the ore consists of more than one component (say k), the mill is represented by m perfect mixers in series, mass fraction of a component flowing into a mixer not equal to the volume of the component flowing

out, it follows that for a particle in size class i of component k in the mth mixer

$$\frac{d(V_k^m \rho_k p_{ik}^m)}{dt} = q\rho_k F_k^m f_{ik}^m - q\rho_k P_k^m p_{ik}^m - s_{ik}^m V_k^m \rho_k p_{ik}^m + \sum_{j=1}^{i-1} b_{ijk}^m s_{jk}^m p_{jk}^m V_k^m \rho_k \tag{3.4}$$

Now,

$$V_k^m = P_k^m V^m \tag{3.5}$$

assuming V^m and ρ_k are constants, the above equation can be simplified as:

$$\frac{d(P_k^m p_{ik}^m)}{dt} = \frac{q}{V^m}(F_k^m f_{ik}^m - P_k^m p_{ik}^m) - s_{ik}^m P_k^m p_{ik}^m + \sum_{j=1}^{i-1} b_{ijk}^m s_{jk}^m P_k^m p_{jk}^m \tag{3.6}$$

Differentiating the left hand side gives,

$$\frac{d(P_k^m p_{ik}^m)}{dt} = P_k^m \frac{dp_{ik}^m}{dt} + p_{ik}^m \frac{dP_k^m}{dt} \tag{3.7}$$

and by definition it is known that

$$p_{ik}^m \frac{dP_k^m}{dt} = p_{ik}^m \frac{q}{V^m}(F_k^m - P_k^m) \tag{3.8}$$

so Equation. 3.6 can be written as

$$P_k^m \frac{dp_{ik}^m}{dt} + p_{ik}^m \frac{q}{V^m}(F_k^m - P_k^m) = \frac{q}{V^m}(F_k^m f_{ik}^m - P_k^m p_{ik}^m) - s_{ik}^m P_k^m p_{ik}^m + \sum_{j=1}^{i-1} b_{ijk}^m s_{jk}^m P_k^m p_{jk}^m \tag{3.9}$$

Suitable rearrangement of terms in equation Equation. 3.9 leads to

$$\frac{dp_{ik}^m}{dt} = \frac{(f_{ik}^m - p_{ik}^m)}{\tau^m} \frac{F_k^m}{P_k^m} - s_{ik}^m p_{ik}^m + \sum_{j=1}^{i-1} b_{ijk}^m s_{jk}^m p_{jk}^m \tag{3.10}$$

The above equation has been used as the basis of the grinding mill model in the simulator. This algorithm is included in the MILL subroutine which requires as arguments simply, the labels of the input and output stream and a counter for the mill number. Further information on developing grinding mill models can be found in Lynch (1977) or Laguitton (1984).

A brief discussion of the breakage and selection functions are necessary at this juncture. First, however, a method to mathematically describe the particle size distribution has to be decided. The most logical choice would be to postulate a continuous function and fit the parameters to sieve analysis data. One of the most common functions used is the Gaudin-Schuhmann distribution expressed as:

$$B = \left(\frac{x}{k}\right)^{\alpha} \qquad x < k \tag{3.11}$$

As the function is continuous over the interval $0 \leq x \leq k$, it will give rise to an infinite number of class sizes. An alternative approach to represent particle size distribution is to make use of a finite number of particle class sizes. In other words, it is convenient to define the size class boundaries by a series of consecutively smaller sieve screen sizes as points of reference. The mass fraction of the particles retained by any screen corresponds directly to the lower bound of a size class that 'passes' the previous screen in the series. This form of discrete representation is capable of describing all possible size distributions and does not necessitate the use of approximations to fit sieve analysis data to a continuous function. The breakage function, b_{ij}, used in this work comes from a simple two parameter normalized Gaudin-Schuhmann cumulative distribution given by:

$$B_i = \left(\frac{x_i}{x_{j+1}}\right)^{\alpha} \quad i = j+1, \cdots, n; \quad \alpha > 0 \tag{3.12}$$

where $b_{ij} = B_i - B_{i+1}$

$B_i = \left[1/(\sqrt{2})\right]^{(i-j-1)\alpha}$

Noting that for $i \leq j, b_{ij} = 0$, and since it is assumed that there is no particle agglomeration and no daughter particles remain in the original size class, the final form of the discretized breakage function is:

$$b_{ij} = \left[\frac{1}{(\sqrt{2})}\right]^{(i-j-k)\alpha} - \left[\frac{1}{(\sqrt{2})}\right]^{(i-j)\alpha}, \qquad i > j \tag{3.13}$$

The parameter, α, in Equation. 3.13 is assumed to be dependent only on the ore type and not on the particular installation. Experimental work by Smith and Guerin (1980) indicated that for the Lake Dufault circuit, $\alpha = 0.676$ for the rod mill and $\alpha = 0.652$ for the ball mill. It is worth noting that the selection function is somewhat analogous to the rate function for a chemical reaction. It determines the rate at which particles are broken from a given size class into small size classes and is therefore dependent on the particular ore and specific grinding mill characteristics. Smith and Guerin (1980) found that for the Lake Dufault circuit the following functional forms were suitable - Rod mill :

$$s_i = \begin{cases} 0.0212 & \text{if } x_i \leq 1000\mu \\ 0.0212(x_i/1000)^{4.48} & \text{otherwise} \end{cases}$$

Ball mill :

$$s_i = 1.045(x_i/1000)^{1.818}$$

To simulate a harder ore the selection elements are simply multiplied by a factor less than one with the breakage elements remaining unaltered. Other functional forms have been proposed in literature. For instance, Rajamani, (Herbst and Rajamani, 1979) uses a selection function which is dependent on the mill power, mill solids holdup and percent solids. While each of these functional forms have their advantages and drawbacks, the simplicity of the models used by Smith and Guerin (1980) make them ideal to use.

3.4 Pump and Sump Model

The Pump Model

Pumps are an integral part of any grinding circuit for transporting the slurry in the circuit. Being such a vital component of the grinding process, pump design

and sizing are critical with respect to the economic operation of the overall grinding circuit. The pump must provide adequate flow rate along with sufficient head at the hydrocyclone inlet for proper operation. Improper sizing will result in pumps performing sub optimally leading to inefficient circuit performance. For simulation purposes, a mathematical model is necessary to describe the dynamic head produced by the pump. For optimum circuit operation, total head produced by the pump must be large enough to overcome the resistance head at all times as defined by the energy balance

$$Total\ Dynamic\ Head - Resistance\ Dynamic\ Head = 0 \tag{3.14}$$

The resistance dynamic head is the sum of all the resistances that the pump has to overcome in order to pump the slurry at the required flow rate. It consists of several factors (Flintoff and others, 1985),

- the static head from the pump centre line to the hydrocyclone inlet centre line
- pressure head required at the hydrocyclone inlet
- friction head due to pipe and fitting losses

Calculating the resistance head is trivial if the required system variables are known. The net static head can be determined as

$$SH = Z - L \tag{3.15}$$

The pressure head, PH, can be calculated with the help of the pressure-flow relationship given by the hydrocyclone model (Plitt, 1976):

$$PH = \frac{KQ^{1.78} \exp 0.0055(\phi)}{D_c^{.37} D_i^{.94} h^{.28} (D_u^2 + D_o^2)^{.87}} \tag{3.16}$$

The friction head, FH, can be calculated by two different methods. If the pressure drop for the nominal flow rate in the pipeline is known *a priori* in terms of the slurry density, the pressure head can be calculated using the well known Hazen-Williams equation for slurries (McDougall, 1987).

For example, if steel pipeline is assumed, this equation can expressed in SI units as:

$$FH = f\rho_s Q^{1.85} \tag{3.17}$$

The other method is arriving at the friction loss by starting from the first principles *i.e.* by calculating the equivalent lengths, friction factor (Churchill's equation), and determining the friction drop (Fanning's equation). The details of this procedure are described in Section 3.6. The resistance dynamic head RDH is, therefore, the sum of Equation. 3.15, Equation. 3.16 and Equation. 3.17, that is

$$RDH = SH + PH + FH \tag{3.18}$$

The total dynamic head, TDH, of the pump has to overcome the resistance head at all times according to Equation. 3.14. It is very convenient to model the TDH by a quadratic equation of the form :

$$TDH = K_{PH1} + K_{PH2}Q + K_{PH3}Q^2 \tag{3.19}$$

which can be used to describe the operating characteristics of a pump with a single or fixed speed drive. Equating Equation. 3.18 and Equation. 3.19 leaves only Q unknown so Q is solved for at each time interval.

The Sump Model

A sump or a pump box is normally used as a tank to collect the mill product stream before it is sent to the classifier. A perfect mixing has been assumed to ease modelling

complexities. Differential equations are set up to determine the the solids mass holdup of individual size fractions and overall solids and water mass holdup within the sump. As the slurry density has an effect on the pump head, it is essential to ascertain the average slurry density (weighted average in case of more than one component) and calculating the water holdup before solving for Q. The level in the sump is found by dividing the holdup slurry volume by the cross-sectional area of the sump base.

3.5 Conveyor and Pipeline Model

Conveyors and pipelines are a major source of time delay in a mineral grinding circuit. To design a realistic simulator it is necessary to be able to model these delays properly and incorporate them in the simulator. Moreover, if these delays, are not accounted for in control system evaluations, implementation in the plant will not be satisfactory.

Conveyor Model

A ball mill feed conveyor can be accurately modelled as a *fixed time delay.* The algorithm used in the simulator is based on one suggested by Franks (1982) with suitable modifications to handle the multi-attribute stream structure. The scheme can be very easily visualized in terms of a 'bucket brigade'. Imagine a line of people passing buckets filled with material from one to another in series. The first bucket is filled while the last is emptied keeping the number of buckets, and hence the material being passed, constant. The number of buckets in the line determines the time it takes for a specified bucket to reach the end of the line and be emptied. This sort of system can be handled quite efficiently on a computer by using a circular buffer as shown in Figure. 3.3. Conceptually, the subroutine allocates N blocks to the conveyor where N

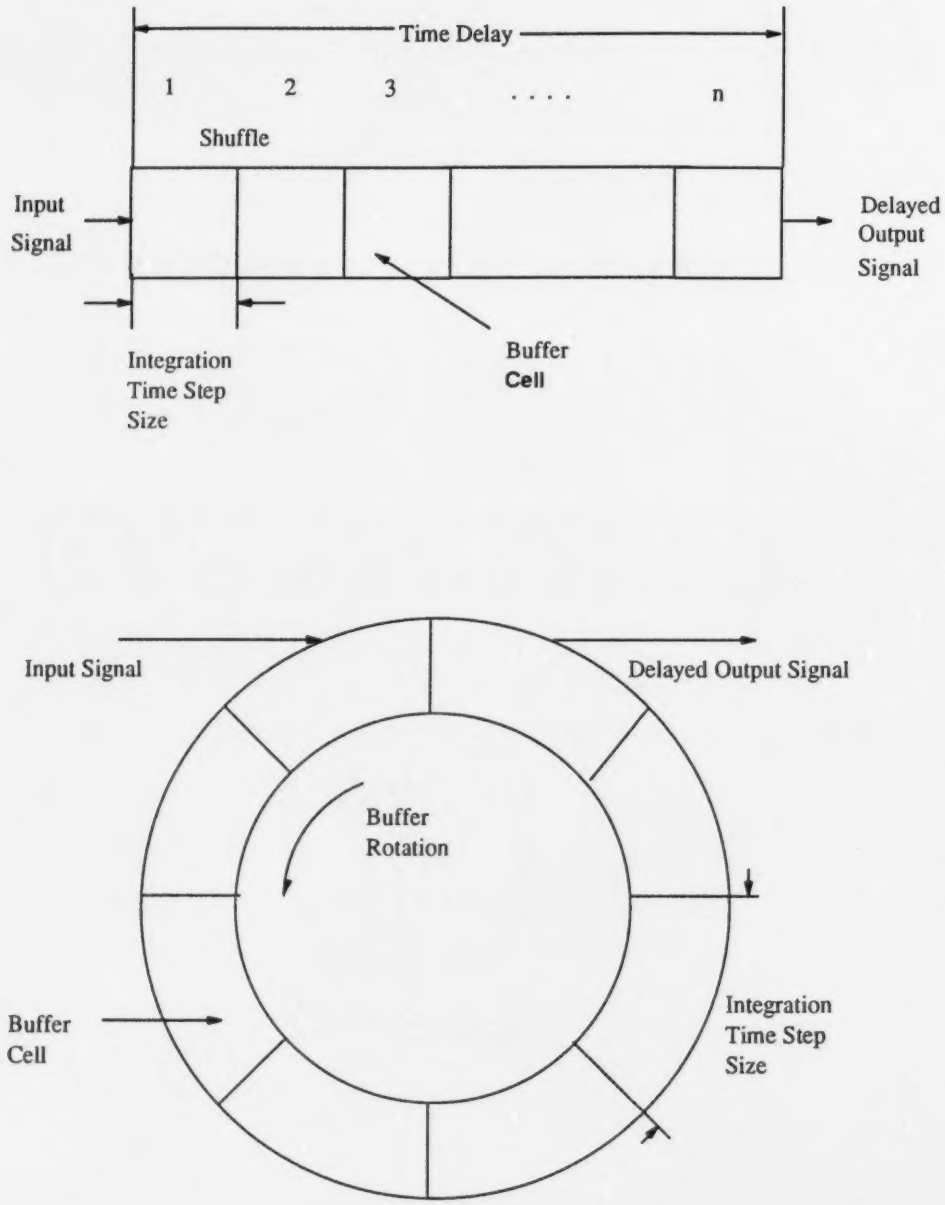

Figure 3.3: Schematic Representation for Digital Computer Implementation of a Fixed Time Delay

is the conveyor time delay divided by the integration interval rounded to the nearest integer. Now, rather than transferring the data from one block to another, it is more efficient to simply increment the block index, which efficiently rotates the buffer, and withdraw the appropriate block as per the value of the index at that particular time interval. To help reach steady state quicker, when starting from initial conditions and to avoid having to store the conveyor cell data from steady state simulations at the end of each run, all the blocks of the time delay model are filled with feed stream material during the first call to the subroutine.

Pipeline Model

It is a known fact that pipelines are another cause for delays and that these delays vary with time. Consequently, these delays pose a special problem in terms of modelling and simulation especially when control system analysis is to be performed. The model for a time delay due to a pipeline *i.e.* a *variable time delay* follows the work by Wood and Flintoff (1982) and is very similar to the model for delay due to conveyors. The primary difference between the *variable time delay* and *fixed time delay* is that in the former, time taken to completely fill the bucket is taken into account *i.e.* after the first bucket empties its contents into the second bucket, the second bucket does not empty till the first is filled again. The 'time' takes into account the variations in flow rate. The schematic diagram given in Figure. 3.4 will further clarify this model. Each of the buckets is represented as a cell. The total volumetric holdup is constant and all but the first cell are assumed to initially be full. The first cell is filled by the input stream; once it is full, the attributes are shuffled down the buffer. Any residual from a given time step is then placed in the now empty first cell. Thus for N cells in the buffer, the shuffle temporarily creates an $(N+1)st$ cell which along with the Nth cell, holds the material that is introduced to the pipe outlet stream.

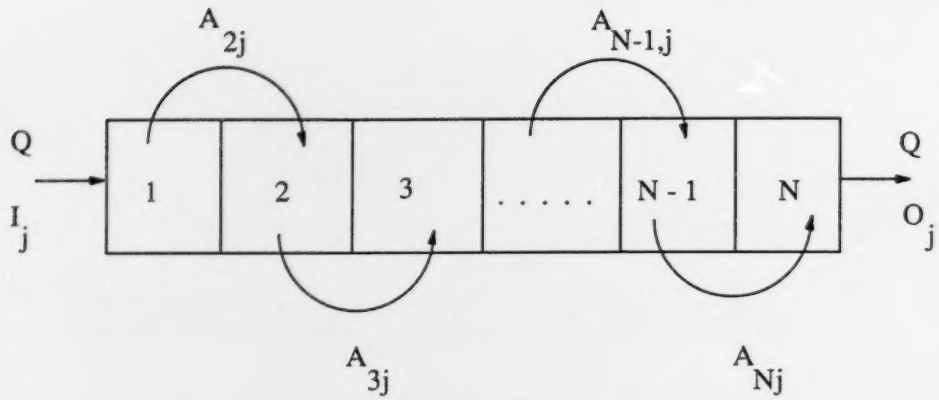

Figure 3.4: Schematic Representation to Explain the Digital Computer Implementation of a Variable Time Delay

As the outlet flow equals the inlet flow at all times, it implies that even if the inlet flow in a given integration interval is insufficient to fill completely the first cell, an equal volume must exit from the last cell. Alternately, if the volume flowing into the first cell is greater than the cell volume, a fractional part will remain in the first cell after the shuffling. In such cases, when the inlet flow per integration interval does not exactly equal the volume of the first cell, the outlet flow attributes are determined from a linear combination of the last two cells in the buffer. The relative weighting of these two cells is related to the residual amount of material in the first cell.

This algorithm has been found to suitably model a *variable time delay.* All the user has to do is to specify, apart from the input and output stream labels, the total volume of the pipeline, number of cells included in the buffer. The rule employed to determine the number of cells to be used in the *variable time delay* model is

$$2 \leq N \leq \frac{V}{3Q_m \Delta t} \tag{3.20}$$

Naturally, the larger the values of N, the more accurate the representation of the

time delay variable. Although there is a loss of accuracy due to discretization, it is felt that this algorithm provides a good compromise between computational efficiency and model accuracy.

The *plug flow element* of a grinding mill model can be modelled by the variable time delay model described above. However, there is one major difference from a physical point of view. While the delay varys depending on the flow rate, it would seem more appropriate to think of this delay as being due to an open launder or weir rather than due to a pipe. The difference can be explained thus. For a pipe, assuming it is completely full, the flow rate out has to equal the flow rate in for incompressible flow. However, in the case of an open launder, for a sudden change in flow rate at one end, there is a definite time delay before the change is realized at the discharge end, a situation very similar to a wave moving down the launder. So a slight modification in the *variable time delay* algorithm. is employed to differentiate between the time delays due to a pipeline and those due to the plug flow element of a grinding mill model.

3.6 Frictional Head Loss

Whenever there is a flow in a pipeline, there will be some loss of pressure due to friction. This head loss termed frictional head loss, FH, must be estimated accurately for correct pump design. Other variables being constant, the head loss usually depends primarily on the flow rate and density of the fluid. In case of slurries, some other factors like percent solids, size distribution *etc.* also come into play. To be able to get a good approximation of the head loss, it is essential to have a good model that can be used in the simulator.

Rigorous Calculation Method

Flow of slurries in pipes differs from flow of homogeneous liquids in many ways. With pure liquids, the complete range of velocities is possible, and the nature of the flow *i.e.* laminar, transitional or turbulent, is defined by the physical properties of the system. However, with slurries, two additional distinct flow regimes and many more physical properties are superimposed on the liquid system. In homogeneous slurries, the solid particles are homogeneously distributed in the liquid media, and the slurries are characterized by high solids concentration and fine particle sizes. Such slurries often exhibit non-Newtonian rheology *i.e.* the effective viscosity is not constant but varies with the applied rate of shearing strain. Heterogeneous slurries, on the other hand, have concentration gradients along the vertical axis of a horizontal pipe even at high flow rates *i.e.* the fluid phase and the solid phase retain their separate identities. Heterogeneous slurries tend to be of lower solids concentration and have larger particle sizes than homogeneous slurries. The most important fact to keep in mind while dealing with slurry flow is to ensure that the flow rate of the slurry is greater than critical velocity. Though there are methods to evaluate the critical velocities of homogeneous and heterogeneous slurries, they are beyond the scope of this research and as such will not be discussed here. For the purposes of this work, it will be assumed that the slurry behaviour is always Newtonian and above the critical velocity. To estimate the friction losses, a number of parameters need to be known. Details like pipe length, diameter, roughness factor, layout and particulars about fittings *e.g.*valves, bends and elbows, *etc.* are essential. Also, knowledge of slurry characteristics like flow rate (nominal), viscosity, density and the volumetric concentration of the solids is required. Once this information is known, the calculation of the pressure drop, ΔP involves the following steps :

- determine Reynolds number
- use the Churchill equation to calculate the friction factor
- apply the Durrand correction for solids loading
- determine the pressure drop using Fanning's equation

$$\Delta P = \frac{2 f L_{eq} V^2 \rho}{D g}$$

Selection of the Churchill equation to calculate the friction factor is arbitrary as many different empirical correlations are available in the literature. Gary and Maria (1985) give a list of some of the more popular ones and their relative merits and demerits. The length L_{eq} in Fanning's equation refers to the equivalent length taking into account the bends, valves *etc.* present in the pipeline.

Pre-calculated Method

Although the method described in the previous section is rigorous and simple to implement, the empirical nature of the equations make the results unreliable under certain conditions. Pump start-up is a case to point. Since initially the velocity of flow will be very low, the Reynolds number will be correspondingly small. In such cases the friction factor calculated using the Churchill equation will be unnaturally high giving a unrealistic value of the pressure drop. Consequently, the method is applicable only when the flow rate is near nominal or at steady state. Another drawback is that an accurate knowledge of all the necessary parameters is required *a priori* to estimate the pressure drop. This could be difficult in some cases. In order to circumvent these problems, there is another way by which the pressure drop can be estimated. The Hazen-Williams equation for friction losses in a slurry pipeline Lee (1978), is :

$$\Delta P_f = 0.2083(100/c)^{1.85}(Q_{USGPM}^{1.85}/d_{in}^{4.8655})$$

After assuming value for c as 100 and converting to SI units, an equation of the following form is obtained :

$$\Delta P_f = K \rho_p (Q^{1.85}/d^{4.8655})$$

$$\Delta P_f = f \rho_p Q^{1.85} \tag{3.21}$$

The assumption that f is almost constant for a range of flow rates and a fixed pulp density may not be too unrealistic. Therefore if ΔP_f can be physically determined for a particular flow rate (for *e.g.* the nominal flow rate) and the density measured, f can be estimated. In cases where, for a particular circuit, f can be determined before the grinding circuit becomes operational, Equation. 3.21 can be used to determine the ΔP_f at all flow rates around the nominal flow rate. This method used in the simulators developed at the University of Alberta (McDougall, 1987 and Neale, 1987) worked remarkably well for the Lake Dufault circuit and has been incorporated in this work.

3.7 Disturbance Modelling

Disturbances to the milling operation can be from different sources and each of these needs to be modelled. The most common and important disturbance is perhaps the change in fresh feed ore hardness. Changes in fresh ore feed hardness happens every time the quality of the incoming ore changes and often the plant operator does not know of this change beforehand. This change will however be reflected, after the appropriate delay, in the product stream. If strict control of the product stream is desired then it is absolutely essential to be able to model hardness changes so that appropriate control strategy can be adopted. Other disturbances that could occur from time to time include changes in the size distribution of the feed, change in ore

density, pressure or flow rate fluctuation in the water supply. These process changes also affect the quality of the product stream and hence should be also be modelled. The following sections will discuss modelling each of these process disturbance. Of course, upsets due to equipment failures or malfunctions are also possible but these have not been considered in this work.

Ore Hardness Disturbance

The parameters which describe ore hardness are those of the selection function S, with harder ore particles being chosen less frequently than softer particles for size reduction. Hardness changes usually appear as load disturbances to the system. On-line measurement of ore-hardness has not been possible thus far although Herbst and Fuerstenau (1980) made use of the extended Kalman filter to identify ore hardness disturbance based on particle size and circulating load measurements in their laboratory at the University of Utah. However this will not be implemented in the current work. Since the selection function is a measure of ore hardness, modelling of ore hardness disturbance could be readily handled done by altering the selection function constants. Implementation of the changes in selection function can be, however, done in two ways. Changes in the ore hardness is achieved, in the first instance, by simply multiplying the selection elements in the grinding mill by a constant McDougall (1987). Although this is convenient, there is one obvious limitation to this method, *i.e.* the time delay has to be chosen *a priori*, and cannot be adjusted once the simulation is started to account for changes in flow rates. The second approach which has been adopted in this work models the feed stream as a two-component system with each component having a different set of selection elements *i.e.* different hardness, Neale (1987). Therefore depending on the relative amount of each component, the hardness of the feed stream will change. Moreover, accounting for each component

separately, the user need not be concerned about the resulting time delays as the time will relate directly to the component flows through the circuit. The user can in fact specify both the time and rate at which the component ratios in the feed material change. An added advantage that this method provides is that even density changes in feed ore can be adequately modelled by assuming each component to have a different density.

Flow Rate Disturbances

Due to the weightometer on the conveyor belt, ore flow rate disturbances can be thought of as non-existent but for checking the reliability of the simulator, such a disturbance is considered. Similarly, even though a large disturbance in the water flow rate is highly unlikely, observing the open loop responses throughout the circuit due to a change in water addition provides useful insight to the dynamics of the grinding process. In this study, the effect of a $\pm$ 10% disturbances in ore feed rate and a $\pm$ 3% disturbances in the water feed rate have been investigated.

Feed Size Distribution

A more realistic and likely disturbance is one to the size distribution of the ore feed. This could occur because of an upset in the upstream primary crusher circuit. This kind of disturbance has been, however, considered beyond the scope of the current work.

Density

A change in slurry density, as discussed in previous sections, can occur due to a change in density of the feed ore or due to a sudden change in water addition to the circuit. The first situation usually happens when there is a change in ore source in which case

there might be an accompanying change in hardness. In a two component stream structure, changes of these nature can be modelled very conveniently. The method of modelling of hardness changes has already been documented. Density changes can be introduced by assigning the second component a density such that the average density is the same as the density of the incoming ore with the percentages of the two components adjusted accordingly. Density changes have been modelled by assuming that the percentage of the second component is 50% and the density of the second component is calculated accordingly as :

$$\frac{m_s}{m_s/2d_1 + m_s/2d_2} = d_a$$

i.e.

$$\frac{1}{d_a} - \frac{1}{2d_1} = \frac{1}{2d_2}$$

or

$$d_2 = \frac{d_a d_1}{2d_1 - d_a}$$

Since the ore density, d_1 is 2.8 $tonnes/m^3$, d_a must be less than 5.6 $tonnes/m^3$, as only changes in the ore density of $\pm 0.5 tonnes/m^3$ are investigated. Modelling density changes due to flow rate changes is implemented by simply reducing the water feed to the first sump.

Chapter 4

Modelling and Characteristics of the Hydrocyclone

4.1 Introduction

Hydrocyclones have been used since the end of last century and the principle of their operation as classifiers is well understood. The first large-scale application of the hydrocyclone came in the late 1940's mainly in the mineral industry for thickening slurries before filtration, removal of unwanted fines prior to floatation, density classification of coal *etc.*They were also used extensively in the paper industry for removing splints and grit from cellulose fine pulp. During these first few years the basic hydrocyclone design was established and has remained essentially unchanged ever since. The 1960's brought about an upsurge in the scale and diversity of hydrocyclone applications which now includes food, chemical, oil, cement, nuclear and metallurgical industries. The diversification has highlighted the limitations in design and prediction methods and consequently, there has been an increase in research effort.

With the advent of these new applications and a greater emphasis placed on efficiency in modern process plants, hydrocyclones have undergone a transformation from a low technology device to a medium or high technology one. Recent advances

in computer modelling now make it possible to simulate the complex multiphase flow inside the hydrocyclone from the fundamental principles. Experimental evidence is still of course necessary for validation, although now the emphasis seems to have shifted from overall performance parameters to internal flow details.

4.2 Operational Principles

The basic separation principle employed in hydrocyclones is centrifugal sedimentation, *i.e.* the suspended particles are subjected to centrifugal acceleration, which causes them to separate from the fluid. The principal difference between a hydrocyclone and a centrifuge, which works on the same principle, is that the hydrocyclone, shown schematically in Figure. 4.1, has no moving parts and the necessary vortex motion is performed by the fluid itself. Separation takes place in the radial direction, with coarse particles moving towards the wall and fine towards the axis. The vortex finder and the spigot are the two exits which yield the classification products along with the medium. Coarse products report to the spigot (or underflow) while the fines report to the vortex finder (or overflow). The standard way of characterizing the performance of any cyclone is to determine the following :

1. The particle cut size
2. The pressure drop
3. The volume throughput (capacity)

The particle cut size is usually given by the hydrocyclone classification efficiency curve presented as Figure. 4.2. This curve represents the percentage of particles entering the hydrocyclone that appear at the underflow for various particle diameters. The corrected efficiency curve represents the classification due to the centrifugal

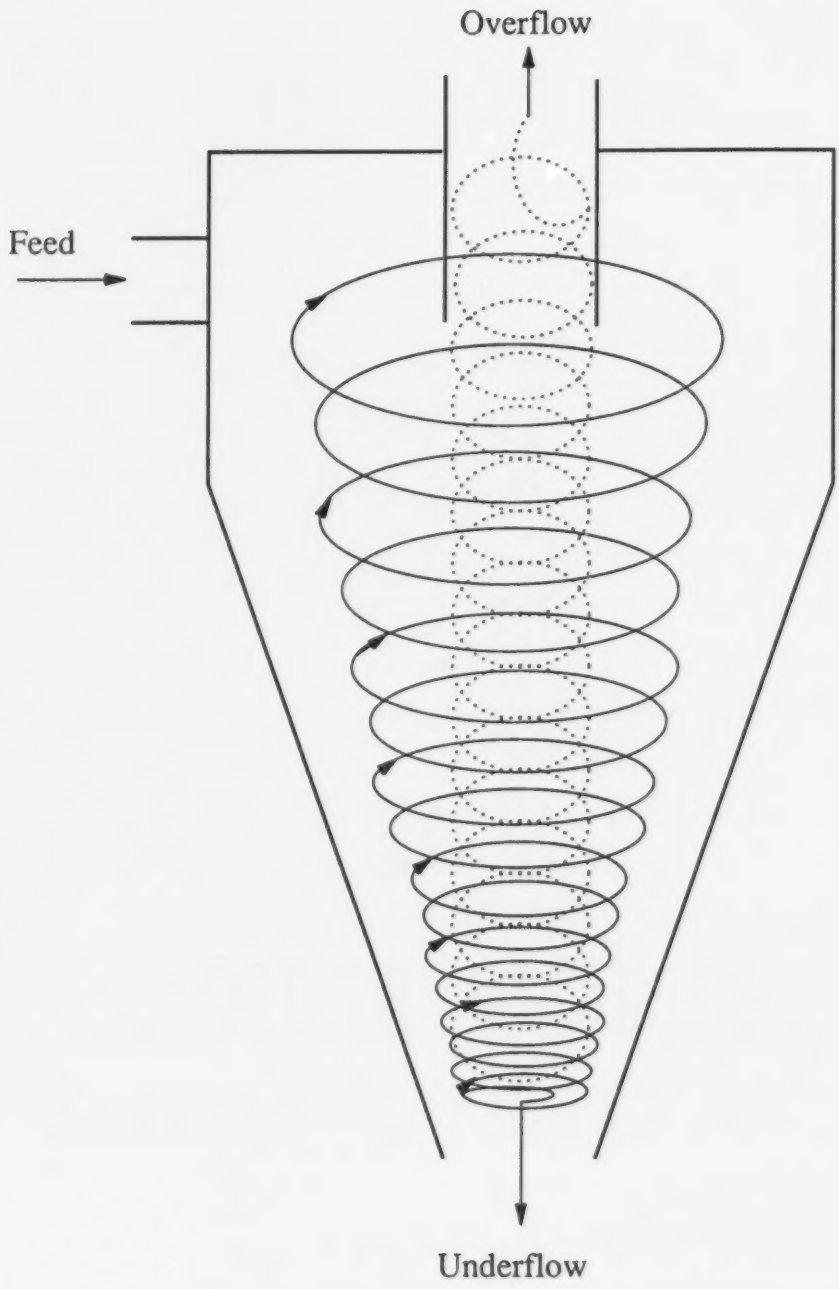

Figure 4.1: A Schematic Diagram of a Hydrocyclone Showing Vortex Formations

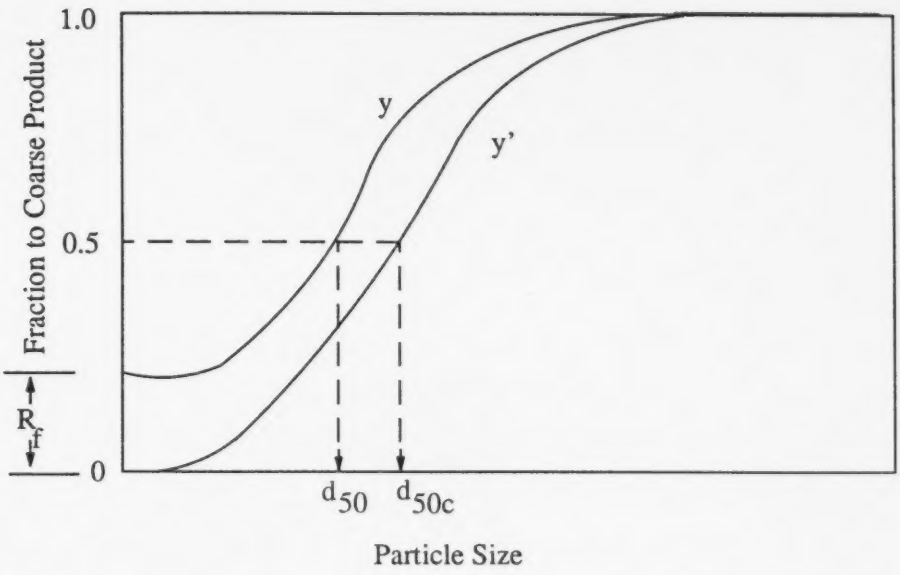

Figure 4.2: Typical Actual and Corrected Classification Partition Curves

effects only and it is more useful for comparing hydrocyclone of different designs. The point on the efficiency curve at which there is a 50% probability of a particle appearing at either exit is called the d_{50c} point or more commonly the hydrocyclone cut size in microns. The slope of the curve at the d_{50c} size represents the sharpness of classification, while the head and tail indicate respectively the coarse particles short circuiting to the overflow and the fines escaping through the underflow.

The second parameter, the pressure drop, is important since it affects the pumping requirements and is especially important where hydrocyclones are operated in series. It represents the energy required to spin the incoming fluid, and the losses associated with inefficient inlet and outlet designs. Due to the vortex flow in the hydrocyclone, the static pressure in the flow increases radially outward. In a working hydrocyclone, the spin of the fluid causes increasing pressure radially outwards and, because the inlet is in the region of high pressure and the overflow at a point of low pressure, the static head must again be overcome in order to pump in additional

fluid. In fact, contrary to common belief, pressure loss in the hydrocyclone is only in a minor part, due to friction component ; the centrifugal head dominates. It should be mentioned here that this 'centrifugal static head' is primarily determined by the distribution of both, the tangential fluid velocities and the suspension densities within the flow. The hydrocyclone throughput is related to the pressure drop, and is important because it determines the amount of slurry that can be processed per unit hydrocyclone at any time.

4.3 Effect of the Design and Operating Parameters on the Performance of the Hydrocyclone

Simple as the structure and principle of operation of the hydrocyclone is, it is evident that the performance of the hydrocyclone is affected by design and operating parameters. An excellent reference on this subject is the book on hydrocyclones by Svarovsky (1984).

4.3.1 Design Variables

The design variables, shown in the schematic representation in Figure. 4.3, which are thought to have a significant effect on hydrocyclone performance are :

- hydrocyclone diameter (D_c),
- vortex finder diameter (D_o),
- vortex finder length and shape,
- inlet diameter (D_i) and shape,
- spigot diameter (D_u),

- hydrocyclone length and cone angle.

The effect of each of these design parameters on operating performance will now be considered.

Hydrocyclone diameter (D_c)

The diameter of the cylindrical part of an operating hydrocyclone is the primary design variable and all other dimensions are usually related to it. For the same pressure drop (*i.e.* specific energy required for separation) and geometrically similar hydrocyclones, the cut size decreases with decreasing hydrocyclone diameter. In other words, a larger diameter hydrocyclone tends to separate at a coarser size than do smaller diameter hydrocyclones because the larger diameter gives rise to smaller accelerative forces. This means that in order to achieve lower cut size and higher mass recoveries, a smaller diameter hydrocyclone should be used.

Vortex finder diameter (D_o)

For hydrocyclones of fixed diameter and operating at constant pressure, the vortex finder (VF) diameter may be altered to influence the d_{50c}. The larger the VF diameter, the coarser the particles in the overflow and vice versa. However, there is a minimum size of vortex finder diameter for every installation below which the cut size starts to increase. This occurs when the outside diameter of the VF becomes smaller than the radius of the maximum tangential velocity (Kelsall, 1953). This is because the particles in the 'short circuit flow' do not encounter strong centrifugal forces as they pass the bottom edge of VF and therefore get carried into the overflow. Bradley (1965) suggested that the minimum VF diameter should be $D_c/8$. Similarly it is recommended that the maximum VF diameter should not be greater than the locus

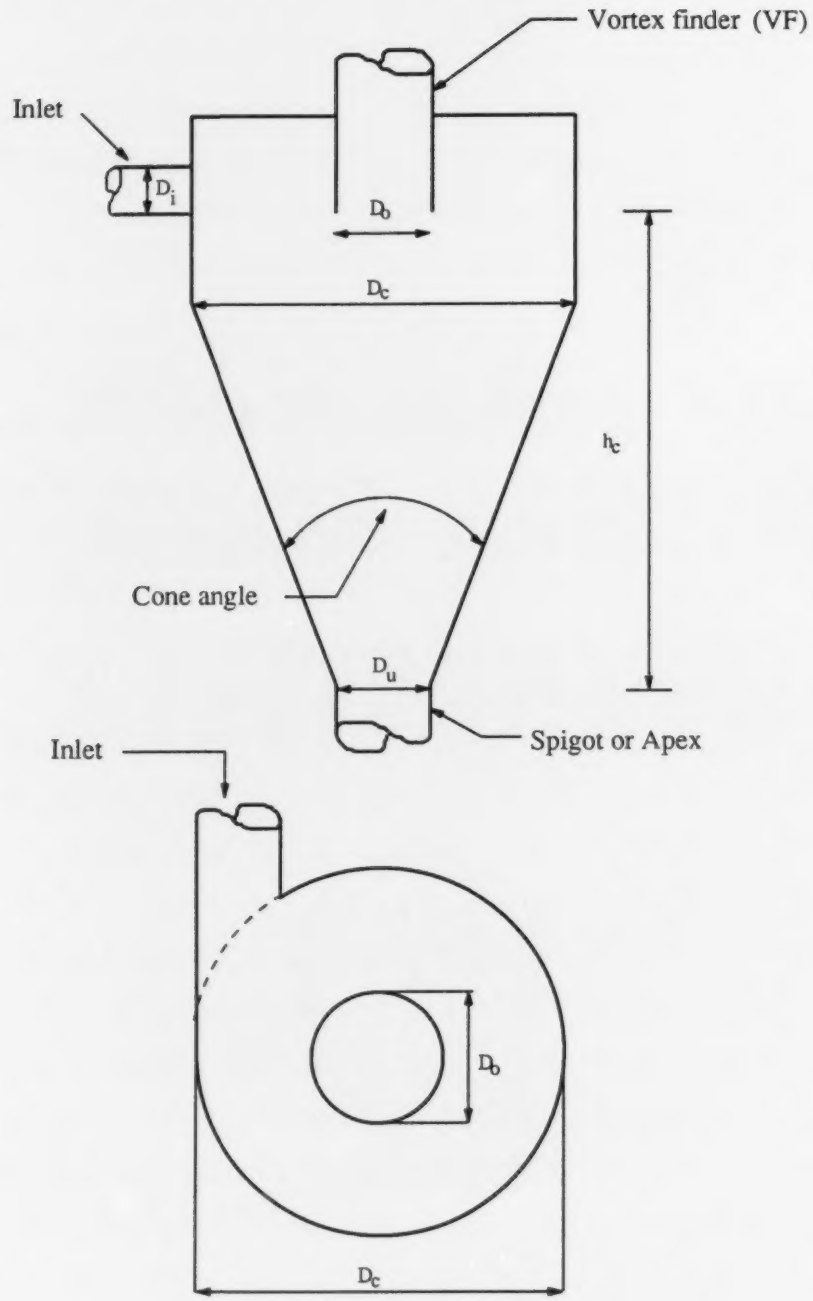

Figure 4.3: Schematic Representation of a Hydrocyclone Showing the Principal Design Variables

of zero vertical velocity because this causes collapse of the normal patterns of inward radial flow. Plitt (1976) has observed that an increase in VF diameter leads to sharper classification.

Vortex finder length and shape

The VF, basically, serves as a barrier against short circuiting of the feed slurry solids. The VF pipe makes it more difficult for the particles in the short circuit flow not to be re-entrained into the main body of the flow when passing the bottom of the VF. The length of the VF pipe should, ideally, terminate below the feed inlet nozzle and above the top of the cylindrical section. Extending the length of the VF, however, shortens the natural vortex in the hydrocyclone body and denies the fine particles a greater opportunity to separate from the vortex. Consequently, a longer VF increases the cut size (Bradley, 1965). In most designs, the VF length varies from 0.3 to 1.0 times the hydrocyclone diameter. The shape of the VF is considered to have very little affect on the efficiency (Bradley, 1965).

Inlet diameter (D_i) and shape

The inlet area determines the entrance velocity and is one of the factors that governs the tangential velocity at various radii. As a consequence, the transition radii between free and forced vortices are affected. Under similar conditions, an increase in inlet area usually involves an increase in flow rate of the feed. Decreasing the inlet area will slightly increase pressure drop at similar capacities. A rectangular shape at the feed entrance is judged to be superior to other shapes (Kelsall, 1953). One important requirement to be satisfied when designing the tangential inlet opening is that the entrance jet should not impinge on the vortex finder, because this would lead to

turbulence as well as to excessive wear due to erosion.

Spigot diameter (D_u)

Spigot diameter determines both solids capacity and the underflow percent solids. For hydrocyclones, particularly those with a diameter greater than three inches, solids capacity changes more rapidly with spigot diameter than does percent solids. A phenomenon related to spigot diameter is *Roping*. *Roping* is a condition where the spigot becomes overloaded with coarse solids or when the underflow is inadvertently throttled, so that the coarse particles are forced in to the overflow stream, a very undesirable situation (Plitt *et.al.*, 1987). Under *roping* conditions, the underflow stream is uniformly thick and tramp oversize can be detected in the overflow. Higher values of the underflow percent solids can be attained without *roping* when the hydrocyclone is operated so as to have a high overflow percent solids.

Hydrocyclone length and cone angle

An increase in the cylindrical section length results in a finer separation, probably because the zone where the coarse particles are being forced towards the axis by the cone wall is further removed from the vortex finder. A small cone angle (cf. Figure. 4.3) tends to decrease the separation size, although the 'sharpness' of classification may be influenced in a detrimental manner. Increasing the cone angle has the reverse effect, that is the separation size increases. The action of the cone is to squeeze coarse solids towards the center to obtain a concentrated underflow product.

Hydrocyclone designs are either geometries obtained by careful optimization by workers such as Kelsall (1953), Rietema (1961) and Bradley (1965) or commercial hydrocyclones that have been well tested (Svarovsky, 1984).

4.3.2 Operating Variables

The separation size is influenced by virtually all the operating variables. Some of the operating variables on which extensive work has been done on the premise that they have the most profound effect on the hydrocyclone performance are :

- pressure - flow rate relationship,
- slurry rheology,
- feed percent solids,
- feed size distribution.

Pressure - flow rate relationship

Increase in the pressure of the feed slurry leads to increase in the pressure head of the slurry at the hydrocyclone inlet. Since the products of classification are released at or near atmospheric pressure, the pressure head associated with the feed slurry relates directly to the pressure drop. As such, pressure (P) and pressure drop (ΔP) are equivalent. Some quantitative relationships have been established between the pressure drop and other performance characteristics of the hydrocyclone. An increase in the pressure drop leads to higher throughput and a finer cut size. Similarly greater pressure drops lead to a more concentrated underflow, cleaner overflow while lessening the underflow - to - throughput ratio (R_f). This behaviour can be explained by the fact that an increase in pressure drop results in a higher flow rate thereby generating greater tangential velocities and hence higher separation efficiencies are achieved. This implies that the efficiency curve, shown in Figure. 4.2 moves to the left, to finer sizes, and the cut size reduces. Consequently, overflow becomes clearer and more particles report to the underflow. The sharpness of classification deteriorates with

increasing R_f ratio and decreasing retention time in the hydrocyclone. The latter implies that low pressure drops, causing longer residence times in the hydrocyclone lead to marginally better sharpness.

Slurry rheology

The performance of a hydrocyclone operating in a grinding circuit can be improved by controlling the slurry rheology. Slurry rheology affects, apart from the separation performance, rate of fine material production. Detailed work has been done on the effect of slurry rheology by researchers like Kawatra and Eisele (1988), Napier-Munn (1980), Klimpel (1982). Although it is generally acknowledged that rheology has a large effect on the efficiency of hydrocyclones (Austin *et al.*, 1984), due to the unavailability of suitable industrial viscometer for use with mineral slurries, control of slurry rheology has been neglected. The chief parameters thought to strongly influence the rheology of a grinding mill slurry output are solids content, particle size distribution, temperature and chemical environment. The d_{50c} size of a hydrocyclone is believed to decrease with increase in temperature. This implies that a decrease in viscosity of the slurry, (assumed since in most cases the carrier fluid is water and the viscosity of water decreases with an increase in temperature) causes a decrease in the d_{50c} size (Kawatra *et al.*, 1989). This is in contrast with the results Klimpel, as reported by Kawatra and Eisele (1988), obtained which contends that the d_{50c} size increases with decreasing viscosity. For both observations to be considered correct it follows that the d_{50c} size must be a function of the manner in which the rheology changes.

Feed percent solids

Oddly, in spite of recognizing the fact that solids concentration in the feed influences the performance of a hydrocyclone, little work has been done in this area in a systematic way. Braun and Bohnet (1990), found that if all the other operating parameters were held constant, an increase in feed solids concentration generally leads to a coarser cut size, reduced sharpness of separation and a rise in pressure drop. Apart from particle-particle interaction which hinders radial motion, the limited capacity of the apex valve and the changes in the flow field within the hydrocyclone cause additional particles to be entrained by the overflow. The flow ratio thus becomes an additional parameter in determining the hydrocyclone efficiency. Also, an increase in the percent solids in the feed also brings about an increase in the effective pulp viscosity as noted by Svarovsky (1980).

Feed size distribution

The particle size distribution in the feed primarily influences the viscosity of the slurry. At constant solids content, a reduction in particle size produces an increase in slurry viscosity. This is a result of the increased surface area, which binds up water molecules and thus increases the effective solids concentration. Under conditions of low solids concentration, feed size distribution effects are not very apparent. However, at higher concentrations, particles in the flow increase the eddy viscosity and, like the liquid viscosity, increase the hydrocyclone flow capacity somewhat (Svarovsky, 1984). Particle size and distribution then begin to affect the cut size too, as is shown by Lynch (1977). Schubert and Neesse(1982), in their two-phase turbulent theory, predict that finer particle size increases the cut size.

4.4 Hydrocyclone Theories and Models

A considerable amount of research has been done in the area of modelling the flow and the separation process in a hydrocyclone. The different approaches, hitherto, to the problem can be divided into two main categories :-

- Physical models
- Mathematical models

4.4.1 Physical Models

The physical models comprise of :

1. Simple fundamental theories
2. Two-phase flow theory
3. Crowding theory

Simple fundamental theories

Each theory in this category gives a relatively simple correlation for the static pressure drop and the cut size of a hydrocyclone. The theories fall into two main groups - the equilibrium orbit theory and residence time theory.

Equilibrium orbit theory : The equilibrium orbit theory is based on the concept of the equilibrium radius proposed originally by Criner and Driessen and reported by Svarovsky (1984). The basic premise for this concept is that particles of a given size attain an equilibrium radial orbit position in the hydrocyclone where their terminal velocity is equal to the radial velocity of the liquid. Particles are hence, 'elutriated' by the inward radial flow according to the balance of the centrifugal and

drag forces, and Stokes' law is usually assumed. Probably the best known and credible approach to the equilibrium orbit theory is that by Bradley and Pulling (1959). The main drawbacks of the equilibrium orbit theory are that it does not take any account the residence time of the particles in the hydrocyclone and the effect of turbulence on the mechanics of particle separation is overlooked. Despite these shortcomings, several of the many forms of the equilibrium orbit theory will yield a prediction of hydrocyclone performance at low feed solids concentration (Svarovsky, 1984).

Residence time theory : The residence time theory assumes non-equilibrium conditions and considers whether a particle will reach the hydrocyclone wall in the residence time available. Rietema (1961) was the first to propose this theory and assumed homogeneous distribution of all particles across the inlet. The cut size will then be the size of the particle which, if entering precisely in the center of the inlet pipe will just reach the wall in residence time T. In mathematical terms, this means that the particle radial settling velocity integrated with time should be equal to one half of the inlet diameter. However, Rietema's theory fails to take into account the radial fluid flow, neglects inertial effects , takes no account of hindered settling at higher concentrations and assumes any influence of turbulence to be negligible. Other investigators such as Holland-Batt (1982) and have worked with this model. Their theories are slight improvements over Rietema's in that they do make provision for the effects of radial fluid flow. Even so, the theory is very simplistic and therefore not a 'true' picture of the actual process. The residence time theory, despite its very different approach and assumptions, often lead to correlations similar in form to those from the equilibrium orbit theory.

The Turbulent two phase flow theory

This theory attempts to address the effect of turbulence on the separation in hydrocyclones. Initial studies were done by Rietema based on the research of Kelsall (1953). Bloor and Ingham (1984), Duggins and Frith (1987) are some of the researchers who have done notable recent work . Bloor and Ingham (1984) obtained variable radial velocity profiles calculated from a simple mathematical theory. The turbulent viscosity was then related to the shear stress in the main flow and the distribution of eddy viscosity with radial distance at various levels in the hydrocyclone was derived. However, Duggins and Frith (1987) challenged the concept of isotropic eddy viscosity. They demonstrated that not only does the eddy viscosity vary with position in the hydrocyclone but its value is different in two mutually perpendicular directions and the ratio of the two values is not constant. They proposed a new method for determining velocities where the eddy viscosity for the axial and radial momentum equations were calculated from the conventional turbulent mode and the viscosity for tangential momentum equation from a mixing length expression. This method, hence allows for anisotropy of turbulence in the swirling flow.

Crowding theory

The crowding theory was first suggested by Fahlstrom (1963) who proposed that cut size is primarily a function of the capacity of the underflow orifice and of the particle size analysis of the feed. He contended that the crowding effect, or hindered discharge through the spigot, can dominate the primary interaction to such an extent that the cut size can be estimated from the mass recovery to the underflow.

The difference between the analytical cut size and the equiprobable size is attributed to the crowding effect. As well, he submits that the difference is a function

of the particle size, but this difference is now known to be due to the non-ideal shape of the grade efficiency curve which exists regardless of whether underflow crowding takes place or not. Bloor *et al.*(1980) have provided a more rigorous evidence. For the hydrocyclone design of Kelsall (1953), these workers using mathematical modelling established a hydrodynamic model of the flow both in the hydrocyclone body and in the boundary layer. The model assumes inviscid flow in the main body and viscous flow in the boundary layer. The predominant effect of underflow control on the cut size indicates that the crowding theory is valid in principle. Since no procedure exists to establish the effect quantitatively, it is to be expected that this area will attract further research.

4.4.2 Mathematical Models

The different types of mathematical models that have been presented in the published literature can be categorized as follows:

1. Regression
2. Dimensionless group
3. Momentum transport (analytical and numerical)

Regression Models

This group of mathematical models are based almost entirely on regression analysis of plant data. The two main performance characteristics taken into consideration are capacity (or pressure drop) and the separation efficiency in the form of the cut size. In most cases, the workers assumed dilute solutions and provided some correction for hindered settling in cases of higher mass concentration. The work of Lynch *et al.*(1968, 1974, 1975) and Plitt (1971, 1976) however, considered the effect of high feed solids

concentration on hydrocyclone capacity. Numerous experiments were carried out by Lynch and co-workers with various hydrocyclones designs and operating conditions with the result regressed to establish 'empirical models' of the hydrocyclone. The models derived were empirical and needed dimensionally dependent constants for application. Another drawback of these models was, since the equations were not based on any physical model of the actual process but on regression of plant data, reliable predictions could only be expected if the constants were determined for each system. The problem is amply illustrated by the variety of equations given by Lynch and co-workers for different studies. Plitt (1976) took the data of Lynch and Rao and added his own to derive by regression analysis, yet another model that characterized the hydrocyclone performance. The formulae proposed by Lynch and co-workers, and by Plitt have been applied to other hydrocyclone sizes and slurries (Apling *et al.*, 1980). Neither model was found to be entirely successful as it was necessary to modify the constants to make the prediction results agree with the experimental data.

Dimensionless Group Models

The model developed mainly through the work of Medronho and Svarvosky (1984) is an example of a chemical engineering approach to the design and scale-up of hydrocyclones. Based on fundamental theory and on hydrocyclone designs proposed by Rietema (1961), dimensional analysis was employed to produce necessary correlations. However the constants, it is revealed, are taken from actual test data rather than being established from theoretical considerations. It is claimed that if a given cut size and underflow concentration are specified, simultaneous solution of the given equations yields the hydrocyclone diameter, the number of hydrocyclones to be used in parallel and the size of the underflow orifice which, in turn, gives the required val-

ues for the hydrocyclone performance and capacity (under the given pressure drop). The geometric similarity usually concerns all internal dimensions of the hydrocyclone except the size of the underflow orifice which has been regarded as an operational variable. The authors claim that as the model is based on a physical model of the hydrocyclone operation and particle behavior, they have, unlike most other models, a better chance of success when applied to conditions outside of those tested. This claim has yet to be validated. There is also no mention if the models are applicable for slurries at solids concentrations greater than 10% by volume.

Momentum Transport Models

The analytical models are based on mathematical solutions of the basic momentum transport equations. The work of Bloor *et al.*(1980) and Hsieh and Rajamani (1988) is worth mentioning. The Bloor-Ingham model assumes inviscid flow in the main body of the flow and is capable of producing particle trajectories for efficiency calculations. It was found that assuming irrotational flow (*i.e.* having zero vorticity) leads to unreasonable results. The theoretical work is still in progress and it is anticipated that future models will provide improved predictions of hydrocyclone behaviour. It is felt that this line of research holds the most promise for describing the actual flow and particle separation in a hydrocyclone and that, in its final form, may not require any experimentally determined constants.

As an alternative to solving the basic equations of fluid mechanics analytically, the methods of computational fluid mechanics can be used to develop a numerical simulation of hydrocyclone operation. Numerical calculation of the complete flow field, using axially symmetric flow models and solving the full viscous equations of motion has been carried out by Rhodes *et al.*(1987). Numerical simulations are more

flexible for design purposes than either analytical models or a full experimental investigation but as yet are not available for high solids concentrations. Numerical simulations should be helpful when considering new geometry for a hydrocyclone.

All models predict hydrocyclone performance satisfactorily for particular hydrocyclone or installations, but none are general. Although models have been developed that can predict flow behavior inside a hydrocyclone, they fail to fully describe the complex separation phenomena occurring in a hydrocyclone . Only by considering the overall hydrocyclone operating characteristics and utilizing the fundamental equations governing the conservations of total mass and of each size fraction of material as well as the momentum equation will a full analysis of hydrocyclone behaviour be possible. A resolution of this difficult problem will likely be the focus of research for many years in the future.

4.5 Description of the Hydrocyclone Model Used in this Work

Subsequent to the discussion in the preceding sections of the various different modelling approaches in the literature to describe hydrocyclone behaviour, it is pertinent to examine briefly, the mathematical model for the hydrocyclone used in this work. At the outset, it must be pointed out that unlike the unit process models described in Chapter 3 the equations modelling the hydrocyclone behaviour are different than the model used hitherto at the University of Alberta. Both McDougall (1987) and Neale (1987) used the model developed by Lynch *et al.*(1968) to describe the hydrocyclone behaviour in their simulators. In this work, the empirical equations developed by Plitt (1976) have been incorporated. Similar to the empirical model outlined by Lynch *et al.*(1968), these equations describe the pressure-flow relationship, the water

split between the discharge streams, reduced or corrected efficiency curve and the equiprobable partition size as a set of nonlinear equations.

The pressure-flow relation of the Plitt model is a function of the various physical dimensions of the hydrocyclone . The equation is stated as :

$$P = \frac{K_1 Q^{1.78} exp(0.0055\phi)}{D_c^{.37} D_i^{.94} h^{.28} (D_u^2 + D_o^2)^{.87}} \tag{4.1}$$

Although K_1 in Equation. 4.1 has to be determined for any given installation from actual operating data, it has been found to remain constant over a wide range of flow rates, pressures and feed slurry compositions.

The next step in modelling the hydrocyclone is determining the ratio of the mass of water that reports to the fines product (overflow) to the mass of water in the inlet feed stream. This operating characteristic known as the water split is expressed by :

$$S = \frac{K_2 (D_u/D_o)^{3.31} h^{.54} (D_u^2 + D_o^2)^{.36} exp[0.0054\phi]}{H^{.24} D_c^{1.11}} \tag{4.2}$$

Again, K_2 is unique to any given installation and once evaluated, remains constant over a wide range of operating conditions. The mass water in the underflow stream is determined by subtracting the solids volume from the total underflow volume.

Next, the sharpness of separation, M has to be evaluated in order to arrive at the cut size of the hydrocyclone classifier. The sharpness of separation is characterized by the equation :

$$M = K_3 exp[-1.58 R_v] \left(\frac{D_c^2 h}{Q} \right)^{.15} \tag{4.3}$$

where

$$R_v = \frac{S}{S+1}$$

Perhaps, the most crucial part of describing hydrocyclone behaviour is correct prediction of the 'cut size'. Many equations have been formulated to predict the d_{50c} of a hydrocyclone . The Plitt d_{50c} equation predicts the 'cut size' in terms of all the major hydrocyclone design and operating variables. The equation is given as :

$$d_{50c} = \frac{K_4 D_c^{.46} D_i^{.6} D_o^{1.21} \mu^{.5} exp[0.063\phi]}{D_u^{.71} h^{.38} Q^{.45} (\rho_s - \rho_f)^{.5}} \tag{4.4}$$

The final part in developing the complete model is to have an equation to represent the entire corrected partition curve. The most widely used equation is the two parameter equation -

$$y' = 1 - exp[-0.693(d/d_{50c})^M] \tag{4.5}$$

However, this equation fails to take into account the entrainment effects of the coarse underflow product liquid. This phenomenon, as can be seen from Figure. 4.2, manifests itself as an intercept on the ordinate of the partition curve and normally corresponds to the fraction of water recovered in the coarse product. The 'classification correction' for the coarse product liquid is mathematically :

$$y' = \frac{y - R_f}{1 - R_f} \tag{4.6}$$

So, to describe the actual classification curve, Equation. 4.5 and Equation. 4.6 are combined to give :

$$y = (1 - R_f)(1 - exp[-0.693(d/d_{50c})^M]) + R_f \tag{4.7}$$

The only parameter that still needs to be determined is R_f. The procedure for establishing a value for R_f till the following method was illustrated by Plitt *et al.*(1990), was to solve for it, iteratively. From Equation. 4.5 it follows that a classification function c_i can be defined as :

$$c_i = 1 - exp[-0.693(d_i/d_{50c})^M] \tag{4.8}$$

With a knowledge of the classification number for each size class, the solids recovery to the underflow, due to classification alone can be expressed as :

$$R_c = \sum c_i w_i \tag{4.9}$$

For a unit volume of feed, the fraction recovered to the underflow is given by :

$$R_v = \phi R_s + (1 - \phi) R_f \tag{4.10}$$

where the solids to the underflow ϕR_s can be written as :

$$\phi R_s = \phi R_c + R_f \phi [1 - R_c] \tag{4.11}$$

substituting Equation. 4.11 in Equation. 4.10 gives :

$$R_f = \frac{R_v - \phi R_c}{1 - \phi R_c} \tag{4.12}$$

where

$R_v = S/S + 1$

After the underflow particle size distribution is evaluated, material balance equations provide a simple means of calculating the overflow product stream particle size distribution.

It is to be noted that the dynamic behaviour is neglected since the residence time within a hydrocyclone is small when compared to other mineral processing equipment.It is also worthy to note that the model outlined above can be solved directly for steady state operation when the feed characteristics are known. For dynamic simulations however, the pressure flow equation must be solved simultaneously with the corresponding pump pressure flow relation in order to accurately determine all the feed characteristics during any transients in the circuit.

Chapter 5

The Grinding Circuit Simulator Structure

5.1 Introduction

As the different unit operations have been described in detail, this chapter presents the overall structure of the simulator, with particular attention directed to the features that will facilitate expansion by future users. The simulator has been coded in FORTRAN 77 which ensures that the simulator is portable and inexpensive. In order to ensure that the simulator is simple to understand, convenient to use and easy to expand it employs a modular in structure with the driver consisting of only a series of calls to various subroutines which in turn call other subroutines and so on. Extensive use of COMMON BLOCKS reduce the argument strings to these subroutines to a minimum. DYFLO subroutines (Franks, 1982) have been included since they offer a choice of several utility routines to handle standard functions like integration, data printing etc. The structure of the simulator follows the same approach as earlier work done in the department of Chemical Engineering at the University of Alberta. The rest of the chapter describes each feature of the simulator in detail and as such can be used as a manual by the user. The next section explains how to initiate operations

of the simulator and the information required as initial inputs. Section 5.2 provides a convenient summary of the specific initialization values required for the use of the simulator, the manner in which the subroutines are structured and called, the kind of data base required to run the simulator and the advantages of the modular design. The next section provides details of the subroutine libraries and how they simulate the unit operations and what the nature of the output is. The last part of the section provides a brief introduction to the DYFLO subroutines. Section 5.4 provides with an example which demonstrates the method to be utilized to set up the simulator for a any milling circuit.

5.2 The Grinding Circuit Simulator

Before highlighting the salient points of the simulator a brief note on the hardware part of the simulator is appropriate. The simulation program is written in Microsoft FORTRAN 77 (version 5.0) and runs on an IBM PC or any compatible. The simulator in the current version requires 284K bytes of RAM. It is expected that as the program is coded in standard FORTRAN 77 syntax, it should be compatible with other compilers. In addition, it is recommended that a math co processor be used to increase the run time speeds. The decision to use the FORTRAN language is based on the fact that this is still is the most widely used computer language among scientists and engineers. Furthermore, use of the FORTRAN language allows the program to rely on the DYFLO subroutines for chemical process simulation (Franks, 1982) which are written in FORTRAN. It was felt that DYFLO2 is an appropriate choice since it has the combination of good documentation and an easy practical approach to simulation necessary for both the beginner and the experienced user. The user not familiar with the DYFLO subroutines may wish to consult the appropriate documen-

tation but this should not be necessary as the simulator is extremely user friendly and guides the user at each stage of the operation.

5.2.1 The User Interface

As has been stated, the framework on which the executive program is based follows from the DYFLO2 programming technique of Franks (1982). This style dictates the partition of the simulation program into four sections each performing specific functions. However, for the sake of brevity, the program could be viewed as being made up of an **initialization section**, an **integration section** and a **termination section**. The initialization section performs two main functions. One is to read in all the initial parameters to initialize the simulator, including the data base. The other function is to keep track of the simulation time and oversee simulation output printing as well as test for completion of simulation. While the first function is performed only once during a simulation run, the latter is carried out at every time step (integration interval). The integration section performs all the integration calculations required in the simulation. Program control is passed sequentially to the various unit processes and the parameter values are updated at each time step. At the end of the the cycle *i.e.* last unit process, the control of the program returns to the initialization section to test for end of the simulation. The termination section basically takes care of all the terminal calculations, data output and stopping the simulation. Needless to say, this function also is performed only once during any given simulation.

5.2.2 The Shell

It is appropriate at this juncture to explain the major functional blocks of the simulator. A schematic diagram of the open-loop simulator is shown in Figure. 5.1 which highlights the modular structure of the program. Each block in the figure represents

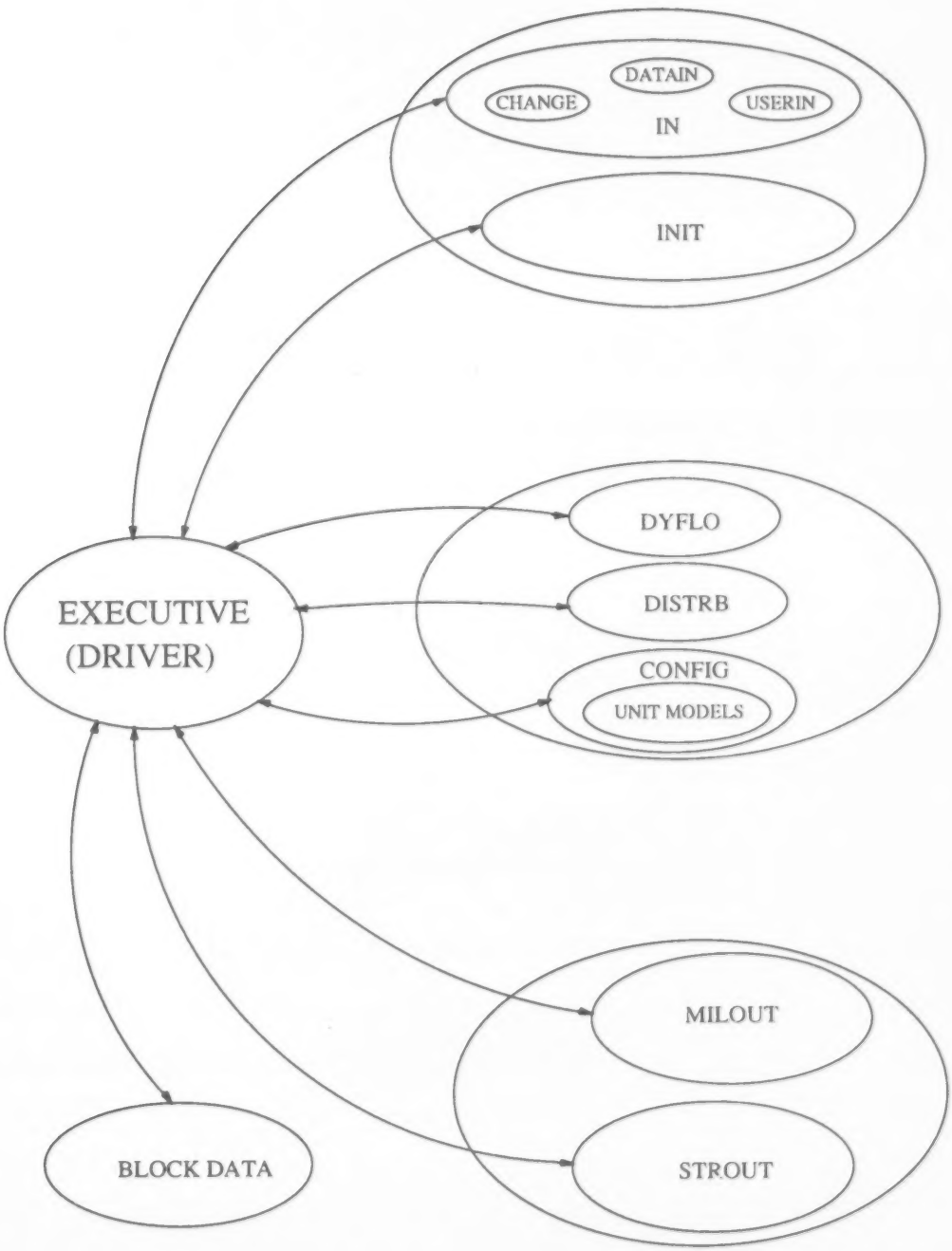

Figure 5.1: Schematic Diagram of the Open Loop Simulator Structure

a specific section of the simulator and the arrowheads indicate the direction of the data flow.

The simulator executive consists of a series of calls to various subroutines. As mentioned earlier, on execution of the simulator, the initialization section of the program takes care of parameter input. The user is offered a choice of specifying the name and type of data file from which stored parameters can be read. Alternately, the user could interactively change some of the input variables to suit the requirements of a particular simulation run. A third option offers the user the choice of specifying all the input parameters interactively. The features of these subroutines are detailed in the next section. Again, it should be pointed out that the structure of the input handling routines conveniently permits further expansion and customization as per the user's need.

Once the block data are loaded, run time parameters need to be specified. The simulator offers the user a default set of run time parameters like integration step size, etc. As well, control options are specified in the menu with open loop as the default. At the end, a complete listing of all the initialization values are shown on the screen before returning the control to the executive . This completes the data input function of the initialization section.

The integration section is responsible for the dynamic simulation calculations and it advances the simulation time by an amount equal to the integration time step each complete integration pass. A complete integration pass depends on the integration order (Franks, 1982). First order integration causes the program to cycle through the derivative and integration sections only once per integration time step, while second and fourth order integration causes the program to cycle two and four times respectively. As well, output of the simulation time and selected process vari-

ables to the output file are handled by this section. Depending on the option chosen, the process disturbance routine may also be invoked during this section. Different kinds of disturbances can be simulated with the help of this routine. In the closed-loop mode the control calculations are also performed at each step in the integration section.

After the completion of the simulation, control is transferred to the termination section which permits the user to specify if and how the simulation results are to be stored. Once again, the user can easily change this section as per personal requirement.

5.2.3 The Database

The simulator is designed to generally perform a simulation starting from steady state conditions. In case of such data being unavailable, the simulator can be used, with suitable precautions, to generate steady state data from 'initial' data. The initial data is the bare minimum data the user must specify in order to start the simulator. Even though the initialization section guides the user through the steps necessary to build the initial data base, an overview of the data base is felt necessary to help the neophyte. At the outset, it must be pointed out that an extensive use of COMMON BLOCKS has been made throughout the simulator. The argument against the use of COMMON BLOCKS due to the possibility of accidental change affected to the wrong variable is granted. However, the danger can be easily minimized if not eliminated by careful and proper coding since the use of COMMON BLOCKS limits the argument strings to each subroutine to a minimum.

Before starting to build the initial database the user must have values for all of the circuit parameters. Needless to mention, the number of parameter values required increase depending on the complexity of the circuit. The crucial parameters are:

- size distribution
- density
- flow rate of the fresh ore
- ratio of the water mixed before the first mill
- physical dimensions of all the process equipment
- numbers of each
- breakage and selection functions
- pump curve equation
- mill mixer volume(s)
- sump levels at steady state
- water flow rate to the sumps
- nominal slurry flow rate to the hydrocyclones
- hydrocyclone model constants
- effective friction factor for the pipeline

The initialization section does provide default values for each of the parameters, but in many cases these numbers may be quite different from the actual value. Care should be taken to enter 'true' values whenever possible because 'approximate' values may sometimes give highly unpredictable results.

5.3 The Closed Loop Simulator

The function of each part of the open loop simulator, *viz.* the initialization section, the integration section and the termination section has been described in the previous section so this part of the chapter will explain the design of the closed loop simulator and provide some details concerning the individual subroutines. As can be seen from Figure. 5.2 the principal difference from the open loop simulator structure is the inclusion of the CONTRL and CIMPL subroutines. These handle the control actions of the simulator and are not operative for open loop simulation.

5.3.1 The Initialization Section

The first statement executed by the simulator driver is a call to the IN subroutine. The IN subroutine interactively sets up various options for loading information for use by the simulator. The options provided allow the user to either load the data directly from a permanent file or selectively change data copied from a permanent data file. The third option permits the buildup of data file interactively. Two types of data files can used to run the simulator as explained in Section 5.2.2. While the data file set up by using the third option contains only the bare minimum information to start the simulator, the permanent file contains all the information necessary to run the simulator. Usually, this comprehensive data is generated by the simulator starting from the bare minimum information. All closed loop simulations are performed using permanent data files only. It should be mentioned though, that some times the permanent data files may not have steady-state data. Instead it might just have information from the simulator that was available at the end of a previous run that created the file.

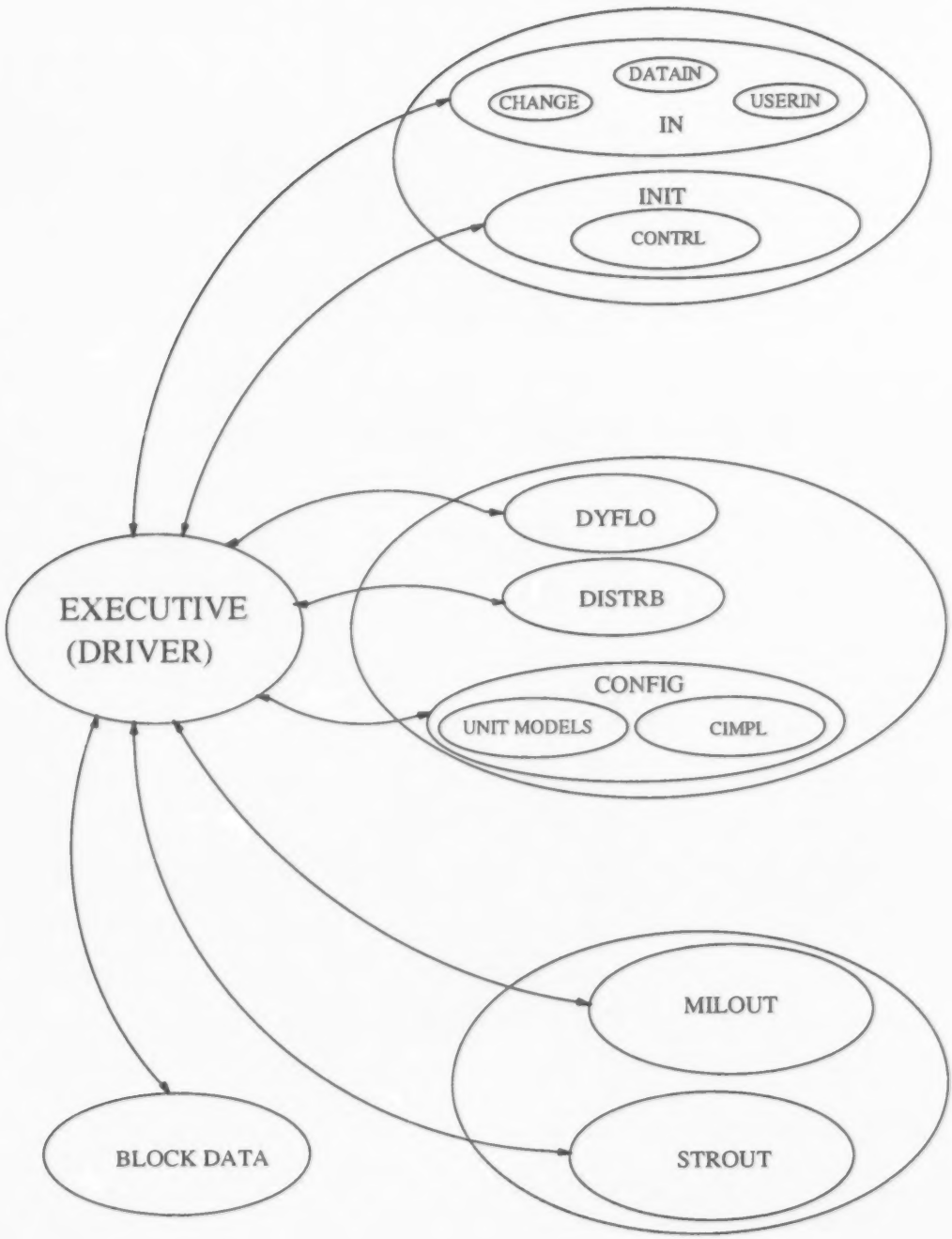

Figure 5.2: Schematic Diagram of the Closed Loop Simulator Structure

The IN subroutine provides the user with the following options:

1. use of an established data file requiring no changes
2. use an established data file with the option to make changes in some of the data
3. interactively set up a new data file

If the first option is selected, the subroutine DATAIN is called which prompts the user to specify further, whether the indicated data file contains data generated by the simulator or whether it has just the information created from the interactive program. Depending on the response, the simulator loads the information and returns the control to the driver.

Subroutine CHANGE is called if option (2) is selected which in turn calls DATAIN, as its first executable statement, in order to load the appropriate data file. The CHANGE subroutine then shows the user the menu of possible parameters that can be changed at the beginning of the run. Care should be taken to change the output data file name as whenever there is a change in the data file the contents of the original file will be lost. Options provided include changes to micro and macro properties of the feed stream and to the equipment model parameters. This part of the program is iterative in the sense that the user can loop back to the menu as many times as required before returning the control to the driver. Complete echoing of the input data is provided for visual error checking. As is the case with other subroutines, this part of simulator is open to expansion *i.e.* if more change options are required for a given application, it is only necessary to append the options to the menu and make the appropriate allowances with the statement numbers that control the program flow.

The choice of option (3) results in a call to the subroutine USERIN which

then allows the user to interactively build a data file that will enable starting of the simulator. This is a very big subroutine due to its interactive nature and extensive error checking. It prompts the user for specified information, does some error checking automatically, and if these constraints are met, echoes the data to the user to ensure that correct values are being read. In many cases this provides default values for the user to help get an idea of the expected value. Also it helps in completing the data file without having to stop frequently. It is felt that the extensive error checking and visual echoing will help keep typographical errors, while entering values, to a bare minimum and the users lead-in time will be significantly reduced. One last point needs to be mentioned before moving on. The interactive subroutines basically starts the simulator from zero initial condition. Consequently, it could take up to 400 minutes, depending on the complexity of the circuit, for the circuit to achieve true steady state, *i.e.* the solids mass flow rate out of the circuit equal to the solids flow rate into the circuit. Also, numerical values produced by the simulator during the initial period should not be construed as being indicative of what takes place in an industrial grinding circuit during a start-up period. Hence, it is advised that the simulator be run in an open loop mode when started from either the interactive subroutine or when using data previously created using the interactive subroutine.

Once the necessary information has been loaded into the simulator, control is returned to the driver which then proceeds to call the INIT subroutine that initializes the simulation run parameters. This is another menu driven interactive program that allows the user to change as many parameters as desired. A list of the default values provided include length of simulation, simulation run time, integration step size, *etc.*. As well, time of disturbance initiation and the type of control strategy (with the default option being the open loop condition). If the user accepts all the default

values, control is returned to the driver, otherwise a menu is provided to allow any of the default values to be changed. This is also an iterative process and the user can make as many changes as desired. The last option in the menu decides whether the simulator runs in open or closed loop condition. From the value of the integer flag ICNTRL which depends on the choice made by the user, the simulator determines the type of control strategy that is implemented. The ICNTRL is actually specified when the INIT subroutine calls the CONTRL subroutine in the closed loop mode. If the default value for this option is accepted it will indicate that an open simulation is desired and the INIT subroutine will not call the CONTRL subroutine. To facilitate use of the interactive CONTRL subroutines, the user must specify only positive values of K_c and τ_i, the algorithm automatically converts these values to the proportional band (PB) and repeats per minute (RPT) variables as required by the DYFLO control subroutines. Only positive values of the controller parameters are entered since the variable AXN is set according to whether direct (AXN=1) or reverse (AXN =-1) control action is required. Some error checking of the user supplied set-points is done to ensure that unattainable or unrealistic set points have not been specified.

Before control is returned to the driver, a complete listing of the initialization values is displayed (on the monitor) for final verification. Acceptance of the listed values returns control to the driver, or the menu is presented again and the user is permitted to make further changes. A return of control to the driver completes the initial work of the initialization section of the package. All pertinent information is now loaded into the simulator.

5.3.2 The Integration Section

The middle part of the simulator is known as the integration section and it is this section that performs the dynamic simulation calculations.This section contains the

DYFLO subroutines used to numerically solve the differential equations and to control progress of the simulation according to the independent variable, time. The DYFLO utility subroutines used in the simulator are explained in more detail in Appendix B. One of the DYFLO subroutines controls the dumping of time dependent data to an output file during the simulation. At every time step through the simulation, depending on the option chosen in the initialization section, a call is made to the DISTRB subroutine to allow the user choices for introducing various disturbances to the circuit. A flag in INIT subroutine can be set to indicate whether the simulation is to be run without disturbances, or if disturbances are to be included, the user can specify the time at which the disturbance is to occur. At the specified time after the simulation starts, the user is prompted, with a menu, of all the different kinds of process disturbances that may be selected, *e.g.* change in the volumetric flow rates in the feed, change in size distribution of the fresh ore, change in the feed composition, *etc.* After the user makes the desired choice, the program prompts for the nature of the disturbance implementation, *e.g.* step change, ramp change, square wave, *etc.* Various flags are used to control the calling of this algorithm throughout the simulation, for example for a single step change the subroutine is called only once, whereas for multiple changes it will be called at every incremental time step. In keeping with the modular structure of the simulator, this part of the program can be expanded to include more disturbance options. Besides the calls to the DYFLO and DISTRB subroutines, the integration section involves only calls to the CONFIG subroutine at each incremental time step. As shown in Figure. 5.3 the CONFIG subroutine orders the calls to the specific unit model subroutines that comprise the circuit. Depending on the layout of the circuit being simulated, the call statements to different unit models are ordered sequentially . An example of the manner in which

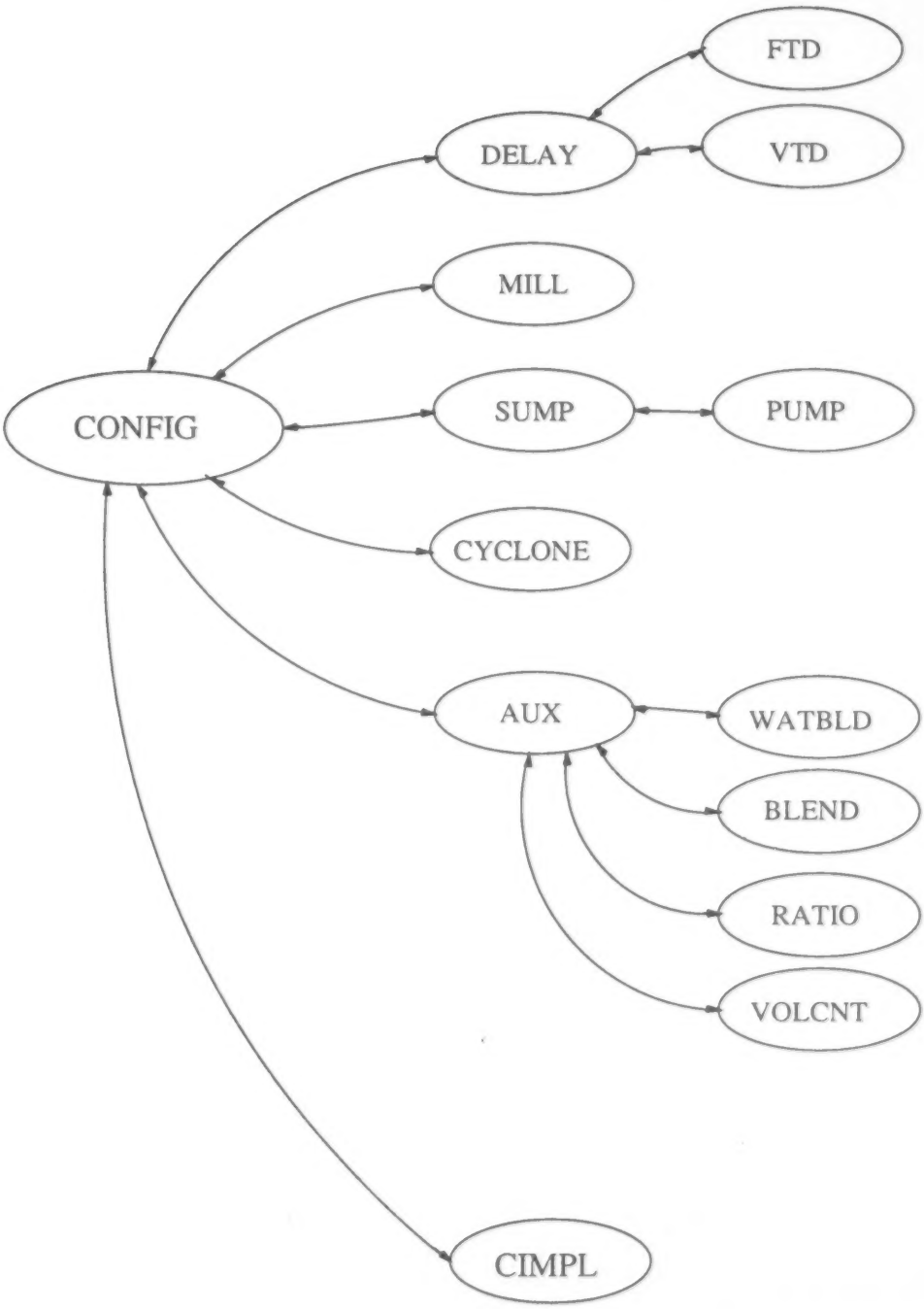

Figure 5.3: Schematic Diagram of the Subroutines Called by the CONFIG Subroutine

the calls to the different unit models are made for a particular layout is given in the last section of this chapter. Obviously, the user has to tailor these calls according to the flow sheet of the relevant circuit. Since CONFIG is called by the driver at every incremental time step, it is quite easy to append various tests or calculations to a particular run. As well, since CONFIG is quite small, it can be altered and compiled without much difficulty. To assist the user in specifying the appropriate unit process models, Table 5.1 gives the name of the subroutine and their functions.

As discussed earlier, if the simulator is operating in closed loop, the CONFIG subroutine apart from calling each unit subroutine sequentially, also calls the CIMPL subroutine at each integration step. The ICNTRL integer flag defined in the INIT subroutine determines the type of control strategy implemented. According to the value of ICNTRL a, specific control algorithm is executed by the CIMPL subroutine. For instance, the DYFLO subroutine CONTR2 is called from the CIMPL to perform a PI control calculation. Since the controller output is a function of the integral of the error signal, a call is made to the INTG subroutine in order to perform the integration. All calculation necessary to establish the controller input signal, and convert the normalized output signal to the appropriate value are performed in CIMPL. Combining all the required calculations in one subroutine makes each control module function as a stand alone unit thereby enhancing the flexibility of the overall system. As with the other subroutines, this part of the simulator can be easily by the interested user.

5.3.3 The Termination Section

As soon as the DYFLO subroutine stops the simulation at the specified point in time, the driver performs its last function by calling the OUT subroutine. This provides the user with two options of retaining the simulation run results in permanent files. Selection of the first option will cause the time dependent values of the circuit variables

Table 5.1: Process Subroutines and their Functions

Subroutine	Function
FTD	This simulates a Fixed Time Delay due to conveyors.
VTD	This simulates a Variable Time Delay due to plug flow.
MILL	This simulates a grinding mill in an ore processing system.
SUMP	This simulates a sump in an industrial circuit.
PUMP	This simulates a pump in an industrial circuit.
CYCLON	This simulates the Plitt model of a hydrocyclone.
WATBLD	This simulates a special case of the stream blender in which two water streams are blended.
BLEND	This simulates a stream blender handling up to four streams.
RATIO	This calculates the mass flow rate of a water addition stream such that pre-determined slurry densities are maintained.
VOLCNT	This adjusts the sump water flow rate to maintain constant volumetric flow in the hydrocyclone feed stream.

to be recorded as the simulator executes and the second, if selected, will contain a tabular record of the grinding mill breakage and selection functions and a complete synopsis of the micro and macro properties of the important streams in the circuit. For this option, two subsidiary subroutines MILOUT for the grinding mill breakage and selection functions, and STROUT for the stream synopsis are called by the OUT subroutine. Furthermore, according to individual cases, the synopsis can be made to record only the details of even numbered or odd numbered streams. A third output file can be defined to dump the entire simulation steady state data to a permanent data file which could be used to rerun the simulator using this data as the starting point. The use of the OPEN command in the output subroutine allows the user to output data to previously established files, with the understanding that any data already present in these files will be lost. Another option is to declare a file name as NEW, and the data will be dumped to a new file that was not in existence before the simulation. A word of caution here is to keep a good record of what files exist on which

disk/drive or account because declaring an existing file as NEW or a non-existing file as OLD will result in a fatal execution error that usually requires rerunning of the simulator. Once control is returned to the driver from the OUT subroutine the simulation is complete.

5.3.4 The DYFLO Subroutine Library

Although the DYFLO utilities have been documented in detail in Appendix B, it is felt that a general introduction needs to be given to indicate the role of DYFLO routines in the overall structure of the simulator. As mentioned earlier, the DYFLO is a set of subroutines designed by Franks (1982)to provide a systematic framework for the development of simulation programs. Of all the subroutines listed in Appendix B, INTI, INTG, PRNTF and CONTR2 are used in this simulator. INTI and INTG control the integration operation. A call is made to INTI at each integration interval, which requires the passing of three arguments, *viz.* the independent variable, the integration interval and the flag indicating the order of integration. The stiff system of differential equations encountered in the MILL subroutine necessitates the use of first order integration. As such, INTI just increments the time variable as the simulation proceeds but for higher orders of integration, INTI allows multiple passes for a single integration interval. The INTG subroutine performs the integration of the dependent variables. It can perform first, second and fourth order integration based on the value of the flag supplied by INTI. The INTG subroutine is called from those unit models in the CONFIG subroutine which require a solution to a first order differential equation. Another DYFLO subroutine used is the PRNTF subroutine which writes user specified time dependent variables at specified time intervals to a permanent file and also tests for the end of the simulation. According to personal requirements the output variables can be changed by making suitable alterations in

the code. In its present form, due to page size limitations, the PRNTF prints only up to a maximum of ten variables.

As referred to earlier, CONTR2 is a subroutine used to implement the proportional plus integral (PI) control. The user specifies the appropriate gains (K_c), integral time constant (τ_i) and the set-points for the output variables. The first part of the CONTR2 subroutine converts the proportional gain to proportional band as $K_c = 100/PB$ and the integral time constant to repeats per minute as $\tau_i = 1/RPT$. To avoid confusion, the user is prompted for the proportional gain and integral time constants only and the requisite conversions are performed by the simulator. A more detailed discussion along with program listings are provided in Appendix B.

5.4 An Illustrative Example to Show the Flexibility of the Simulator

To appreciate the operation of the dynamic behaviour of the simulator, the circuit shown in Figure. 3.1 will be considered. Besides the standard sump, pump and a bank of hydrocyclones, it has two grinding mills and the associated transportation equipment. To begin with, the required information about the details of the circuit have must be supplied to the simulator. This can be done interactively by choosing the third option from the first menu on the screen. Once all the necessary circuit parameters has been provided, the simulator then prompts the user to define the run time parameters. It is recommended that until steady state values of the operating variables have been generated by the simulator, the simulator should be run without disturbances and in open loop mode. This means that initially the user needs to change only the fifth item in the on-screen menu showing the default initialization values. Off course, subsequently, it might be necessary to change the simulation

run time and integration step size values but the default values are suitable initial specifications.

The next step in involves specifying the circuit configuration to the simulator ready to set up the calls to various unit models in the correct order in the CONFIG subroutine. Referring to Figure. 3.1, the CONFIG subroutine would be structured as shown schematically by way of a flow sheet in Figure. 5.4. Briefly, this is how the CONFIG subroutine is established for the circuit shown in Figure. 3.1. The fixed speed conveyor is simulated by the FTD subroutine. Though not present as a physical unit, the BLEND subroutine is used as a front end to avoid excessive passing of arguments to the MILL subroutine. The RATIO subroutine is employed to calculate the amount of water required to keep the slurry density of the material flowing into the mill constant. The box consisting of streams 5 and 6 denotes the rod mill. As mentioned in Chapter 3, the mill has been modelled as having a mixer in series with a time delay to account for the plug flow characteristics. Again a BLEND subroutine is used to act as a summer for stream 6 (from the grinding mill), stream 7 (the water flow to the sump) and stream 14 (the ball mill product). The sump and pump in the circuit is simulated by the SUMP and PUMP subroutines and the set of hydrocyclones are simulated by the CYCLONE subroutine. As can be seen, a combination of a mixer with a time delay in series is used to model the ball mill. This completes the CONFIG subroutine for the circuit shown in Figure. 3.1.

As is obvious, any circuit can be thus, very conveniently set up in the CONFIG subroutine to describe the actual process. However, before trying to go through this exercise, it is advised that the user look at an existing CONFIG file to understand the arguments that need to be provided for each subroutine. Care should also be taken while numbering the streams as unwarranted changes to these numbers, since

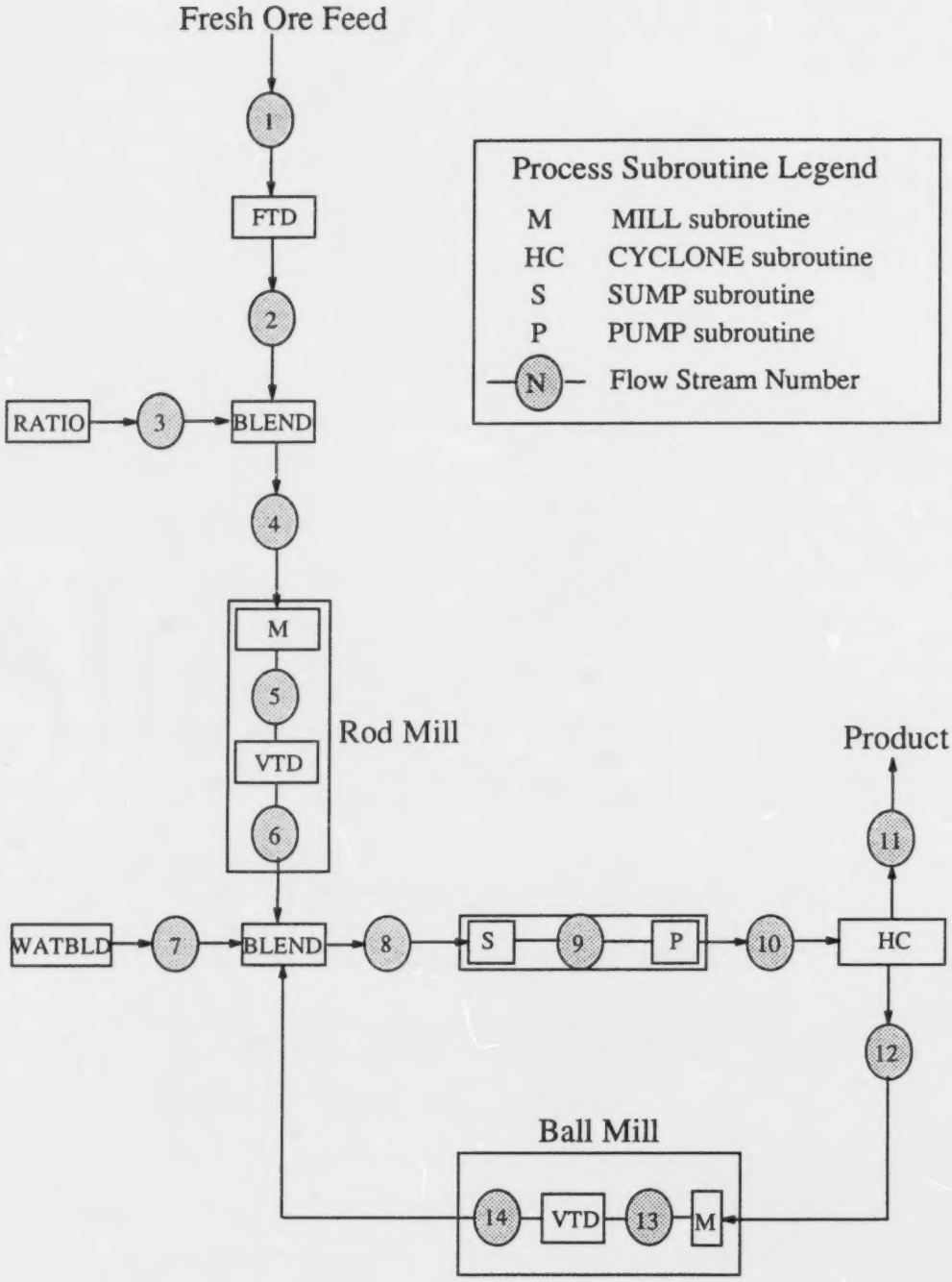

Figure 5.4: Illustration of the CONFIG Structure for Figure 3.1

they are in the COMMON BLOCK, can cause fatal errors in the program. As a final note it should be mentioned that setting up the CONFIG file, which must be done independently, and loading the required data must be the first steps to simulating any circuit. Once these are established, the CONFIG subroutine should be in the code and the entire program recompiled. At this stage simulator is ready to be used to simulate the circuit of interest.

Chapter 6

Simulation of the Hemlo Grinding Circuit

6.1 Introduction

With the availabilaty of a grinding circuit simulator such as developed in this work the operation various different grinding circuit flow sheets operating under different control schemes can be studied. This chapter will describe the results of a simulation study on an existing circuit at the Hemlo Gold Mines Inc.

The Hemlo Gold Mines Inc. operate the Golden Giant Mine, Hemlo, Ontario. This is an underground gold mine with 3000 *tonnes/day* capacity and ore averages of 0.39 *oz./tonne*. A recovery of about 95% is achieved through a combined complex process which includes crushing, grinding, cyanidation and carbon in pulp processes Larsen and Tessier (1986). The following sections give details of the Hemlo grinding circuit parameters that are relevant to the simulation. To begin with, particulars about the equipment used and the layout is discussed. Next, matching of simulator structure with the actual circuit is described. Section 6.3 presents the open loop responses to various disturbances. Some of these disturbances are common in the plant while others are used to assist in controller design.

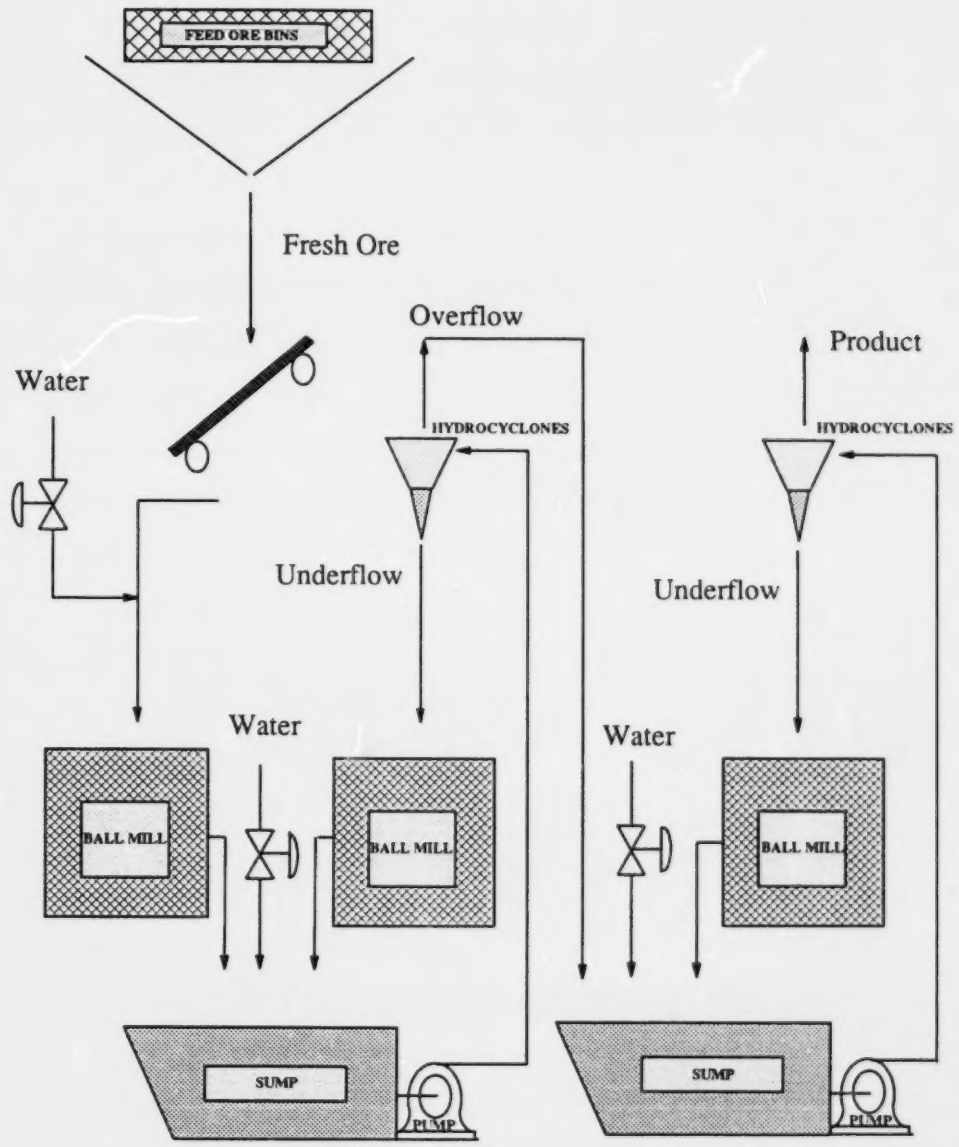

Schematic Representation of the Hemlo Grinding Circuit

Figure 6.1: Schematic Representation of the Hemlo Grinding Circuit

6.2 The Hemlo Circuit

The flow sheet of the Hemlo grinding circuit is shown in Figure. 6.1. Fresh ore from the feed ore bins is fed to a variable speed conveyor where it is weighed. Depending on the weight, a calculated amount of water is added to the solids and the slurry of constant pulp density flows into the first ball mill. The product overflows from the first ball mill to the sump. Water is added to the slurry at this stage and the mixture is pumped to the first set of hydrocyclones. The underflow from these hydrocyclones is fed to the second ball mill. The ground product from the second ball mill overflows into the first sump. The overflow from the first set of hydrocyclones is fed to the second sump where more water is added to the slurry before pumping it to the second set of hydrocyclones. The underflow from the second set of hydrocyclones is again gravity fed to the third ball mill. The product from this mill is returned to the second sump thus completing the closed circuit. The overflow product from the second set of hydrocyclones flows from the vortex finder (VF) and through a particle size monitor (PSM) exits as the final product.

Since a PSM is susceptible to frequent breakdowns and hence not a very reliable instrument to monitor the overflow particle size distribution, it has been proposed by Kawatra *et al.*(1985)that overflow size be inferred. These workers developed an inferential model that uses the pulp feed density to the hydrocyclones to infer the particle size distribution in the overflow stream.

Before considering the physical parameters, it is appropriate to establish the necessary unit process models to be combined in the CONFIG subroutine to represent the circuit. This will also provide a direct summary of the parameters that are required. of parameters one is looking for. As described in the example given in the previous chapter, each of the pieces of equipment can be adequately represented either

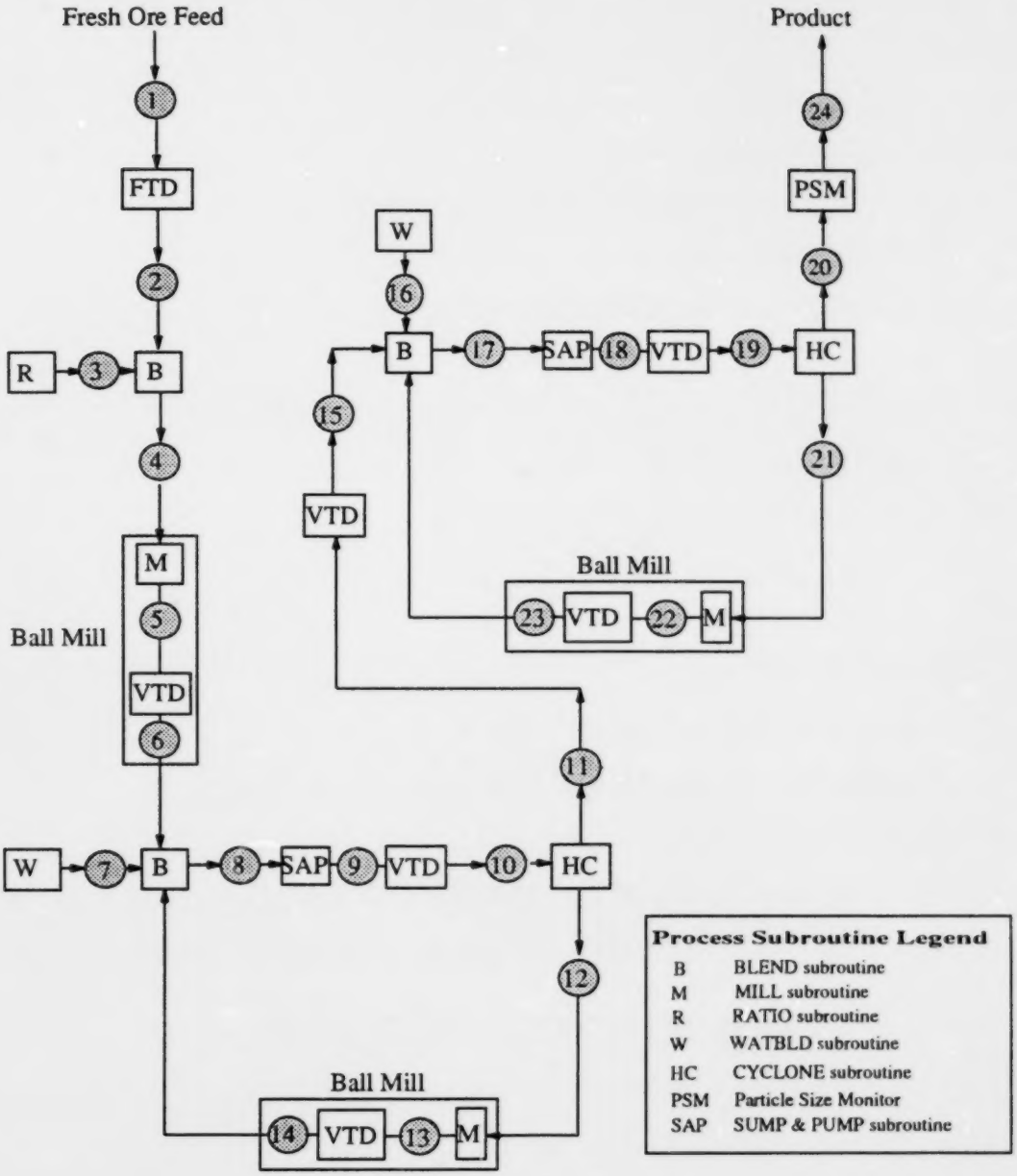

Figure 6.2: Schematic Representation of the CONFIG Subroutine for the Hemlo Grinding Circuit

as a unit operation or as a time delay. Figure. 6.2 shows a schematic illustration of the simulation models characterizing the Hemlo grinding circuit. Flow stream numbers shown correspond to the ones used in the simulator. The fresh ore feed enters as stream 1 through the feed ore bins (FOB) where it is delayed by a fixed time delay (FTD) representing the fixed speed conveyor in Figure. 6.1. Stream 2 from the FTD is blended with the ball mill feed water (stream 3) in the BLEND subroutine before being fed to the ball mill (stream 4). As described earlier, the milling operation is represented by a call to the mill subroutine (M) and a call to the variable time delay (VTD) subroutine. The output stream *i.e.* stream 6 is blended with the sump water stream (stream 7) and the product of the second ball mill (stream 14). The sump and pump subroutine (SAP) is then called and the pump outflow stream is fed to the hydrocyclone (CLASS) routine through a variable time delay due to the feed pipeline. The underflow from the first set of hydrocyclones, stream 12, is then fed to the second ball mill which means that the mill subroutine is called in series with the VTD subroutine. The product stream 14 is sent to the blender as described above. The overflow from the CLASS subrotuine, stream 11 is delayed by the VTD and fed to another BLEND which mixes the water feed to the second sump (stream 16) and the product from the third ball mill. The product stream from the blender is then fed to the sump and pump (SAP) subroutine with the output stream being the feed to the second set of hydrocyclones. The oversize stream is then passed to the third ball mill while the undersize is the product stream.

In order to use the simulator to study the behaviour of Hemlo circuit, actual operating data are used to define the necessary parameters for the models. The fixed time delay due to the fine ore conveyors is determined to be 0.19 minutes. Each grinding mill is modelled using Equation. 3.10. The first parameter that should be

Table 6.1: First Column of Breakage Matrix for the Grinding Mills

Lower Bound on Particle Size (microns)	Ball Mill Number 1	Ball Mill Number 2	Ball Mill Number 3
3327	0.000	0.000	0.000
2362	0.270	0.270	0.270
1651	0.189	0.189	0.189
1168	0.134	0.134	0.134
833	0.096	0.096	0.096
589	0.070	0.070	0.070
417	0.052	0.052	0.052
295	0.039	0.039	0.039
208	0.030	0.030	0.030
147	0.023	0.023	0.023
104	0.018	0.018	0.018
74	0.014	0.014	0.014
52	0.011	0.011	0.011
37	0.053	0.053	0.053

established is the number of screen sizes sizes n to be used to define the particle size distribution. Although it is true that the larger the number n, the better the model, a practical limit needs to be set due to computational considerations. For this work, 14 particle sizes have been chosen. As explained in Chapter 3, for the purpose of simulating a hardness disturbance, it is more convenient to assume the ore to be made up of two components. This assumption has to be kept in mind while establishing the breakage matrix and selection functions. The breakage function b_{ij} given by Equation. 3.13 turns out to be the same for both components in all the three mills. For $n = 14$, the first column of breakage matrix for each mill is calculated and summarized in Table 6.1. Similarly, the selection functions are calculated and summarized in Table 6.2. The initial steady state feed and product particle size

Table 6.2: Selection Function Associated with the Hemlo Circuit Grinding Mills

Lower Bound on Particle Size (microns)	**Ball Mill Number 1**		**Ball Mill Number 2**		**Ball Mill Number 3**	
	1^{st} Comp. (min^{-1})	2^{nd} Comp. (min^{-1})	1^{st} Comp. (min^{-1})	2^{nd} Comp. (min^{-1})	1^{st} Comp. (min^{-1})	2^{nd} Comp. (min^{-1})
3327	4.969	2.4845	38.348	19.1740	15.397	7.6985
2362	3.741	1.8705	38.348	19.1740	9.755	4.8755
1651	2.683	1.3415	17.996	8.9980	6.231	3.1150
1168	1.832	0.9160	8.666	4.3330	4.012	2.0060
833	1.191	0.5955	4.282	2.1410	2.605	1.3025
589	0.738	0.3690	2.171	1.0855	1.705	0.8525
417	0.435	0.2175	1.130	0.5650	1.125	0.5625
295	0.244	0.1220	0.603	0.3015	0.749	0.3745
208	0.131	0.0655	0.330	0.1650	0.596	0.2980
147	0.067	0.0335	0.186	0.0930	0.361	0.1805
104	0.032	0.0160	0.107	0.0535	0.212	0.1060
74	0.015	0.0075	0.063	0.0315	0.120	0.0600
52	0.007	0.0037	0.039	0.0195	0.067	0.0335
37	0.000	0.0000	0.000	0.0000	0.000	0.0000

distribution for the three ball mills are shown in Table 6.3 in terms of weight percent retained in the size classification.

The residence time of each mill is dependent on the inlet volumetric flow rate Q. As well, in order to determine the residence time, the mill volumetric holdup V is required. For the ball mills in the Hemlo circuit, the volumetric holdup of the first ball mill (after excluding the volume due to the balls) is 8.50 m^3 and that of the other two is 5.20 m^3 each. Based on the initial steady state volumetric flow rates of 130 m^3/h to the first ball, 256.87 m^3/h to the second ball mill and 130.88 m^3/h to the third ball mill, the residence times are respectively, 3.92 minutes, 1.21 minutes, and 2.38 minutes. The variable time delay elements in each mill are arbitrarily assigned nominal values of one minute. The number of blocks used in the variable time delay model for the first ball mill is 8 while those for the other two are 6 each.

The physical dimensions along with model constants for each hydrocyclone set are listed in Table 6.4. The steady state inlet and outlet particle size distribution for

Table 6.3: Steady State Particle Size Frequency Distribution for the Hemlo Circuit Grinding Mills' Feed and Product Streams

Lower Bound on Particle Size (microns)	**Ball Mill Number 1**		**Ball Mill Number 2**		**Ball Mill Number 3**	
	Feed (wt%)	Product (wt%)	Feed (wt%)	Product (wt%)	Feed (wt%)	Product (wt%)
3327	54.49	1.96	1.006	0.016	0.00	0.000
2362	4.87	0.91	0.474	0.012	0.00	0.000
1651	4.14	1.24	0.665	0.035	0.00	0.000
1168	3.52	1.75	0.989	0.104	0.00	0.000
833	2.93	2.50	1.563	0.298	0.00	0.000
589	2.94	3.68	2.718	0.856	0.00	0.000
417	3.48	5.49	5.155	2.400	0.071	0.002
295	3.00	7.33	9.362	5.94	0.853	0.290
208	3.88	9.61	15.466	12.21	4.907	1.990
147	4.80	11.42	18.595	17.41	14.602	8.01
104	4.13	11.04	14.826	16.27	20.550	14.98
74	4.10	10.20	9.792	12.32	18.502	16.90
52	2.65	7.70	5.406	7.95	11.122	13.19
37	5.07	25.18	13.984	24.17	29.293	4.62

the hydrocyclone sets are determined in a similar fashion to that used to determine this information for the mills. The simulator was started using the minimum data generated with the help of the interactive routine and run without disturbance till the mass flows of outlet streams matched with mass flows of the inlet stream. Table 6.5 summarizes the results thus obtained. It can be seen, in keeping with the circuit layout, that the particle size distribution of the underflow stream from the first set of hydrocyclones matches that of the feed to the second ball mill. This is also the case with the size distribution of the second set of hydrocyclone underflow and the feed to the third ball mill. The size specification of the product in this work is based on the percentage of solid material in the overflow stream that passes through the 200

Table 6.4: Physical Dimensions and Model Constants of the Hemlo Circuit Hydrocyclone Sets

Dimension	**Hydrocyclone Set # 1** (cm)	**Hydrocyclone Set # 2** (cm)
Hydrocyclone dia (D_c)	38.10	25.4
Inlet dia (D_i)	9.51	6.28
Vortex finder dia (D_o)	15.24	10.8
Apex (Spigot) dia (D_u)	7.62	5.08
Free vortex ht.(h)	94.3	70.5
Model Constants		
K_1	44.02	52.92
K_2	1.088	1.037
K_3	3.78	2.482
K_4	0.9761	2.582

mesh screen. Using this criterion, from Table 6.5 it can be seen that about 90 mass percent of the product stream passes 200 mesh at steady state.

Finally it should be mentioned that the steady state flow rates for the simulation were taken as 130 $tonnes/h$ for the fresh ore feed, 370 $tonnes/h$ water flow rate to the first sump and 31 $tonnes/h$ water flow rate to the second sump. The slurry to the first mill had a 70% by weight solids concentration.

6.3 Open Loop Simulations

The first use of the simulator in selecting a control strategy for the Hemlo circuit is the using it to simulate the open loop response of the output variables for different changes in the process inputs. The three major input streams, *i.e.* the fresh ore feed and water feeds to the sumps are obvious choices for disturbances. The water added to the slurry before the first ball mill is not considered here since it is ratioed to the incoming fresh feed ore. Other probable sources of disturbances include feed ore hardness and

Table 6.5: Steady State Particle Size Frequency Distribution for the Hemlo Circuit Hydrocyclones' Feed and Product Streams

Upper Bound on Particle Size (microns)	Hydrocyclone Set Number 1			Hydrocyclone Set Number 2		
	Feed (wt%)	Overflow (wt%)	Underflow (wt%)	Feed (wt%)	Overflow (wt%)	Underflow (wt%)
3327	0.668	0.000	1.006	0.000	0.000	0.000
2362	0.315	0.000	0.474	0.000	0.000	0.000
1651	0.442	0.000	0.665	0.000	0.000	0.000
1168	0.657	0.000	0.989	0.000	0.000	0.000
833	1.037	0.000	1.563	0.000	0.000	0.000
589	1.805	0.000	2.718	0.000	0.000	0.000
417	3.441	0.053	5.155	0.036	0.000	0.071
295	6.407	0.569	9.362	0.431	0.060	0.853
208	11.336	3.176	15.466	2.580	0.237	4.907
147	15.397	9.079	18.595	8.545	2.447	14.602
104	14.513	13.895	14.826	14.439	8.286	20.550
74	11.606	15.190	9.792	16.048	14.030	18.502
52	7.864	12.722	5.406	12.958	14.807	11.122
37	24.512	45.316	13.984	44.963	60.133	29.393

feed ore size distribution change. These disturbances can not be measured on-line and the only way to detect such disturbances is by the effect they have on the output variables. As discussed in Chapter 3, besides these process disturbances, other upsets would relate to hardware (machinery) malfunction but these types of changes are not considered in this work.

The menu driven DISTRB subroutine described earlier in Chapter 5 provides a choice for four types of disturbances :

1. Change in feed stream components (simulates a change in hardness)

2. Change in feed stream ore flow rate

3. Change in feed stream size distribution

4. Change in water flow rate to the sumps

Although individual users can append other options, it is felt that given the scope of the simulator, the above choices are reasonable. The first option which is employed to simulate hardness changes in the ore has two suboptions. While dealing with hardness changes, it must be kept in mind that hardness change could either be accompanied by a change in the density of the ore, as the case maybe if the ore is from a different source, or a hardness change could occur with no change in density. Although the magnitude of the change in density is in most cases is quite small and hence insignificant, it is felt that one should be able to differentiate the effect of each disturbance on other circuit variables and therefore need to be modelled separately. This becomes all the more crucial when one realizes that the effects of these two parameters have on the controlled variable *i.e.* the overflow size from the second set of hydrocyclones. Whereas an increase in hardness results in a coarser slurry reporting to the underflow, a change in density affects the separation characteristics of the hydrocyclone. Often, the changes occur in such a way that the effects end up cancelling each other.

The third option *i.e.* the feed stream size distribution has negligible effect on circuit performance (McDougall, 1987; Neale, 1987) and consequently, has not been considered in this work. However, it has been included for reasons of completeness. The other three options have been examined in detail and the results are presented in the following pages.

6.3.1 Increase in the Fresh Ore Feed Rate (FOF)

First of all it must be mentioned that fresh ore feed rate in itself is not a disturbance, but rather a manipulated variable. Consequently, a knowledge of how the other

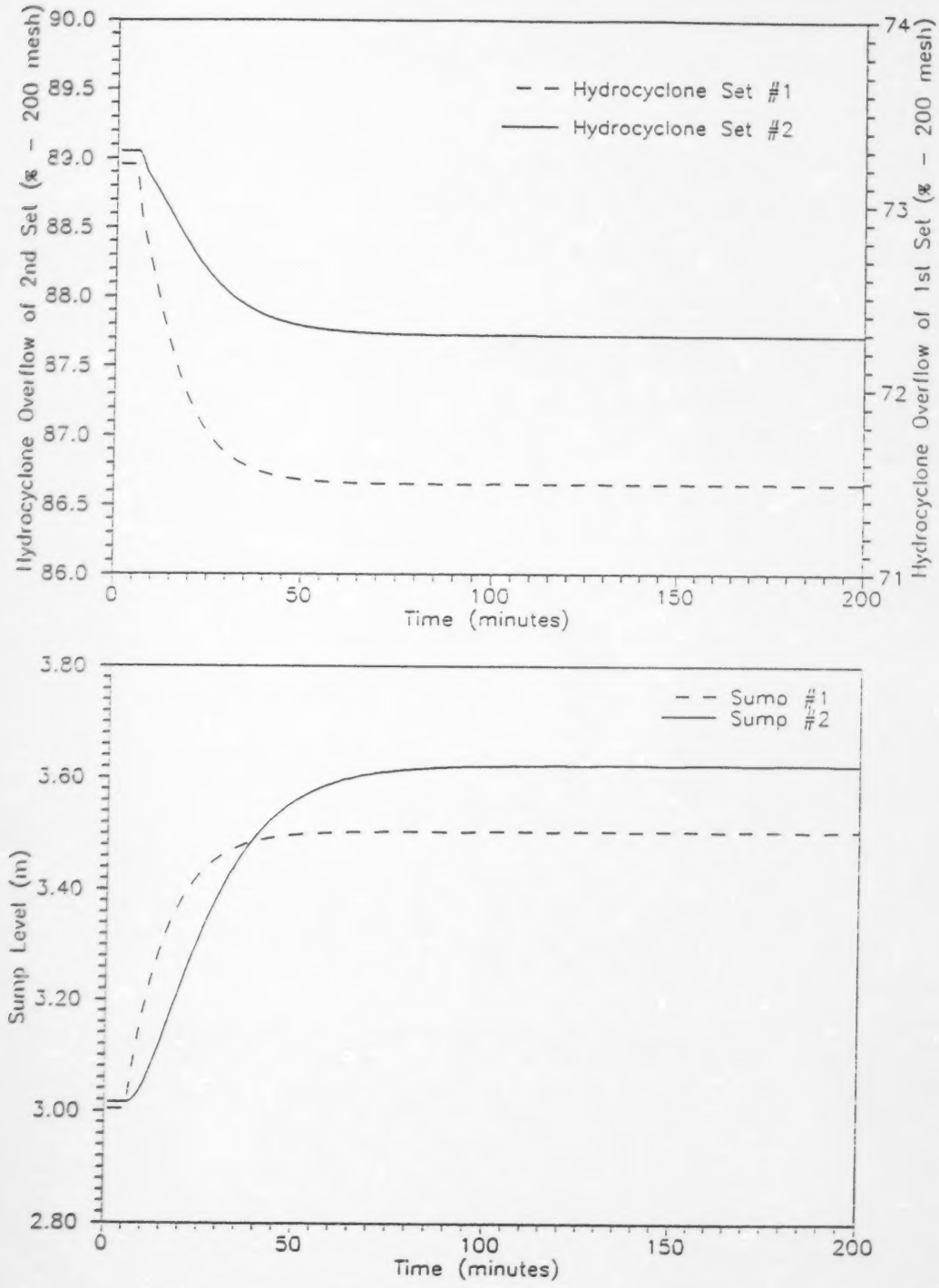

Figure 6.3: Open Loop Response of the Hydrocyclone Overflows and Sump Levels to a 10% Step Increase in the Feed Ore Flow Rate

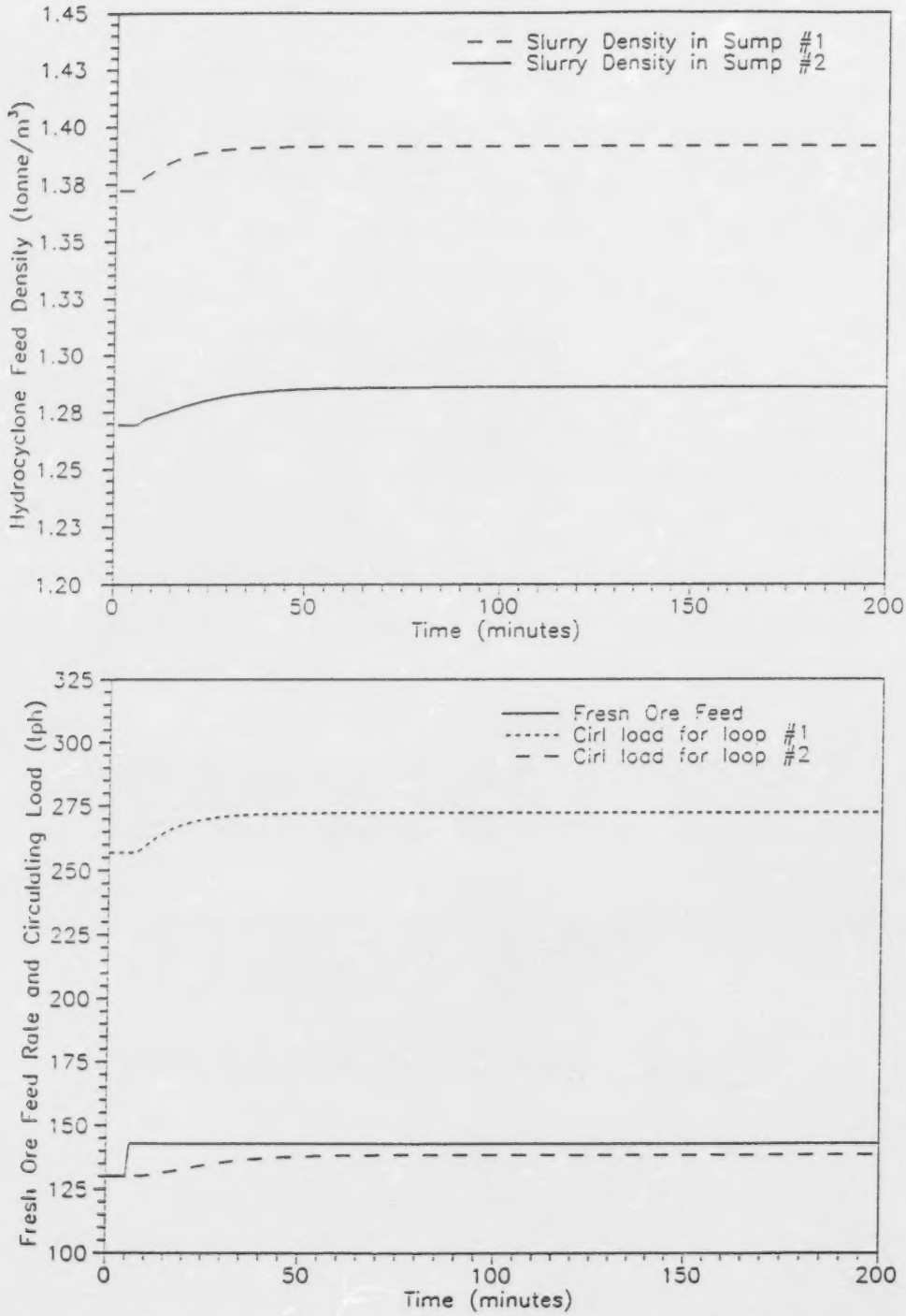

Figure 6.4: Open Loop Response of the Slurry Densities and Circulating Loads to a 10% Step Increase in the Feed Ore Flow Rate

variables behave to a change in the feed rate is essential in designing a good control system. Figures. 6.3 and 6.4 show the circuit response to a 10% step increase in the fresh ore feed rate introduced 5 minutes from the start of the simulation. It should be noted that the magnitude of the change used in generating the responses shown in Figures. 6.3 and 6.4 was chosen so that the steady state values of the output variables was attained in a reasonable length of time (about 200 minutes of simulation time). Furthermore, larger step changes in the ore rate would likely result in a sump overflow condition.

The effect of increasing the fresh ore feed rate on the overflow stream of the two hydrocyclone sets is as expected given the dynamics of the circuit. As can be seen, the overflow of the hydrocyclone set #1 responds quicker to the change than hydrocyclone set #2. However, both responses show that the percent less than 200 mesh decreases when there is an increase in the feed ore flow rate. This behaviour is appropriate when one realizes that that the 'grind' from the mills will be poorer due to the increase in feed rate of the ore. Given the fixed holdup volumes of the mills, an increase in ore rate would imply a decrease in the residence time which would in turn, mean that the slurry is not ground as well as before the change. As a consequence of this, the underflow streams increase giving rise to higher circulating loads. This coupled with the increase in the feed rates cause a rise in the sump levels until new steady states are achieved. The increase in circulating load also results in an increase in the hydrocyclone feed densities at the two sumps. The net effect of increasing the fresh feed rate by 10% is a drop in the product stream size distribution from the steady state 89% -200 mesh to 87.7% -200 mesh. The transient responses of the output variable exhibit typical first order plus delay response.

The response of the system to a 10% decrease in the fresh ore flow rate is

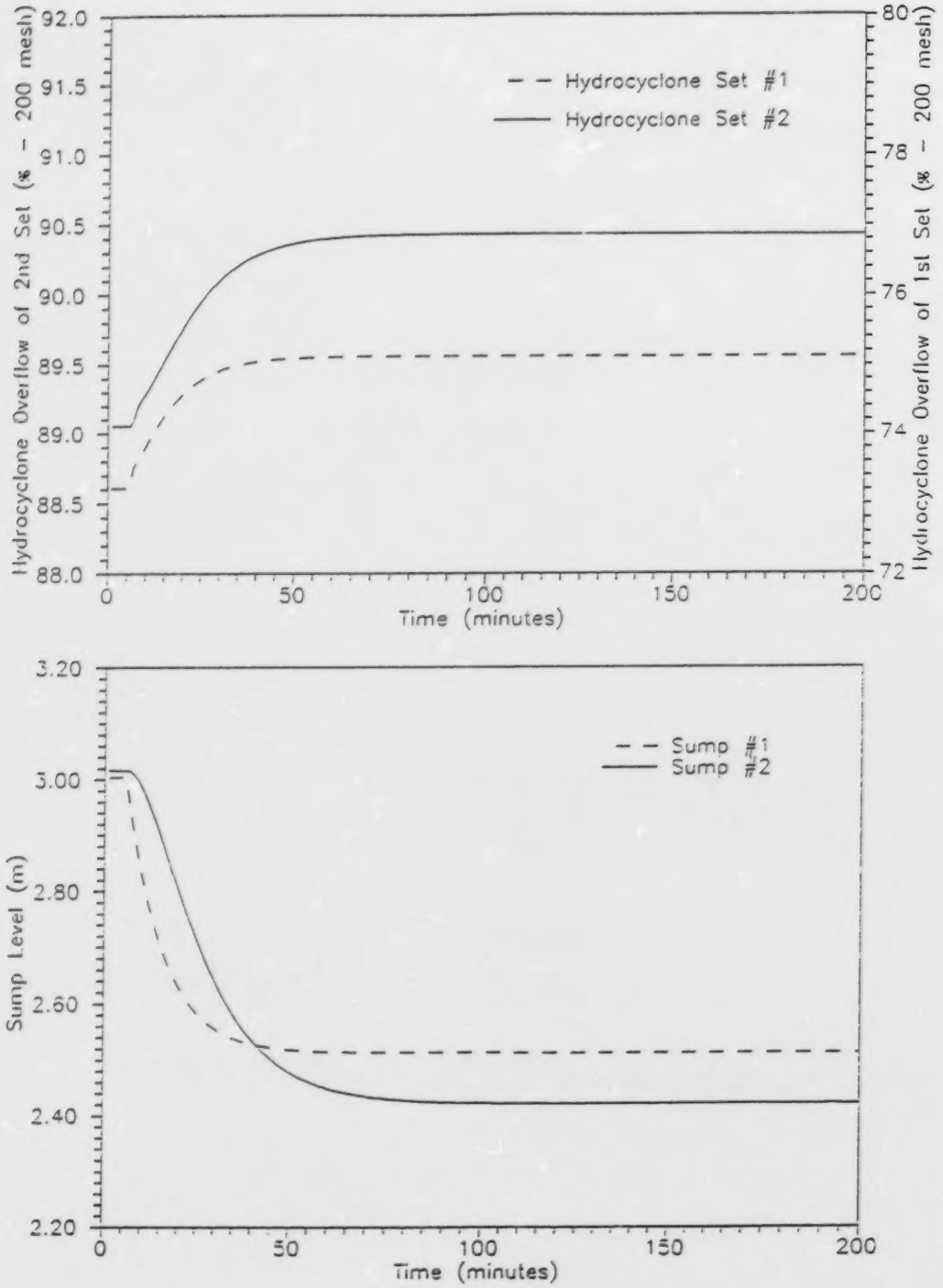

Figure 6.5: Open Loop Response of the Hydrocyclone Overflows and Sump Levels to a 10% Step Decrease in the Feed Ore Flow Rate

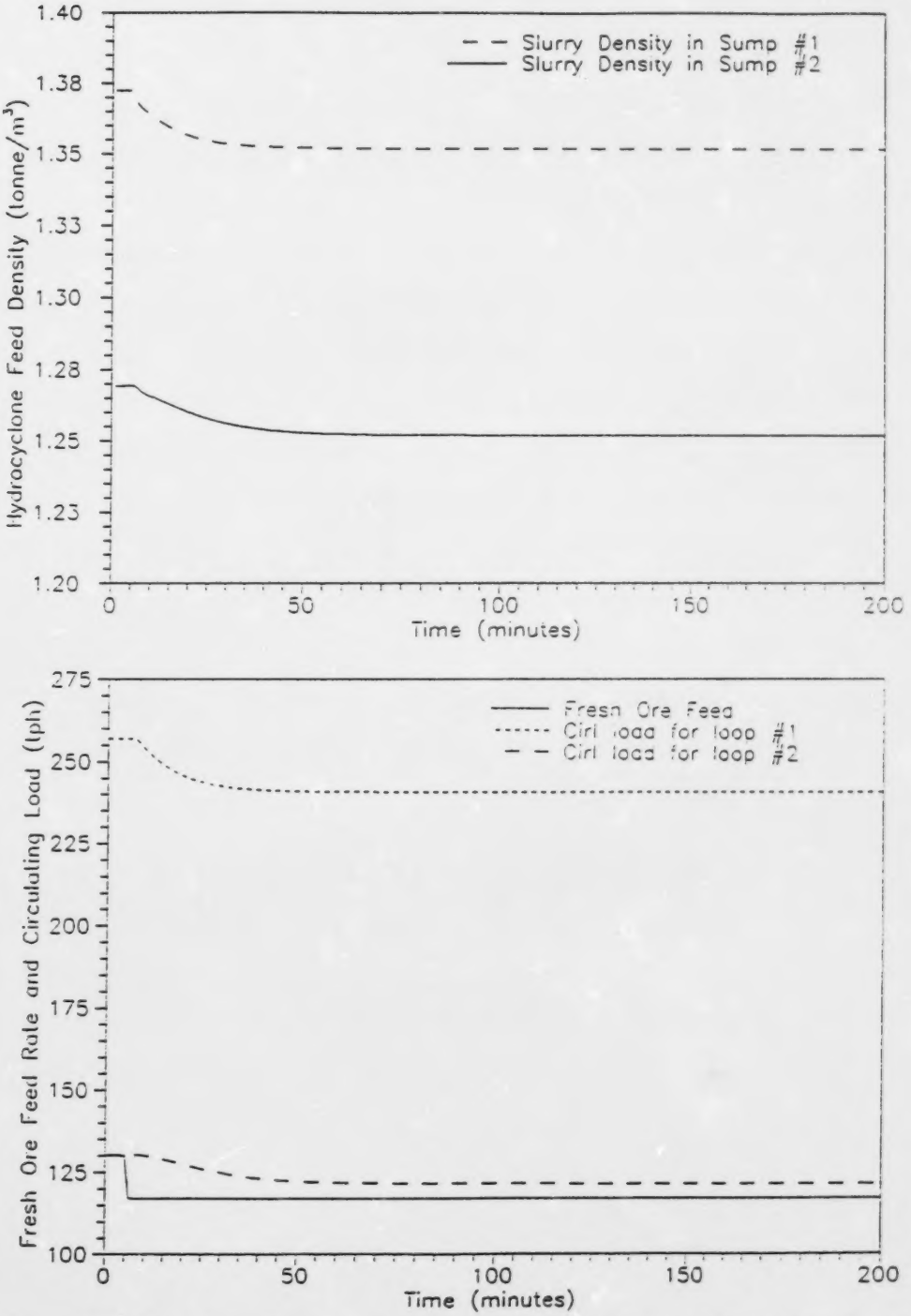

Figure 6.6: Open Loop Response of the Slurry Densities and Circulating Loads to a 10% Step Decrease in the Feed Ore Flow Rate

exactly opposite to that for an increase, as shown in Figures. 6.5 and 6.6 In this case there is an increase in the percent less than 200 mesh in the overflow streams of the two hydrocyclone sets after the necessary time delays. This increase is obviously due to more grinding of the slurry by the mills resulting from an increased residence time. Consequently, the circulating loads decrease which makes the hydrocyclone feed densities decrease. As well ,the sump levels reduce due to the combination of reduced feed rate and smaller circulating loads. The net result of decreasing the ore rate by 10% is a rise in the product stream size distribution from the steady state 89% -200 mesh to 90.4% -200 mesh. The process reaction curves, as in the previous case, exhibit a first order plus time delay response.

6.3.2 Increase in the Sump Water Flow Rate (SWF)

The flow rate of water to the two sumps can be manipulated to adjust other circuit parameters, or under certain conditions, can act as a disturbance to the circuit. In other words, one can consider the water flow stream as being made up of two separate streams. One stream behaving as the manipulated stream while the other acts as the extraneous water which causes the disturbance. The simulator handles this scenario by blending the two streams using the WATBLD subroutine and then monitoring the blended stream as it flows into the sump. Hence, this open loop simulation serves two purposes since it indicates the effect of extraneous sump water on circuit performance as well as produces data required for the process reaction curves necessary for selection of controller parameters. Figures. 6.7 and 6.8 show the circuit response to a 3% increase in the water flow rate to the first sump. Before proceeding further, it must be mentioned that although there are two sumps in the circuit and hence two options for selecting the sump water addition to evaluate open loop response, the first sump was chosen since it was more likely affect the whole circuit than if the disturbance had

been the water addition to sump #2. Disturbance in the water to the second sump will bring about a corresponding change only in the third ball mill feeds while the first and second ball mill feeds will remain unaffected. However, it is also true that a disturbance in the water flow to the second sump would produce a more immediate and profound effect on the product size than if the disturbance is to the first sump. Still, to refrain from overstating the sump water disturbance effects, only the case of changes in water feed to the first sump have been investigated here.

As the sump is modelled as a perfect mixer and as it is assumed that there are no dynamics associated with the hydrocyclone, there is almost an immediate response in the hydrocyclone set #1 feed density and overflow stream size distribution. The same effect is apparent in the hydrocyclone set #2 after the associated delay. While the sump levels increase to reach a new steady state value, the percentage overflow less than -200 mesh initially increases and then drops back to a value in between the initial and the maximum values. The exact opposite response can be observed in the case of hydrocyclone feed densities with the slurry densities initially decreasing and then imperceptibly increasing to its original value. This phenomenon can be explained as follows. Due to the step increase in the water flow rate to sump #1, the hydrocyclone feed slurry density decreases which causes a decrease in the d_{50} size and increases the fineness of the overflow stream from hydrocyclone set #1. Reduction of the d_{50} size results in an increased routing of material to the underflow corresponding to an increase in the circulating load. There is a little delay due to the mills before this effect translates itself on the slurry to the sump as a slight increase in the hydrocyclone feed density. Increase in the hydrocyclone feed density means a resultant increase in the d_{50} size and a coarsening of the overflow stream. The same phenomenon happens in the other loop after the time delay. The hydrocyclone

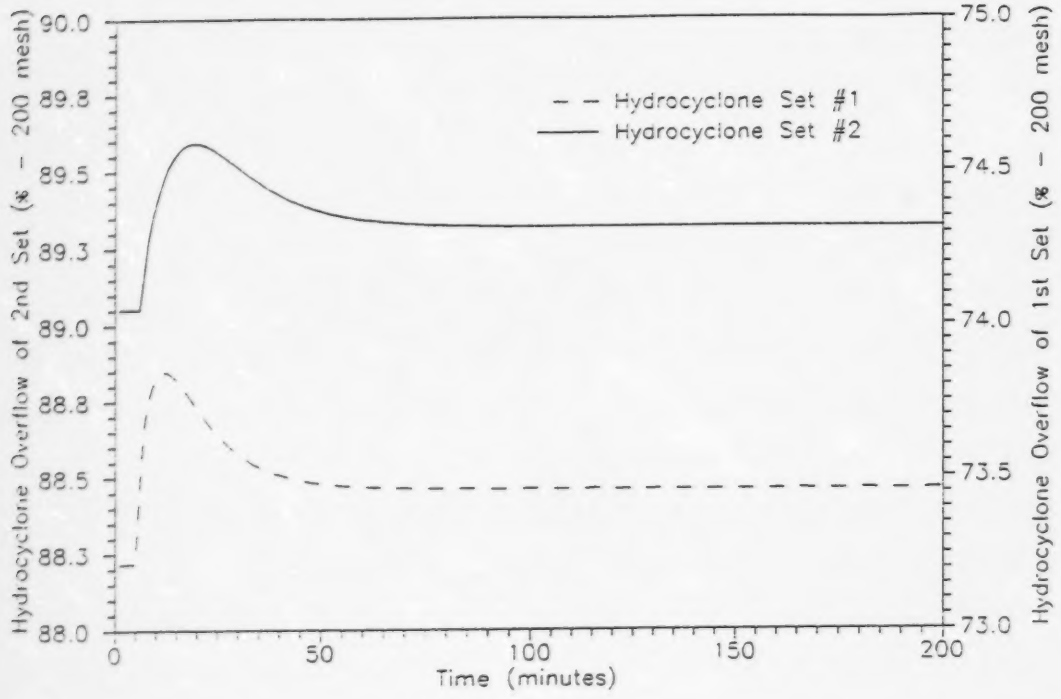

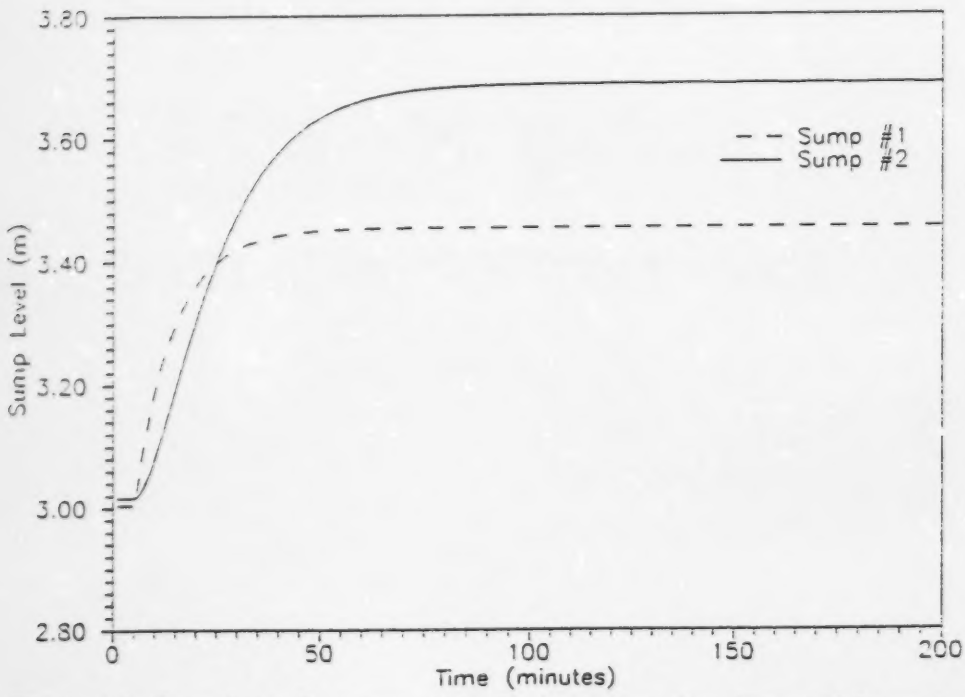

Figure 6.7: Open Loop Response of the Hydrocyclone Overflows and Sump Levels to a 3% Step Increase in the Water Flow Rate to Sump #1

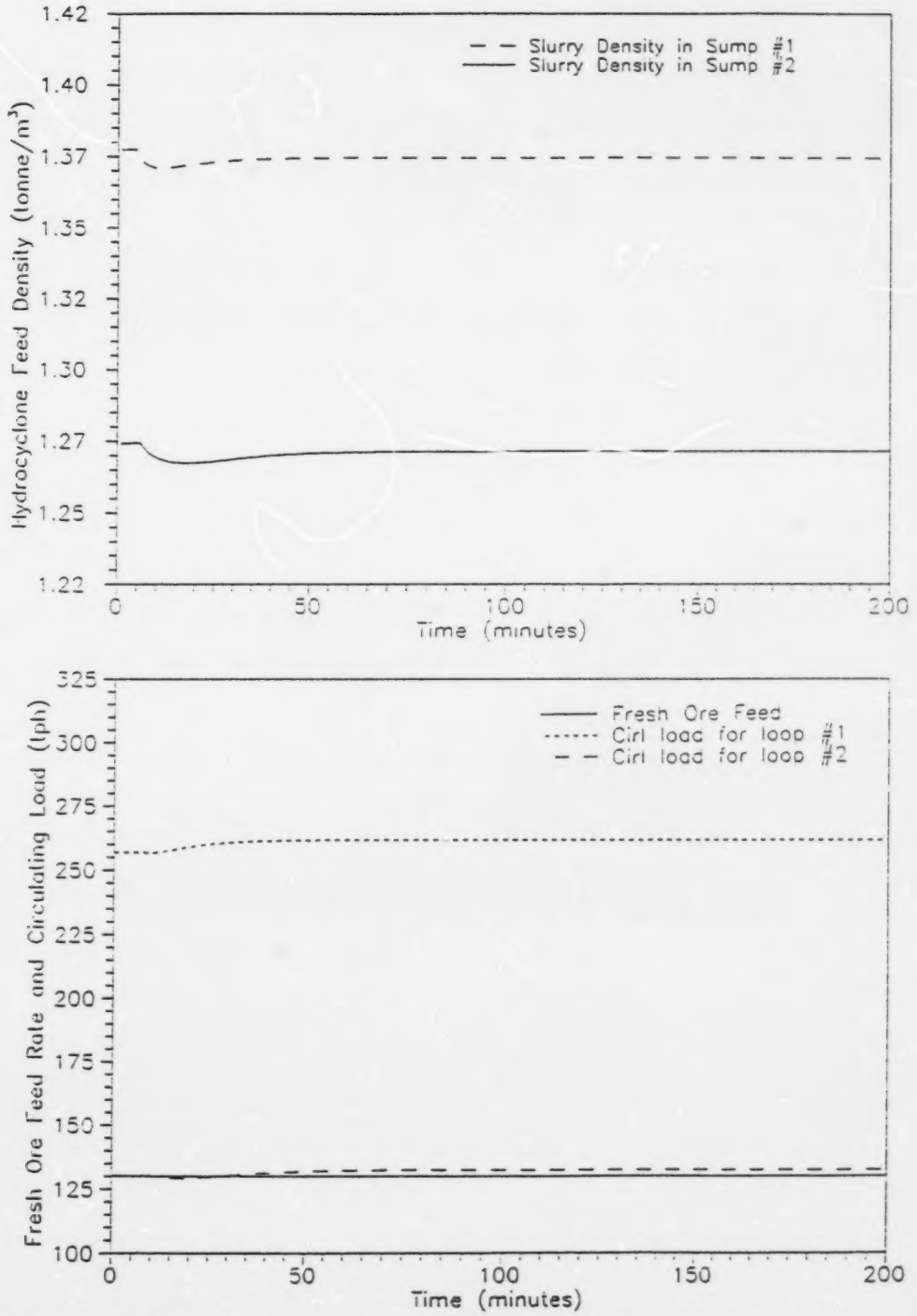

Figure 6.8: Open Loop Response of the Slurry Densities and Circulating Loads to a 3% Step Increase in the Water Flow Rate to Sump #1

feed density has a more pronounced effect on the d_{50} size than does the volumetric flow rate (Plitt, 1976), but in this case both effects combine to move the response in the same direction. After about 75 minutes the circuit reaches a new steady state with an increase in circulating loads, higher sump levels, reduced feed densities and finer product streams than before the change is imposed. The product stream size increases from 89% -200 mesh to 89.4% -200 mesh which is not a significant change. However there may be a loss of efficiency due to overgrinding of the ore. One can observe second order dynamics in the output trajectories due to opposing effects of increasing circulating loads and decreasing hydrocyclone feed densities.

The results of a 3% decrease in the water feed to the first sump are shown in Figures. 6.9 and 6.10. As expected, these responses are symetrically opposite to the responses due to a 3% increase in the water flow rate. Suffice to say that since the simulator produces an 'opposite' response to an 'opposite' change, the circuit response to water feed flow rate to the first sump exhibits linear dynamic behaviour.

6.3.3 Increase in the Fresh Ore Feed Hardness

As mentioned earlier, testing the effects of a change in the hardness of the feed ore on other circuit parameters is difficult if not impossible in an industrial circuit. However, with a simulator such changes can be easily performed. As explained in Chapter 3 hardness changes have been modelled by considering the ore to be composed of two components having the same breakage function but different selection elements. In other words, a hardness change can be brought about by making a step change from component #1, the soft ore to component #2, the hard ore. Two questions immediately come to mind. First, what are the initial and final ratios of the two components in the ore and second, is there difference in their densities. Given that an increase from 100% of component #1 to 100% component #2 is an extreme case and

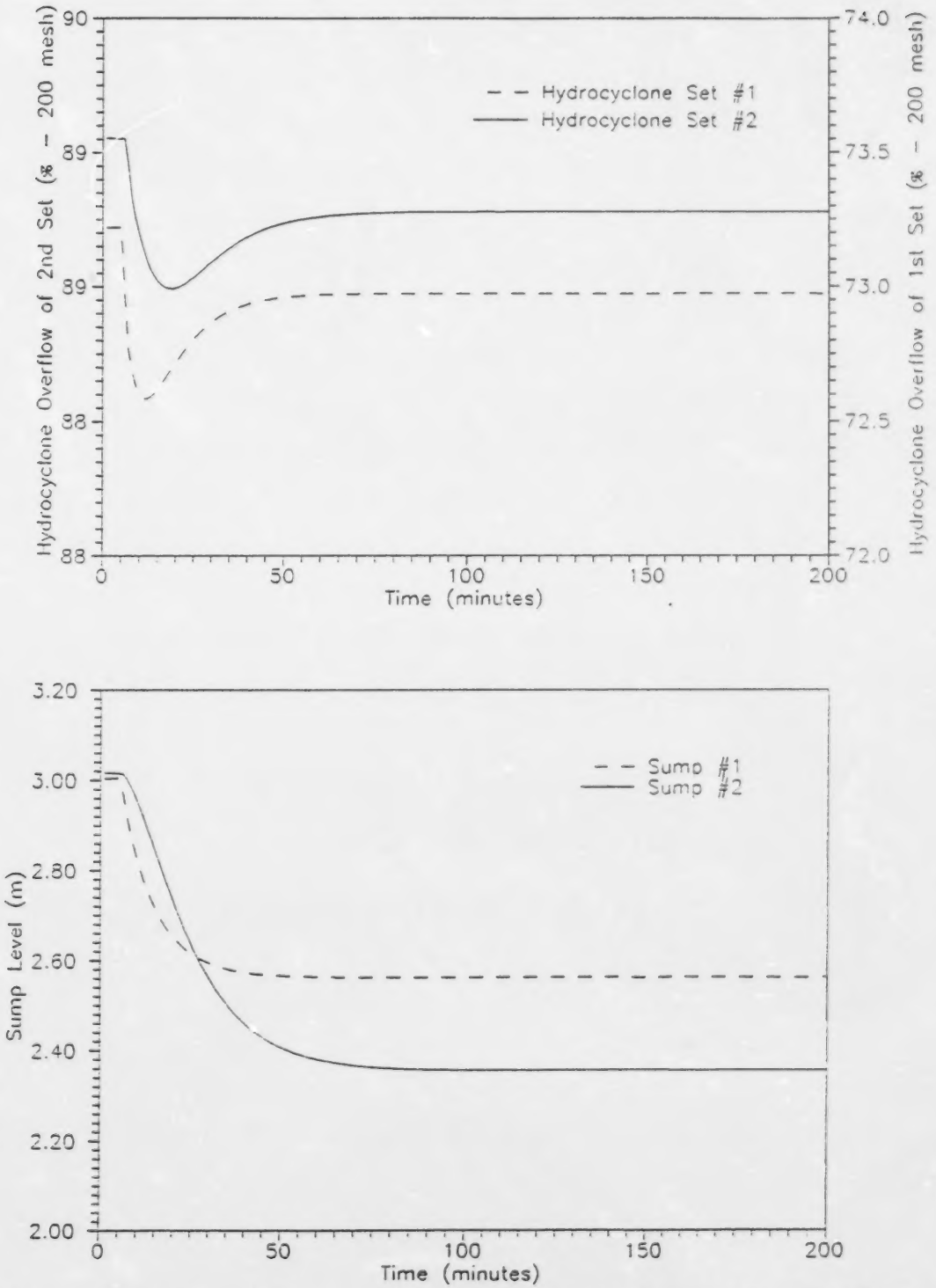

Figure 6.9: Open Loop Response of the Hydrocyclone Overflows and Sump Levels to a 3% Step Decrease in the Water Flow Rate to Sump #1

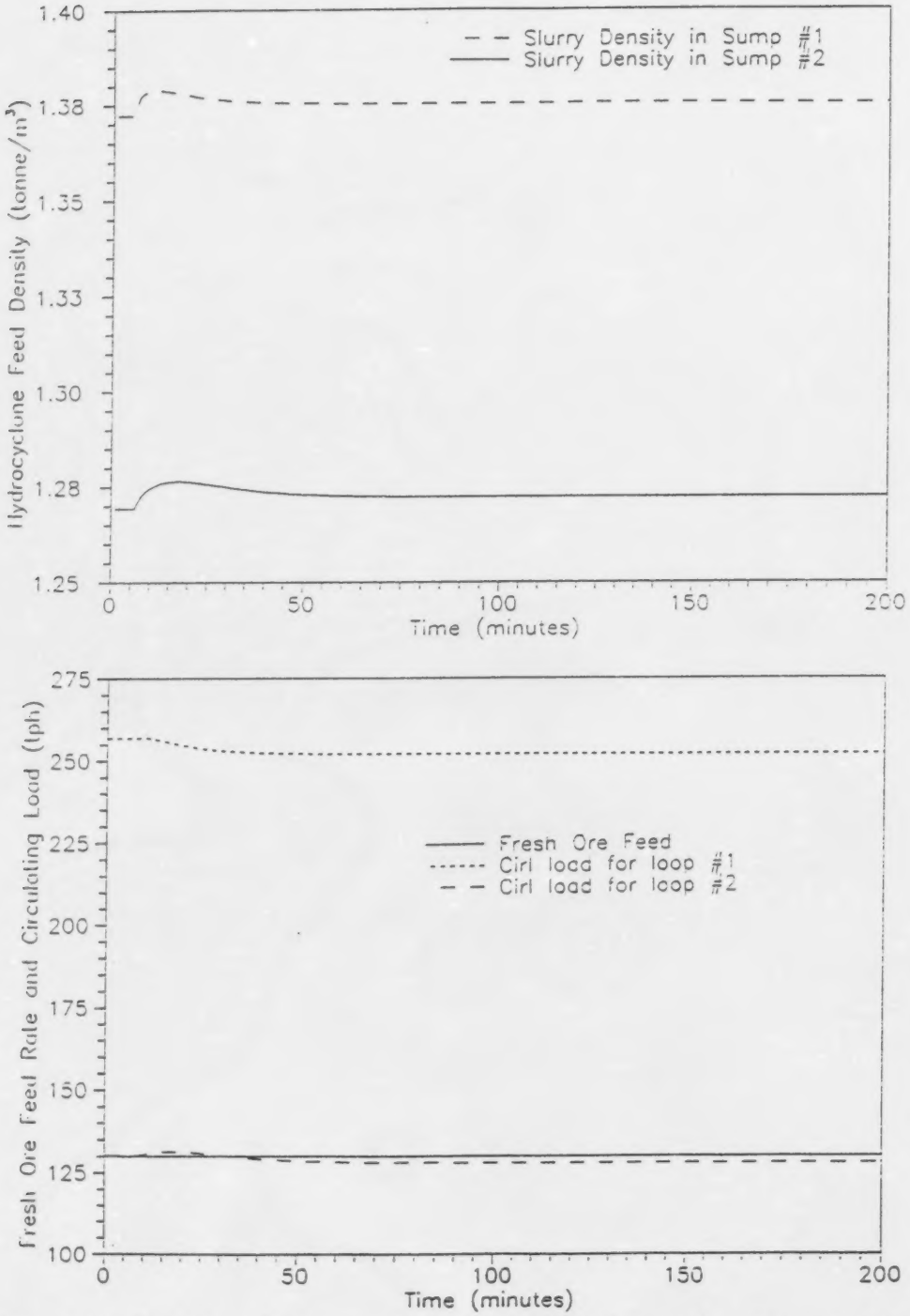

Figure 6.10: Open Loop Response of the Slurry Densities and Circulating Loads to a 3% Step Decrease in the Water Flow Rate to Sump #1

hence unlikely, the ratios after the change could be realistically anywhere between 75-25, 50-50 or 25-75 of the first and second component respectively. One would expect the three cases to behave similarly with the absolute values of the parameters depending on the actual ratios. Consequently, it should be sufficient to investigate only the case where the ore which for the base case contains only component #1, changes abruptly to one consisting of an equal percentage of components #1 and #2 (*i.e.* 50% of each component). Since the ore is initially assumed to be made up solely of component #1, a change to an ore that contains 50% of each component represents an increase in hardness.

Figures. 6.11 and 6.12 show the effect of a step increase in the hardness of the fresh ore feed. The selection elements of component #2 are one-half of the corresponding elements of component #1 and the ore contains 50% of each component with the fresh ore flow rate and density constant. As expected, there is a significant lag period before the effects are felt in the circuit variables monitored. Due to the increase in hardness, the mill product is coarser than before the change, which after due delay in the sumps, results in an increase in the mass fraction of the material reporting to the underflow streams. The circulating loads, as a consequence, start to increase leading to higher flows to the sump. The sump levels, therefore, increase as do the hydrocyclone densities. The hydrocyclone feed density to hydrocyclone set #2 decreases initially due to the fact that the overflow from the first set of hydrocyclones, which is its feed stream, decreases as a result of the hardness change. Eventually, however, densities in both the sumps reach new steady states greater than their original value.

As a consequence of higher density slurries being pumped to the hydrocyclones, the d_{50} sizes associated with both the hydrocyclone sets increases resulting in coarser

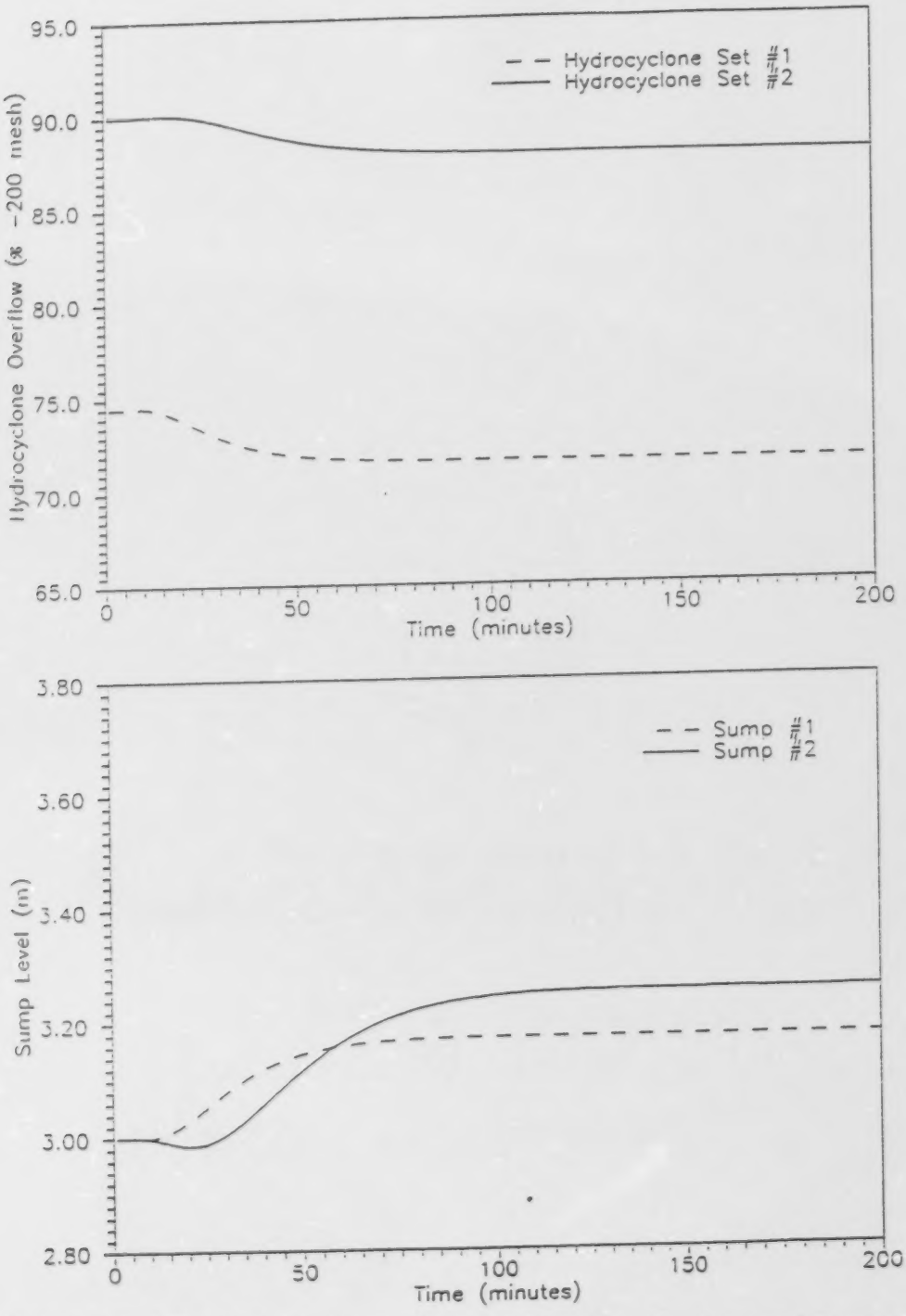

Figure 6.11: Open Loop Response of the Hydrocyclone Overflows and Sump Levels to a Step Increase in the Fresh Ore Feed Hardness

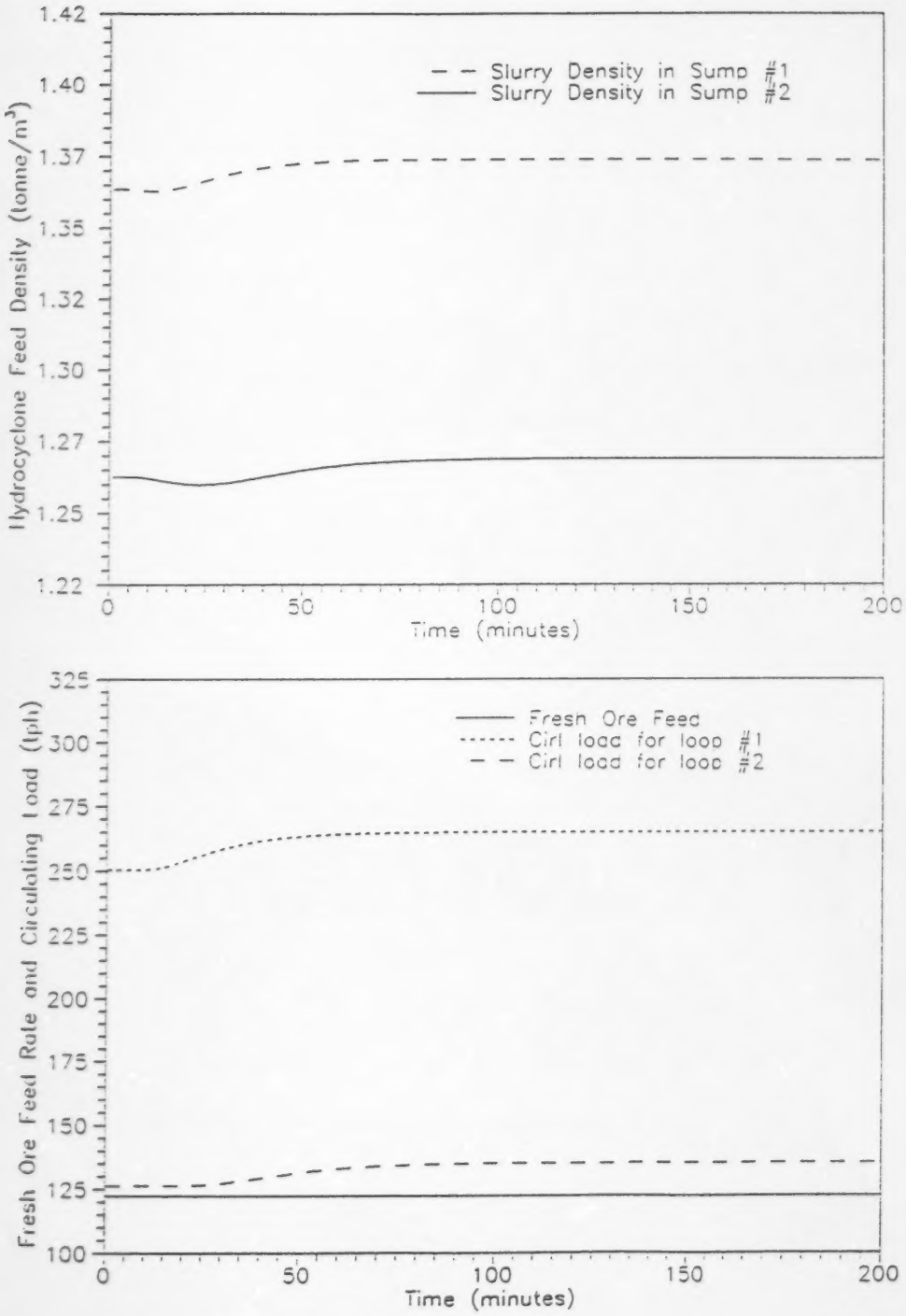

Figure 6.12: Open Loop Response of the Slurry Densities and Circulating Loads to a Step Increase in the Fresh Ore Feed Hardness

overflow streams with the final steady state value of the product stream being about 5% below the desired size distribution of 90% less than 200 mesh. Having observed the consequence of a step change in feed ore hardness in one direction *i.e.* increase in hardness, it would be relevant insofar as determining whether hardness changes produce linear responses, to look at a case where the hardness of the ore decreases. This could be simulated by changing from an ore that is composed of 100% of component #2 to an an ore consisting of equal ratios of the two components. Since the initial steady state values are quite different, it is not possible to compare the actual magnitude of the changes but it can be safely concluded from Figures. 6.13 and 6.14 that the circuit is linear in response to changes in hardness.

6.3.4 Increase in Fresh Feed Ore Density

Although this situation unlikely to occur in an operating plant, it is instructional to observe the effect of a change in the fresh ore feed density without a corresponding change in the ore hardness. Analyzing this situation will give an insight to the expected response when a change in fresh ore hardness is accompanied by a change in ore density. Assigning an arbitrary value of 4.2 $tonnes/m^3$ to the second component, the ore is assumed to consist of two components in equal proportions and hardness but different densities.

Figures. 6.15 and 6.16 show the effect of a change in density in the fresh feed ore. One can observe an 'inverse' response in the case of sump levels momentarily after the change is imposed. The increase in ore density at constant flow rate implies a decrease in the volume of the ore coming into the circuit. This causes a decrease in the level of solids in the sumps. As well, the decrease in d_{50} is immediate since it is assumed that there is no dynamics associated with the hydrocyclone . It must be realized that the the simulator is designed such that the effect of a change in densities

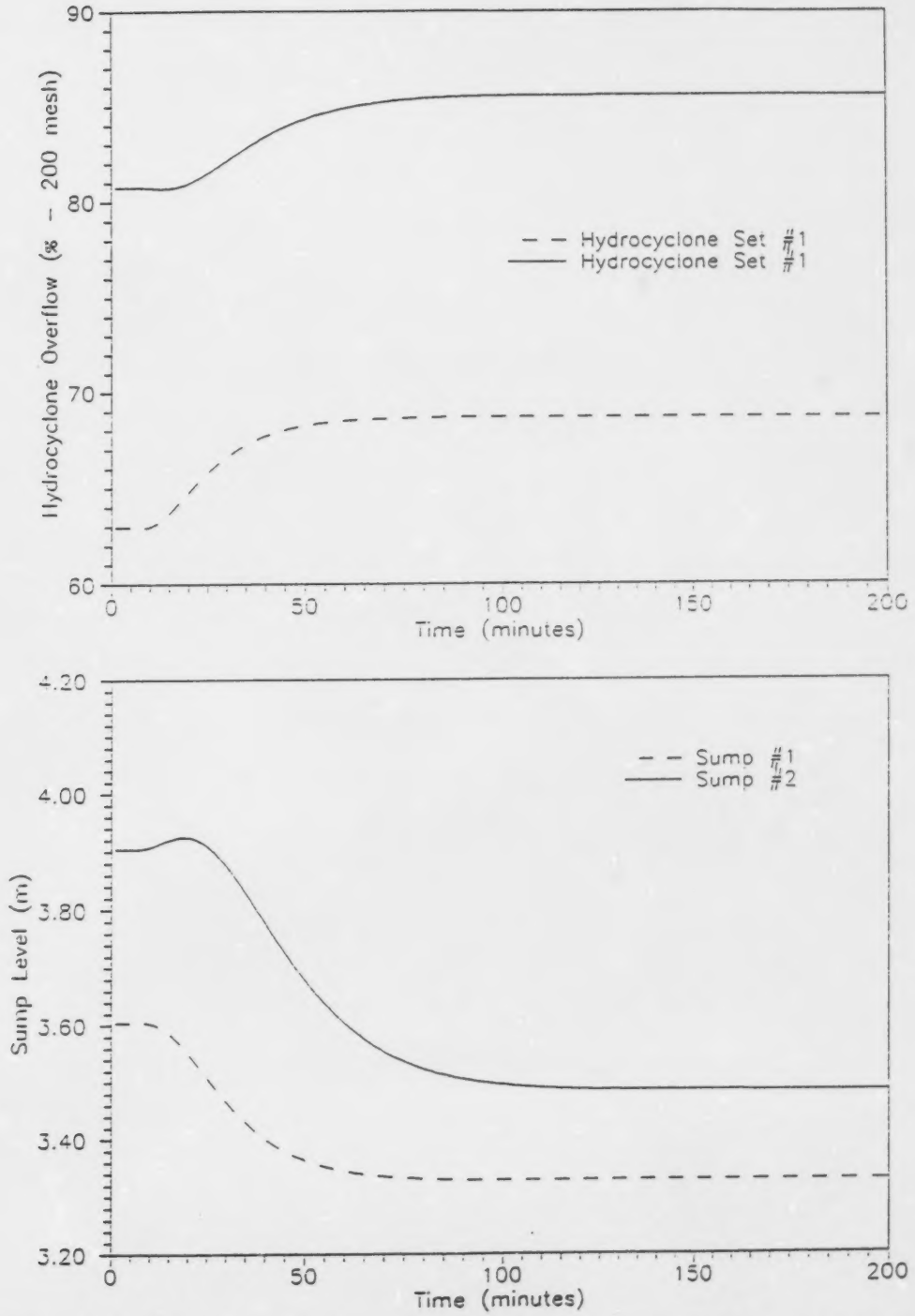

Figure 6.13: Open Loop Response of the Hydrocyclone Overflows and Sump Levels to a Step Decrease in the Fresh Ore Feed Hardness

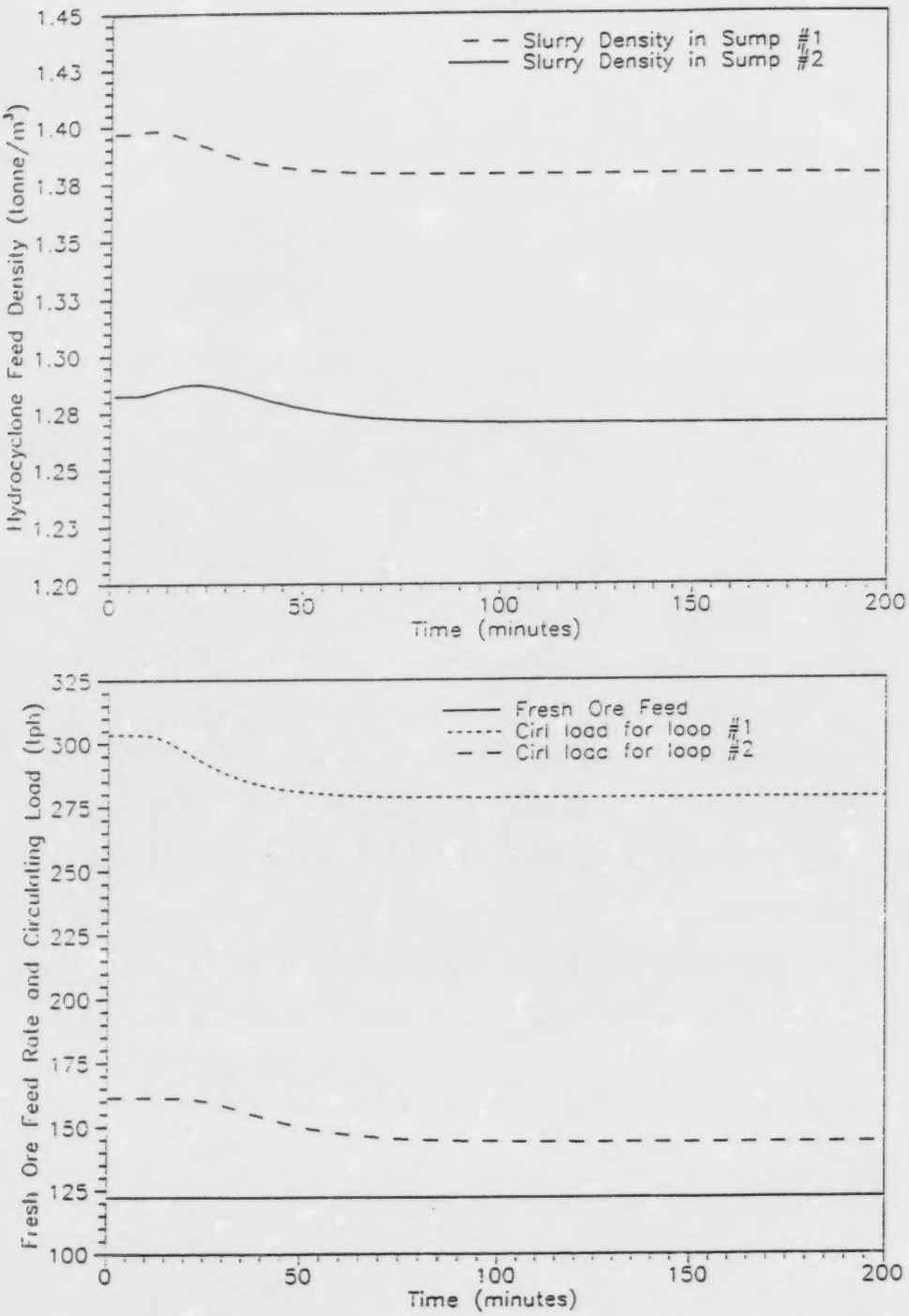

Figure 6.14: Open Loop Response of the Slurry Densities and Circulating Loads to a Step Decrease in the Fresh Ore Feed Hardness

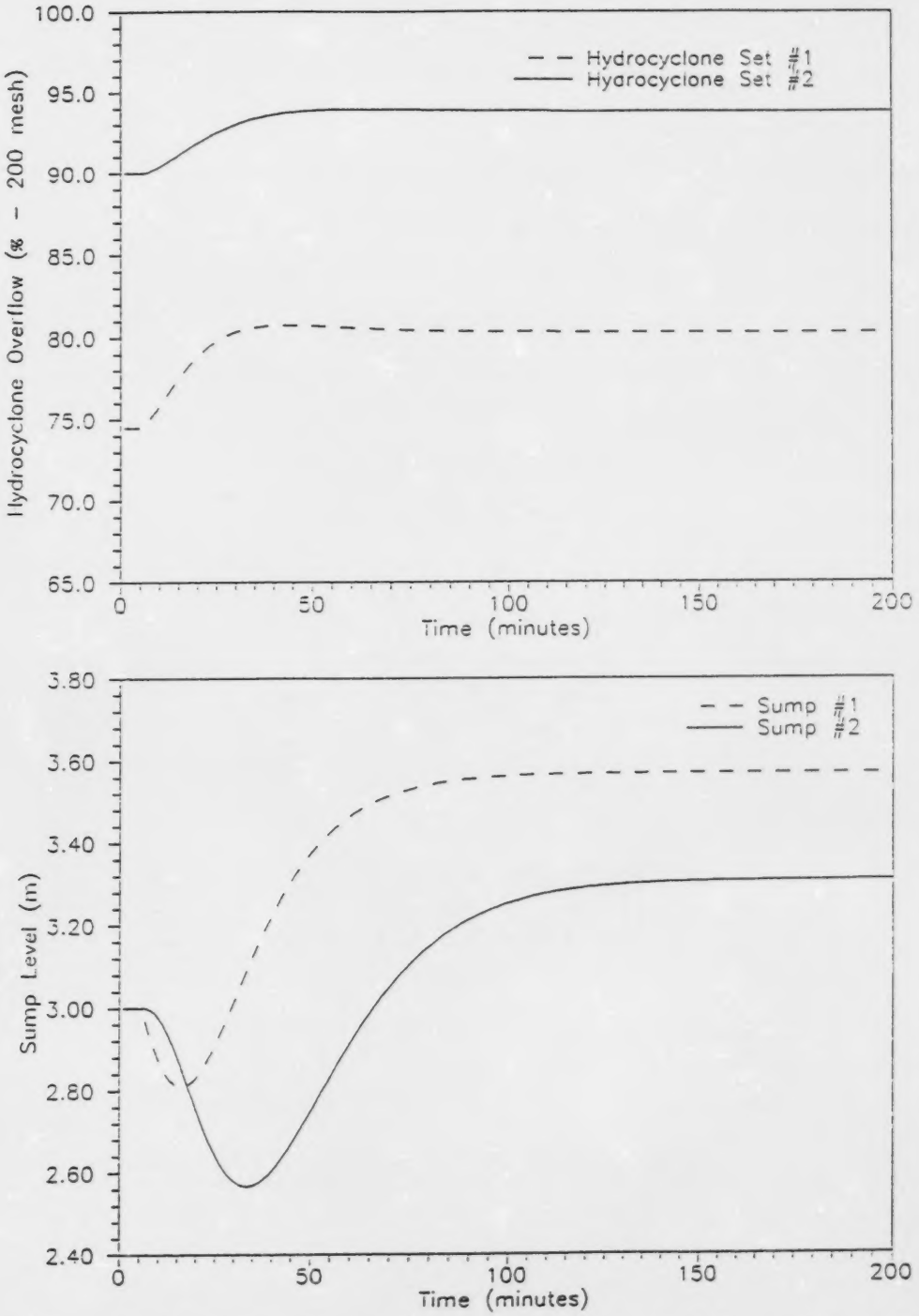

Figure 6.15: Open Loop Response of the Hydrocyclone Overflows and Sump Levels to a Step Increase in the Fresh Ore Feed Density

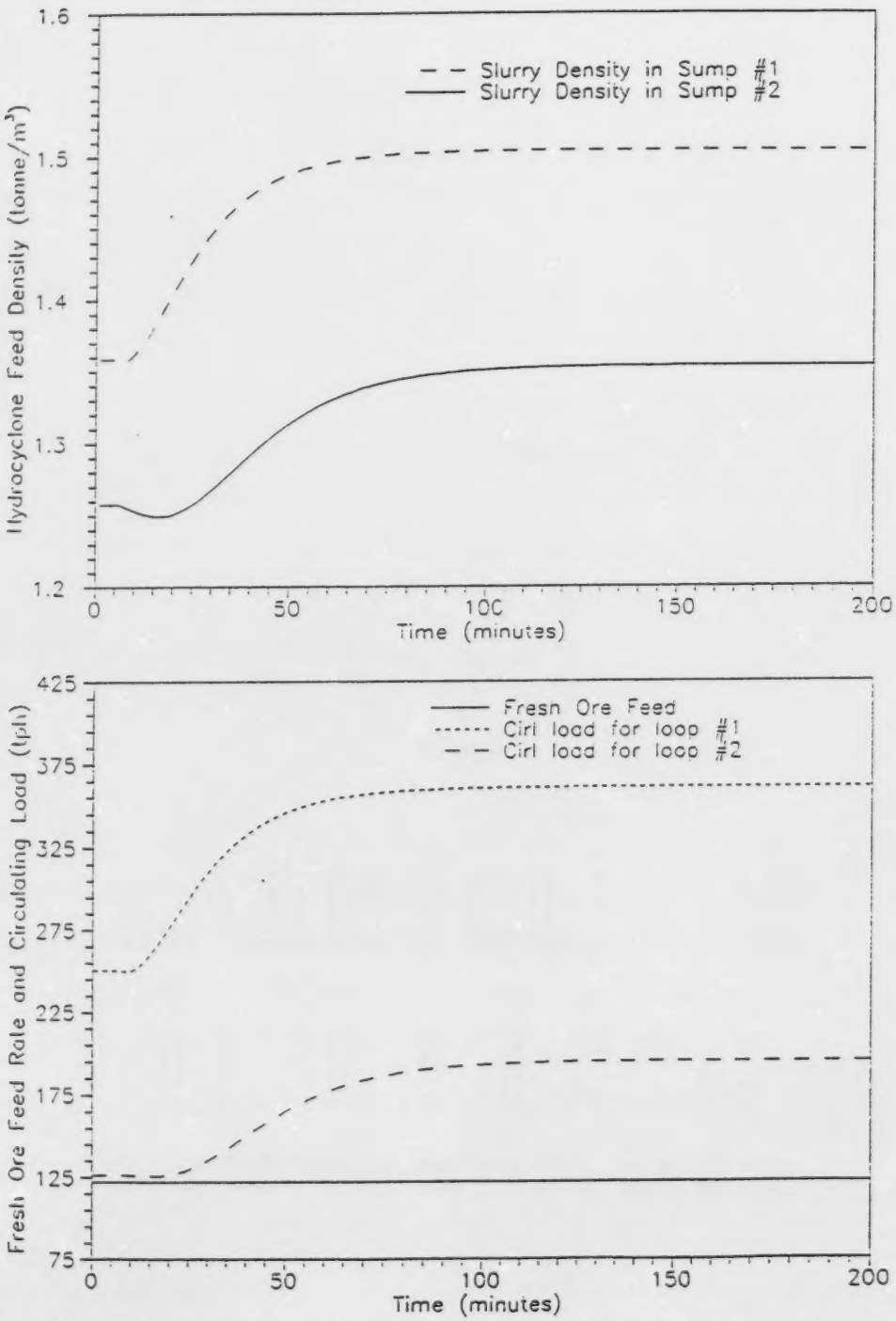

Figure 6.16: Open Loop Response of the Slurry Densities and Circulating Loads to a Step Increase in the Fresh Ore Feed Density

shows up only in the classification part of the grinding process. It has no effect on the way the MILL subroutine is designed. The decrease in the d_{50} results in a coarser underflow which helps in bringing the level of the pulp in the sumps, up. In other words, reduction in d_{50} gives rise to higher ciculating loads, higher sump levels and higher hydrocyclone feed densities (after an initial decrease). It should be noted that the effect of changing any parameter at the respective feed points is diluted by the time this disturbance propogates to the second hydrocyclone set. In a sense, the first and second sumps act as buffers to the rest of the circuit.

6.3.5 Increase in the Fresh Ore Hardness and Density

After taking the case where the two components that comprise the feed ore possess the same density and the case where the components have same hardness but different density in the previous two sections, it is appropriate to consider the more complex case where the ore components have different hardness as well as different densities. The second component is again assigned values such that its selection elements are one-half of the corresponding element of component #1 and its density is 1.5 times that of the first component. In effect then, the components are such that the first component is of low density and soft while the second component is hard and has a higher density. The effect of the combined disturbance is shown in Figures. 6.17 and 6.18. The change in hardness results in producing a similar response as in the previous case. However, this response lags behind the effect due to a change in the density of the ore. In other words, the effect of the simultaneous changes in two properties of the ore get superimposed with the response due to the density predominant initially and the effect of the hardness change manifesting itself later. In this case, both the grinding mills and the hydrocyclone affect the product output. As discussed in the previous section, an increase in density leads to an initial drop in the sump levels . In

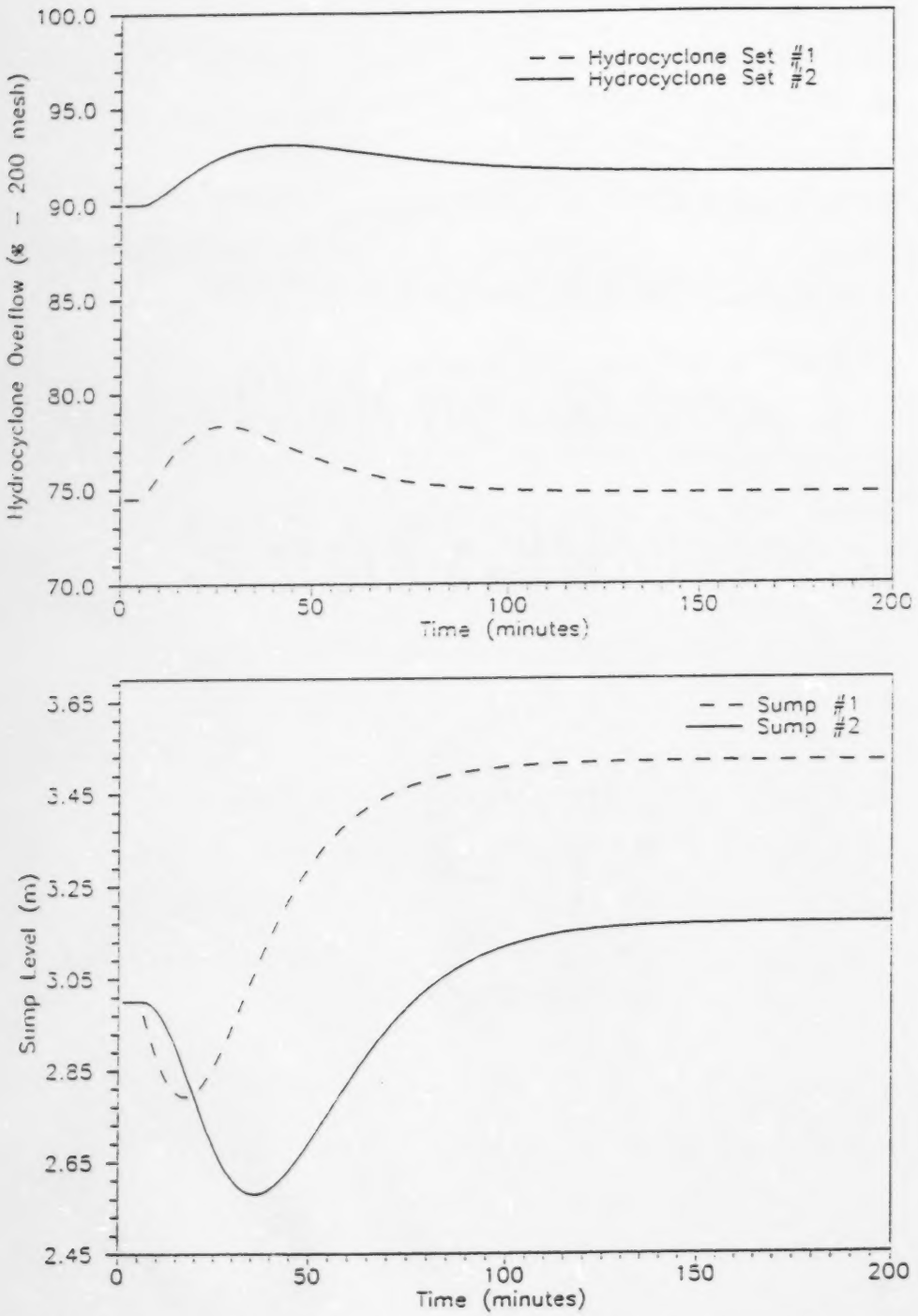

Figure 6.17: Open Loop Response of the Hydrocyclone Overflows and Sump Levels to a Step Increase in the Fresh Ore Feed Density and Hardness

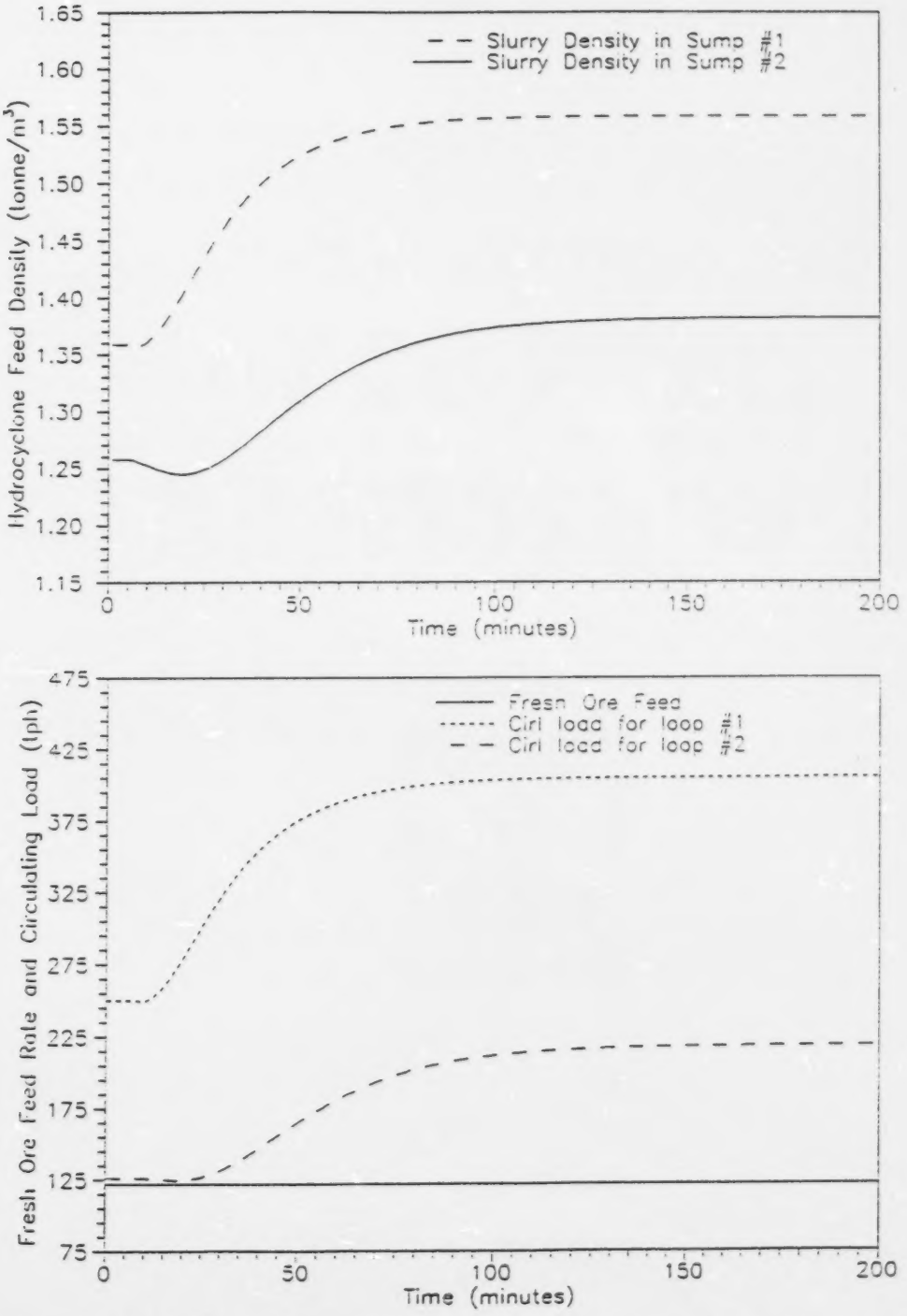

Figure 6.18: Open Loop Response of the Slurry Densities and Circulating Loads to a Step Increase in the Fresh Ore Feed Density and Hardness

this case, a decrease in the hydrocyclone feed density coupled with coarser feed from the mills due to an increase in hardness results in reducing the d_{50} to a level where the percent less than 200 mesh in the hydrocyclone overflow stream decreases after an initial increase. The circuit stabilizes to a new steady state with higher circulating loads, higher hydrocyclone feed densities, higher sump levels and a marginally finer product.

Chapter 7

The Hemlo Circuit Feedback Control

7.1 Introduction

Provided the dynamic responses and steady state conditions calculated by a simulator are representative of the measured variables in a grinding circuit the next logical step would presumably be evaluation of different control strategies. In view of the frequent disturbances that occur in a real plant, regulatory control *i.e.* disturbance rejection is thought to be more important than servo control.

The usual practice in designing a control strategy is to start by properly understanding the management policy *vis-a-vis* operating goals. The most common objective is the production of an optimal grind at a specified tonnage for the lowest unit cost. Alternately, it might be desired to maximize the throughput while maintaining a specified grind. While there are numerous such philosophies, in most cases these are mutually exclusive objectives and selecting the best course of action will be a compromise dependent on the relative importance of each objective.

Having decided the control objective, it is then appropriate to define the nature of the control algorithm. It is common practice in classical control methods

the control scheme will initially consider the process as a single input single output (SISO) system or a collection of such systems. Control action for such systems involve a direct measurement of the controlled variable(s) with the value of the manipulated variable(s) changed so that the desired value of the controlled variable(s) are maintained. This kind of control strategy termed as feedback control implies that an error signal is used to drive the manipulated variable till the error reduces to zero. Among the many different controllers used to implement this strategy, most widely employed feedback controllers utilize a PID algorithm. There are many variations of this and one of the more popular is given as:

$$c(t) = K_c\varepsilon(t) + \frac{K_c}{\tau_i}\int \varepsilon(t)dt + K_c\tau_d\frac{d\varepsilon(t)}{dt} + c_s \tag{7.1}$$

where

$$\varepsilon(t) = y_{sp}(t) - \hat{y}(t) \tag{7.2}$$

In situations where some offset from the set point is allowed, it is enough if a proportional only type of controller is employed. However, if it is desired to have a control strategy such that there is no offset, one has to use a proportional plus integral (PI) controller. The integral time constant τ_i in Equation. 7.1 determines how quickly the proportional action of the controller is repeated. The integral action of the PI controller in a closed loop increases the order of the overall system through the addition of a lag into the characteristic polynomial, thus slowing down the system response. The other shortcoming of the integral action becomes evident when large errors persist for long time periods. A condition known as reset windup or controller saturation can develop because the integral action continues to integrate and attempts to add to the controller output even after the final control element has reached its maximum (or minimum) position. The usual method to correct this problem is to limit the controller output to the operating range of the final control element and use a reset

feedback structure implementation of the control action.

The addition of derivative action further improves the overall control system by anticipating the error in the near future and applying control action proportional to the rate of change of the error term. Again, the system response becomes slower due to the increase in the effective system constant. However this reduction in the response speed has a stabilizing effect which improves the robustness of the controlled system. The problem with derivative action is that it is extremely sensitive and hence may produce an undesirably large control action or derivative 'kick' for small errors. This fact is especially true when such controllers are applied to industry. As in most industrial applications, measurements have some associated 'noise', the anticipatory action of the derivative controller may result in poor or incorrect control action.

In general, the single input single output (SISO) systems discussed thus far are the exception than the rule in most industrial processes. The industrial grinding circuit with multiple inputs and outputs is a typical example of a multiple input multiple output (MIMO) system. In order to take advantage of the control strategy described above, the methodology followed in these situations is to design a multiple SISO system such that each loop links one input with an appropriate output. However, this, as can be observed from the open loop response curves in the previous chapter, results in system interactions. System interaction, a well recognized limitation to good control, is a situation where a change in any given input results in changes to more than one of the outputs. The standard practice in such cases is to detune one or more of the loops in order to obtain satisfactory, if not optimal, control. Before detuning any of the control loops it must be ensured that the pairing of the input-output variables is chosen so that there are minimal system interactions.

Herbst and Rajamani (1979) identified four output variables that must be

controlled and four input variables that could be manipulated to control these output variables. A summary of these combinations is given in Table 7.1. For the current work, these combinations can be reduced from four to three since the mill water is ratioed to the fresh ore feed rate resulting in a constant pulp density into the first ball mill. Also the use of pumping rate as a manipulated variable to control sump level is not possible for the Hemlo circuit since only fixed speed pumps are being used.

Given that there is no choice in the manipulated variable for controlling sump levels, two distinct types of classical control strategies can be identified (referred to as Type I and Type II by Herbst and Rajamani, 1979). The Type I control strategy manipulates the fresh ore feed rate to control product particle size and uses sump water addition rates to control the circulating load, whereas the Type II control strategy controls the product particle size by adjusting the sump water addition rate and trims the fresh ore feed rate to maintain a fixed circulating load. The possible variable pairings for the Hemlo circuit are given in Table 7.2.

Once the possible input-output variable pairings have been selected, it is necessary to determine the possible disturbances that could occur which might require regulatory control. From the simulation results in Chapter 6, it is obvious that changes in hardness of the fresh ore, feed size distribution, and sump water addition rate are possible disturbances. Of these, it has been shown by McDougall (1987), that disturbances in feed size distribution does not significantly affect the other circuit variables and as such can be ignored. Since the sump level is controlled by sump water addition rates, extraneous water to sump can also be neglected as a potential disturbance. This leaves only hardness changes in the fresh ore as the most serious control problem and this chapter will deal mostly with designing a control system that maintains a desired grind size specification in the hydrocyclone overflow stream

Table 7.1: List of Possible Pairings of Controlled and Manipulated Variables

Controlled Variable	Manipulated Variable
(1) Sump Level	(1) Sump water addition rate or (2) Slurry pumping rate
(2) Product particle size (or Hydrocyclone feed density)	(1) Fresh ore feed rate (2) Sump water addition rate
(3) Circulating load (or Mill throughput)	(1) Fresh ore feed rate (2) Sump water addition rate
(4) Mill percent solids (or feed percent solids)	(1) Fresh mill water rate

by manipulating the fresh ore feed rate for changes in ore hardness.

7.2 Design and Evaluation of Feedback Controllers

As discussed in the previous section, the control engineer must decide upon the type of control algorithm most suitable for the given circuit, P, PI or PID *etc.*, and establish optimum input-output pairings. Subsequently, appropriate values of initial controller constants K_c, τ_i and τ_d and some form of criterion for non-subjective evaluation of the controller performance must to be determined. Most of the better known techniques to estimate controller constants are classified as either on-line procedures such as the Ziegler-Nichols ultimate gain technique or are based on the assumption that the process can be adequately described by a first order plus time delay model. The choice of a particular method is usually based on personal preference and the

Table 7.2: List of Possible Pairings of Controlled and Manipulated Variables for the Hemlo Circuit

Controlled Variable	**Manipulated Variable**
(1) Sump Level	Sump water addition rate
(2) Product particle size (or Hydrocyclone feed density)	(1) Fresh ore feed rate (2) Sump water addition rate
(3) Circulating load (or Mill throughput)	(1) Fresh ore feed rate (2) Sump water addition rate

nature of process being controlled. Regardless of the method employed, almost always subsequent tuning is required.

For this work, the process reaction curve method was selected. From a simulation point of view, this technique is the simplest because for every control loop to be tuned only one open loop simulation is needed. On the other hand, the ultimate gain technique requires multiple simulations to obtain the required cyclical behaviour in the process output. Cohen and Coon have suggested controller constants for SISO systems provided the open loop behaviour of these systems is identical to that produced by a transfer function of the form:

$$G(s) = \frac{Ke^{-T_d s}}{\tau s + 1} \tag{7.3}$$

The simulation results in the previous chapter indicate that the response is not first order plus time delay, but rather an overdamped second order (or higher) process with time delay. As there are no standard technique for systems with such process reaction curves, an *ad hoc* method has been employed. For the current work, initial tuning was performed using proportional control only, with the controller gain being

adjusted until offset in the controlled variable and oscillation in the input and output signals were minimized. The resultant gain was subsequently reduced by almost 20% and the amount of integral action slowly increased until the offset was zero.

In order to evaluate the controller performance objectively, it is imperative to choose some kind of performance criteria. The closed loop performance for set-point changes is often characterized by such measures as rise time, overshoot, settling time, decay ratio etc. In the case of closed loop control for handling disturbance inputs it is appropriate to characterize the closed loop performance by selecting one of the time integral performance criteria as listed by Stephanopoulos (1984). For this work the integral of absolute error (IAE) is used as the performance index, where

$$IAE = \int_0^\infty |\varepsilon(t)|\, dt$$

Controller constants were tuned using the IAE value as the measure of performance.

7.3 Type I Control Behaviour

As shown in Table 7.1, the overall circuit can be described as a 3x3 MIMO system. To make things easier, however, it would be more expedient to consider a simpler 2x2 system for developing the control scheme. Subsequently, one can add the third dimension with little or no extra effort. Referring to Table 7.2, we can see that for the current work, there are three variables to be controlled *viz* the sump level (SPL), the product particle size (COS) and the circulating load (CL) while there are, in the absence of a variable speed pump, only two manipulated variables in FOF and sump water addition rate (SW). Forsaking the circulating load (CL) as a controlled variable, one possible pairing would be to use the FOF to control the COS and the water addition rates to maintain the levels. The choice of linking COS to FOF follows from the work of McDougall (1987)who did control studies on a similar simulator for

the Lake Dufault circuit. Another reason is that if sump water feed rate is used to control the COS, controlling sump levels might pose a problem. The decision to control sump level rather than circulating load needs some explanation. While it is true that as long as the sump does not run dry or overflow, strict level control is not essential, it must be pointed out that in this particular circuit the situation is a bit more complicated. There are two sumps in the Hemlo grinding circuit. Since sumps act as holdup vessels, the effect of a change in flow rate of the ore is not reflected in the second sump for some period of time. In the extreme case, this could result in an overflow from the second sump before the control action in the form of a reduction in the fresh ore rate reaches it. At such times the validity of the simulation might be questionable since the product prediction is strongly dependent on the second sump variables. Whereas if one controls the sump level and links the FOF to COS, the circulating load will always remain within limits. As well, one could use the sump levels to provide an indication of the system operating conditions *i.e.* with high sump levels the inertia is increased such that high frequency disturbances can often be absorbed, with minimal effect of the desired control variable, but on the other hand the system becomes more more 'sluggish' in terms of regulatory control. The opposite effect is evident in case of low sump levels, the system becomes more 'susceptible' to various disturbances but easier to manipulate from a control standpoint. Once again, a compromise is necessary so by maintaining fairly constant sump levels, the dominant time constants of the units involved in the system will not fluctuate as much as it would in case of an oscillating sump level. With regard to designing a control strategy, it is much easier to tune a system with relatively stable time constants.

7.3.1 Controlling a Step Change in Hardness

The result of a change in hardness of the fresh ore at constant density has been shown in Figures. 6.11 to 6.14. Employing FOF to control COS means that for an increase in hardness, FOF has to decrease and conversely as hardness decreases, FOF should increase to maintain a fixed COS. In the first case, a reduction in FOF means that the volumetric flow of slurry to sump decreases. To maintain a constant sump level, SWF will increase to make up the shortfall in flow to the sump. From Figures. 6.7 and 6.8 it is clear that changing the flow rate of water to the sump affects all system outputs. As mentioned earlier, there are two sumps in the Hemlo grinding circuit. To get a better picture of the circuit response behaviour to load disturbances it is more prudent to focus attention on only one of the sumps. Since the first sump handles a bigger circulating load, is the first to get affected in cases of disturbances it is a better indicator of the way the circuit behaves than the second sump. Consequently, heretofore all references to 'sump' will mean the first sump of the circuit and SWF will indicate water flow to this sump. As can be observed from the open loop plots in the previous chapter, the second sump behaves in an identical fashion as the first one but with a time delay. Coming back to the problem of controlling COS with FOF for an increase in ore hardness, it is apparent that a reduction in FOF will lead to a higher SWF. From Figures. 6.7 and 6.8 it can be seen that for a 3% increase in the SWF, the percent less than 200 mesh material in the product stream increases, the hydrocyclone feed density decreases, the circulating load increases slightly and the sump level increases steadily. Thus it can be expected that if sump water is used to control level, while FOF is being reduced to compensate for the coarsening of the product stream, various interactions occur that could compound the control problem. As the flow rate out of the sump is for all practical purposes, independent

of the sump level, *i.e.* the static head effect is minimal, the response of the sump level to changes in SWF is not first order and has practically no time delay. Under these conditions, the first choice for the sump level controller constants would be large values of K_c and small τ_I to effect fast control without causing stability problems. The method to test this argument is to implement a hardness change with the COS - FOF controller disconnected and the SPL - SWF controller active. These studies showed that for a $K_c = 2$ and $\tau_I = 0.7$, sump level control was excellent. Similarly, activating the COS - FOF controller with the SPL - SWF controller disconnected indicated that for $K_c = 3.8$ and $\tau_I = 1.8$, good COS control was achieved. In a perfect world *i.e.* for a system with no interactions, it would have been possible to implement both controller settings and expect perfect control. However, such is not the case. Simulating the circuit with these controller constant resulted in oscillatory behaviour of the manipulated and controlled variables. The value of the integral of the absolute error (IAE) was 7975 compared to 29.3 and 17.8 for the tuned closed loop simulations done with individual controllers. This situation can be resolved to a great extent by detuning one or both the loops till acceptable control behaviour is observed. Various combinations of controller constants were examined and the closed loop response shown in Figures. 7.1 and 7.2 represent the best performance *i.e.* minimum IAE. It must be mentioned that initially a proportional (P) only controller was employed to control the sump levels and inspite of a very low IAE of 17.32 it was decided to add the integral action to remove a steady state error of about 1.2 %.

For a decrease in ore hardness, all responses are opposite in direction. Again as was seen Figures. 6.13 and 6.14, the open loop response for a step decrease in hardness results in a higher COS, lower sump levels, densities and circulating loads.

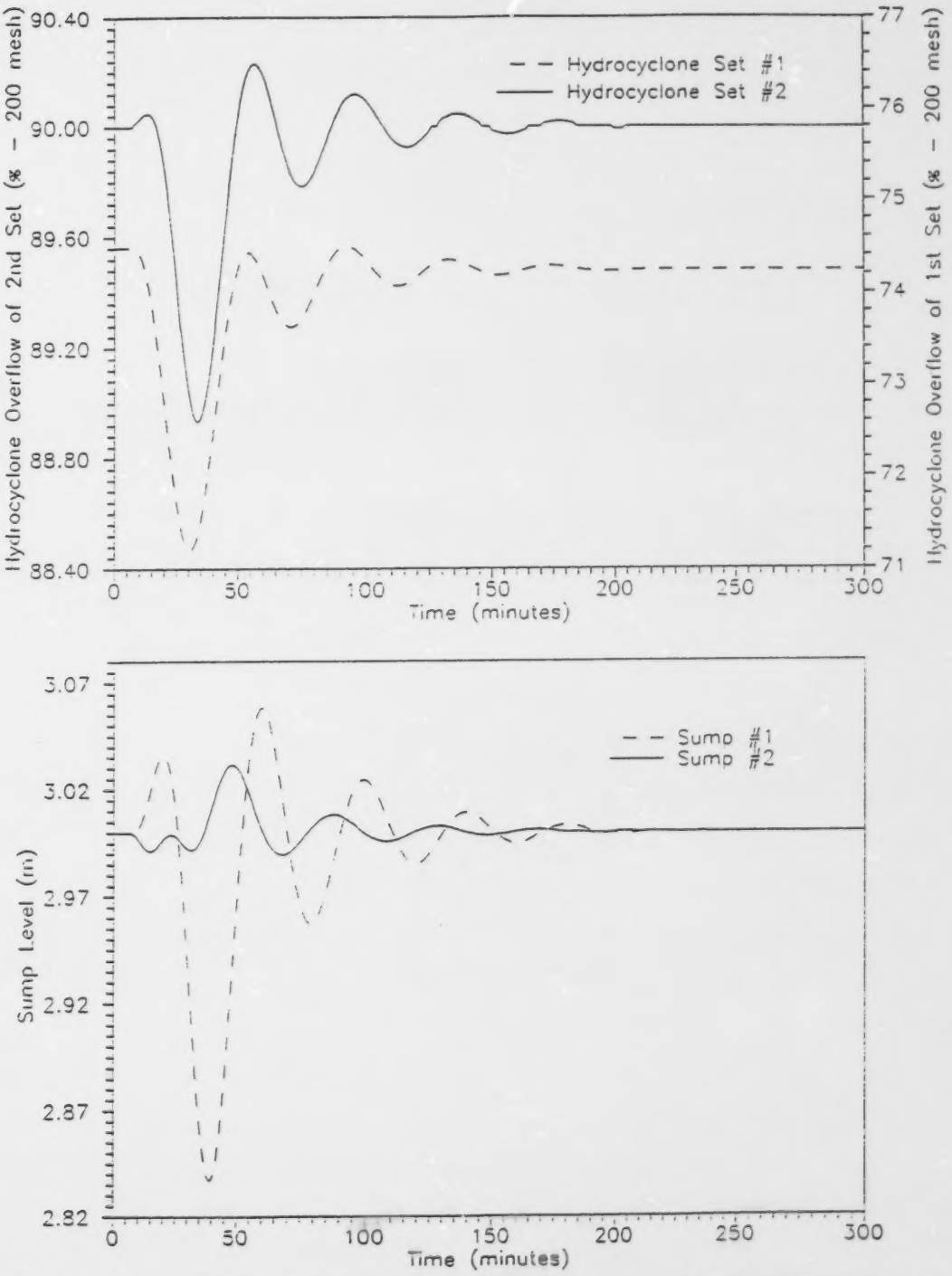

Figure 7.1: Closed Loop Response of the Hydrocyclone Overflows and Sump Levels to a Step Increase in the Fresh Ore Feed Hardness with $K_f = 1.7$, $\tau_I = 0.9$, $K_{s1} = 1.5$, $\tau_{I1} = 1.0$, $K_{s2} = 1.2$, $\tau_{I2} = 1.0$ and IAE=29.3

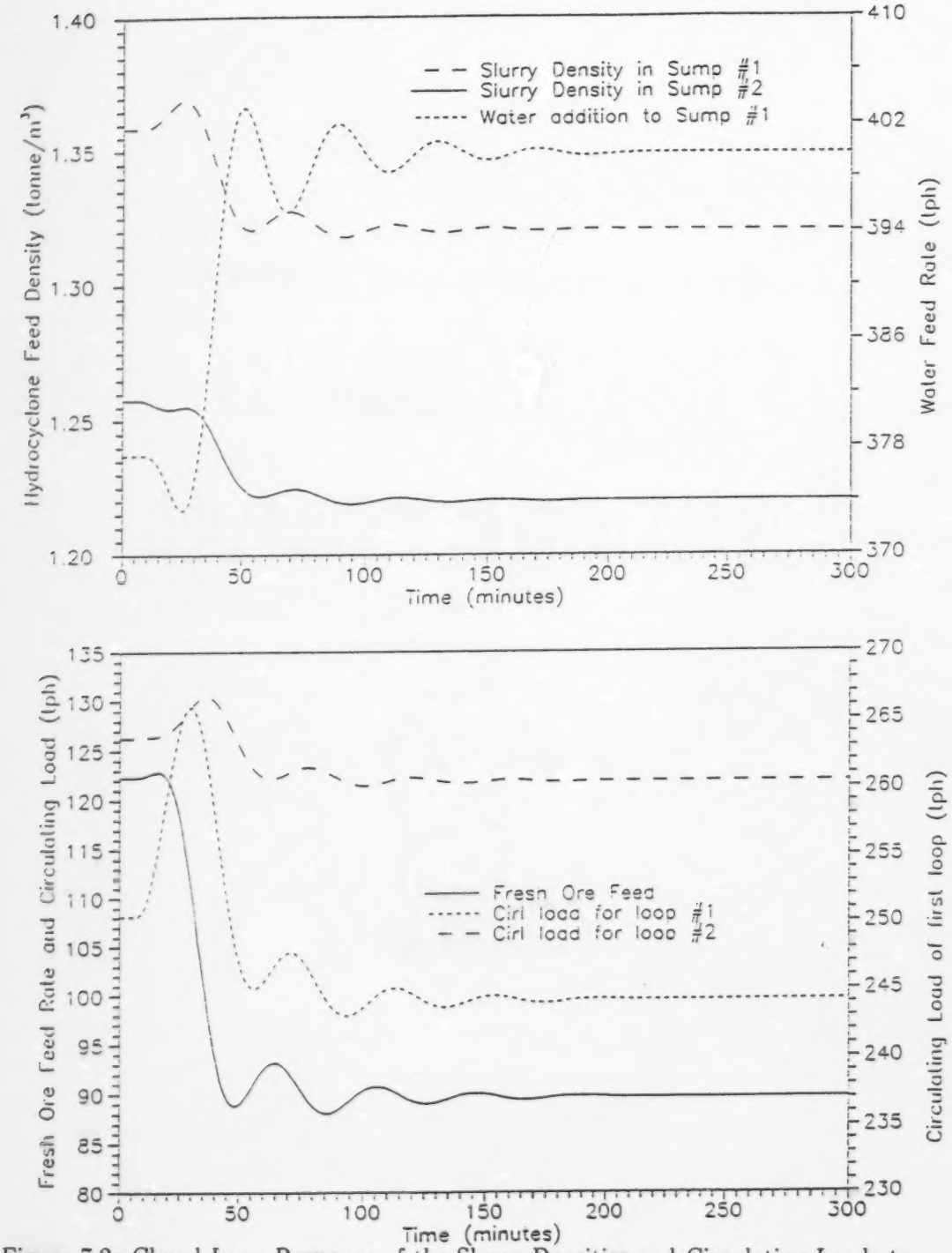
Slurry Density in Sump #1
Slurry Density in Sump #2
Water addition to Sump #1
Hydrocyclone Feed Density (tonne/m³)
Water Feed Rate (tph)
Time (minutes)
Fresh Ore Feed
Circ load for loop #1
Circ load for loop #2
Fresh Ore Feed Rate and Circulating Load (tph)
Circulating Load of first loop (tph)
Time (minutes)

Figure 7.2: Closed Loop Response of the Slurry Densities and Circulating Loads to a Step Increase in the Fresh Ore Feed Hardness with $K_f = 1.7$, $\tau_f = 0.9, K_{s1} = 1.5, \tau_{I1} = 1.0, K_{s2} = 1.2, \tau_{I2} = 1.0$ and IAE=29.3

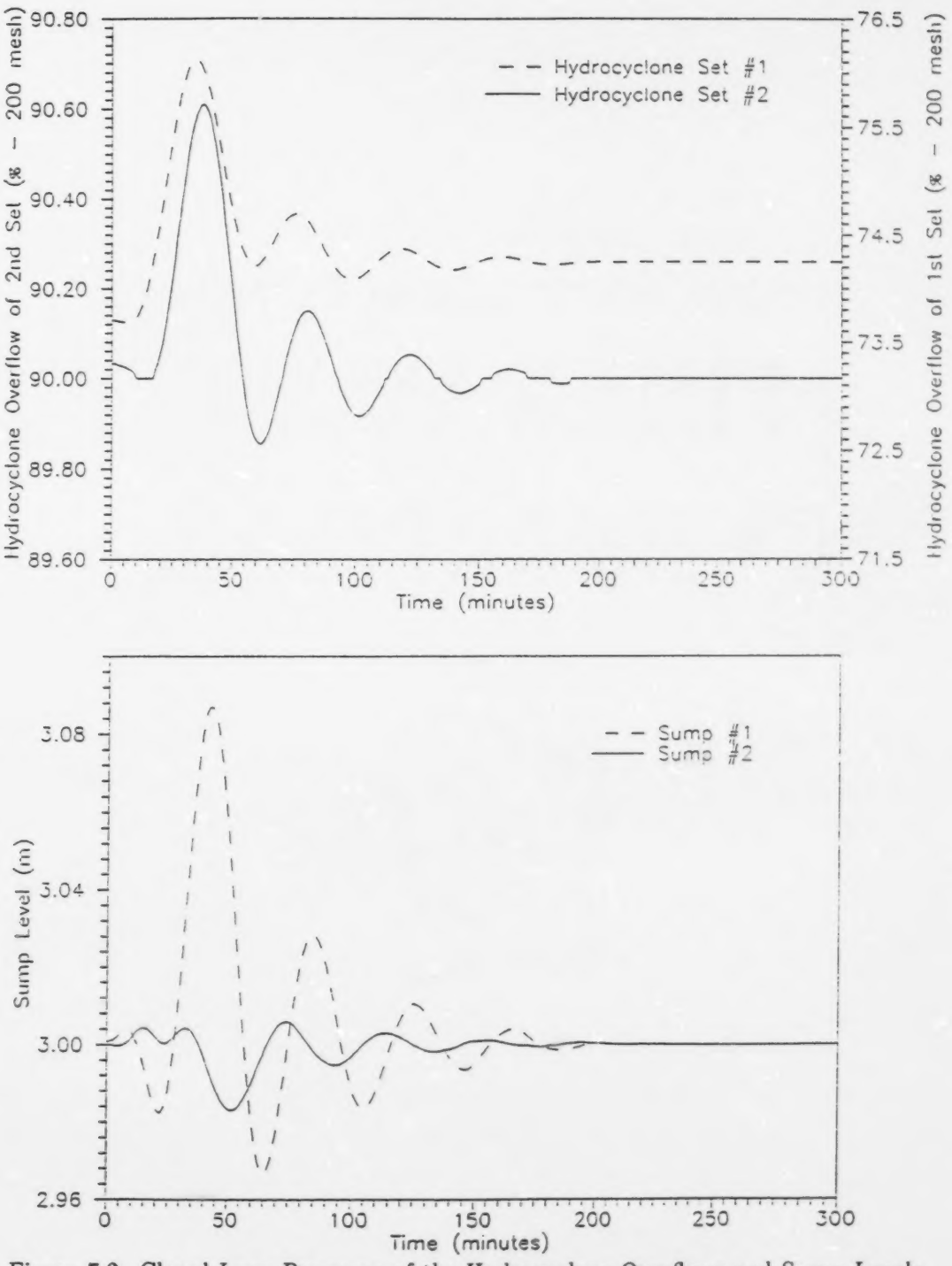

Figure 7.3: Closed Loop Response of the Hydrocyclone Overflows and Sump Levels to a Step Decrease in the Fresh Ore Feed Hardness with $K_f = 1.7$, $\tau_I = 0.9$, $K_{s1} = 1.5, \tau_{I1} = 1.0, K_{s2} = 1.2, \tau_{I2} = 1.0$ and IAE=21.9

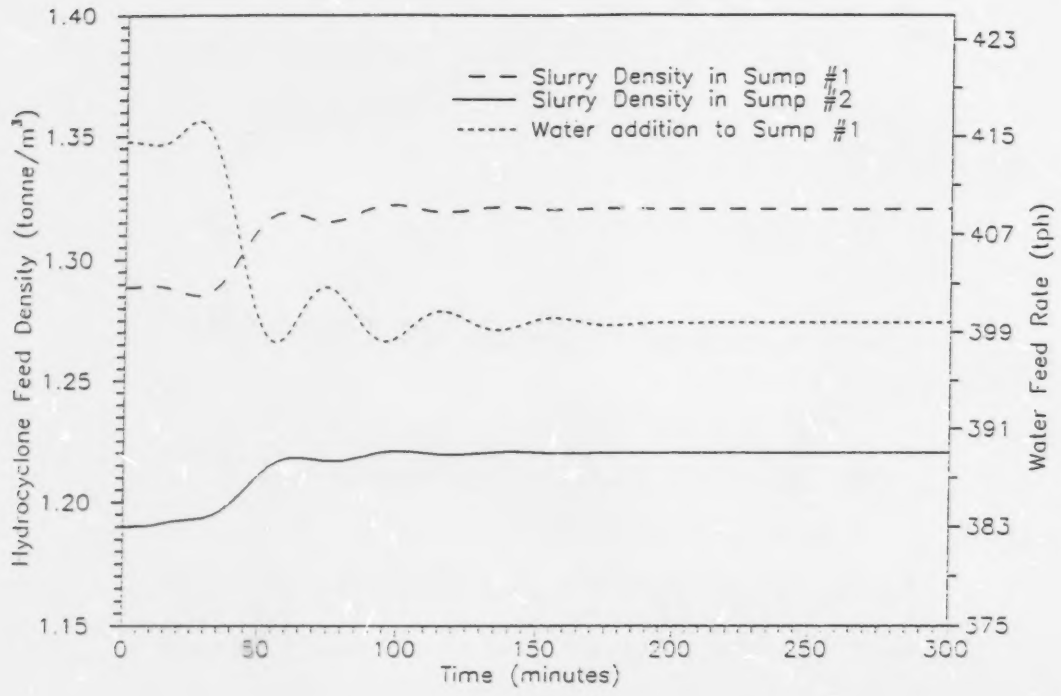

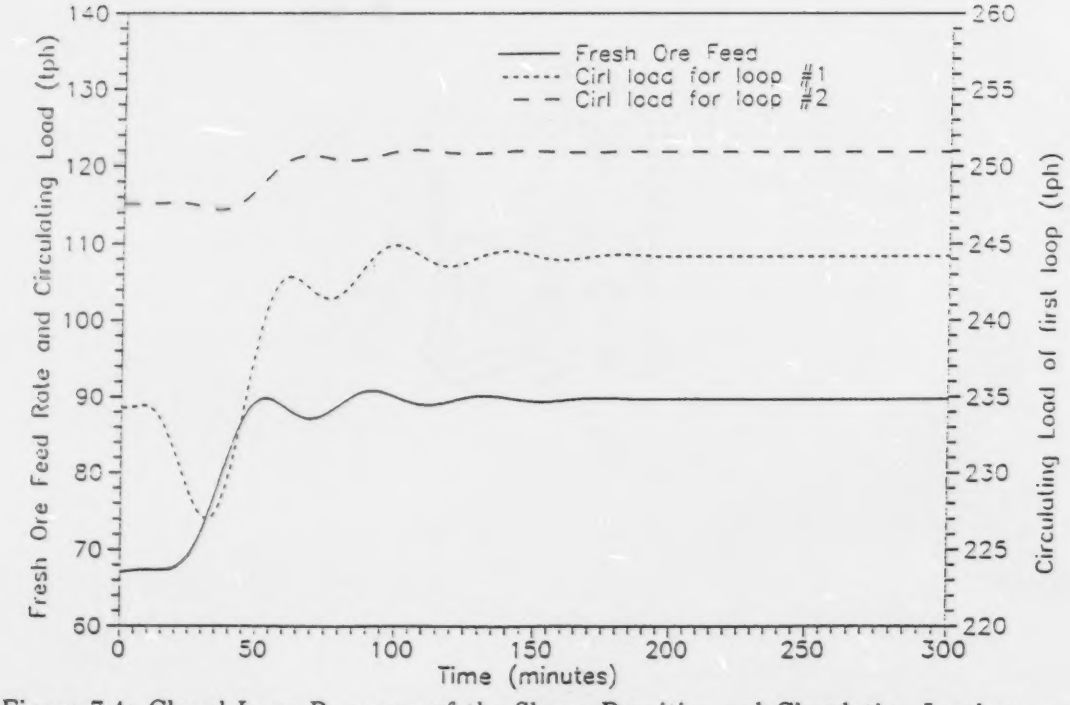

Figure 7.4: Closed Loop Response of the Slurry Densities and Circulating Loads to a Step Decrease in the Fresh Ore Feed Hardness with $K_f = 1.7$, $\tau_I = 0.9, K_{s1} = 1.5, \tau_{I1} = 1.0, K_{s2} = 1.2, \tau_{I2} = 1.0$ and IAE=21.9

As a consequence one can expect a behaviour opposite to that observed for an increase in hardness. The procedure of using controller setting established individually for each loop was discarded in favor of utilizing the same controller constants as for the increase in hardness. The result of this approach is shown by the responses in Figures. 7.3 and 7.4. Further tuning of the controller constants did not yield any significant changes in the IAE value so the controller constants were not changed.

7.3.2 Controlling a Step Change in Density

As mentioned earlier in Chapter 6, even though a change in density without an accompanying change in hardness is a purely hypothetical situation, it was decided to test the performance of the controller in the presence of only a disturbance in the density. As was observed from the open loop response in Figures. 6.15 and 6.16, an increase in density of the fresh ore leads to a higher COS which would imply an increase in the fresh ore feed. As a consequence, one can expect an increase in the flow of slurry to the sumps. To maintain the levels, the sump level controller will decrease the water flows to the sumps leading to an increase in the cyclone feed slurry density. As well the circulating loads will increase, both due to increase in FOF and the increase in density. The initial the controller constants were taken the same as for the case of a hardness disturbance, and the IAE value was 58.7. The value of the IAE was reduced by tuning of the controller constants and the closed responses are as shown in Figures. 7.5 and 7.6.

7.3.3 Controlling a Simultaneous Disturbance of Hardness and Density

A simultaneous change in hardness and density is one that is most likely to occur in a typical plant and hence requires special mention. Once again, the initial controller

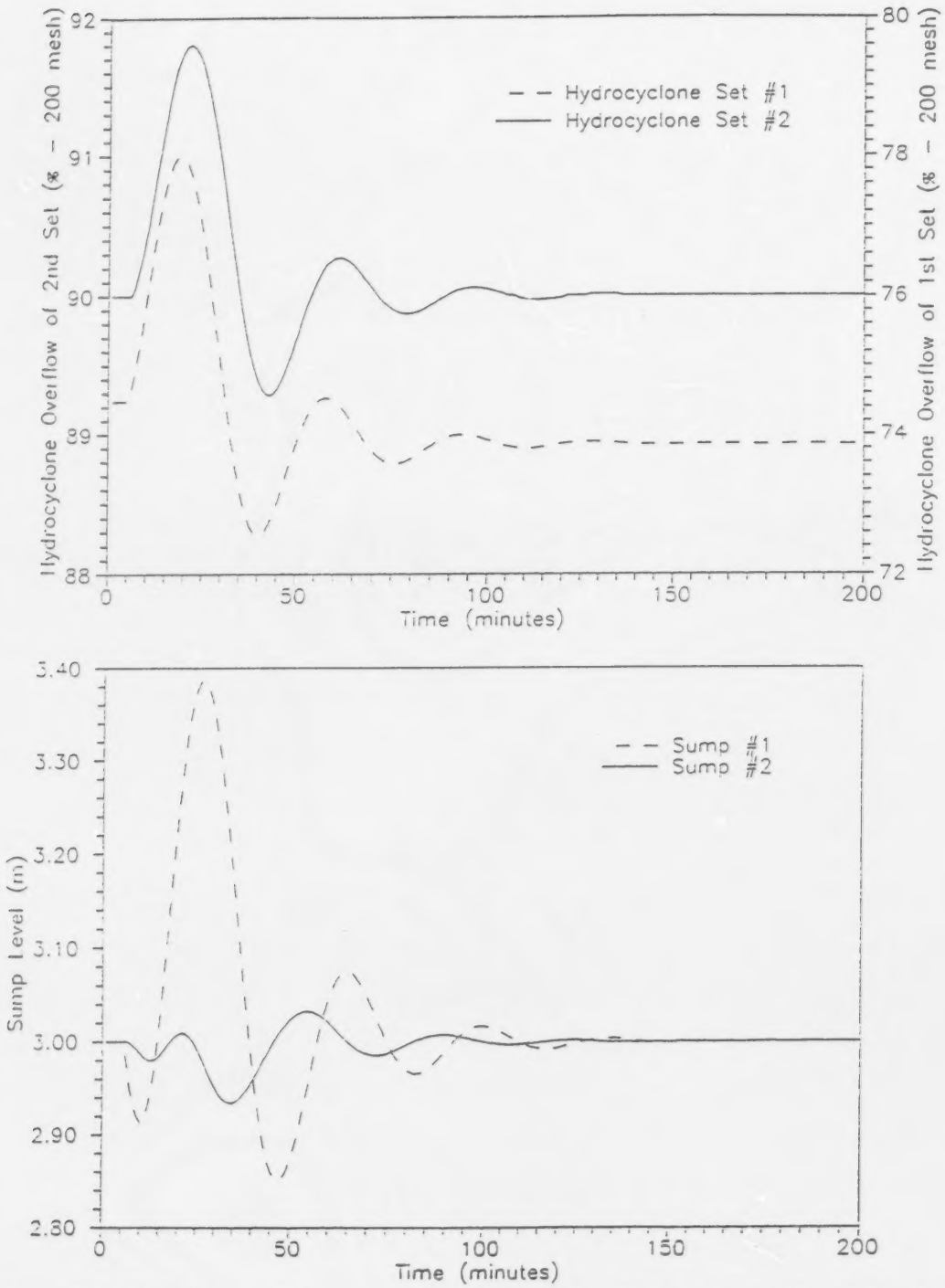

Figure 7.5: Closed Loop Response of the Hydrocyclone Overflows and Sump Levels to a Step Increase in the Fresh Ore Feed Density with $K_f = 1.5$, $\tau_I = 0.9, K_{s1} = 1.3, \tau_{I1} = 1.0, K_{s2} = 1.0, \tau_{I2} = 1.0$ and IAE=37.4

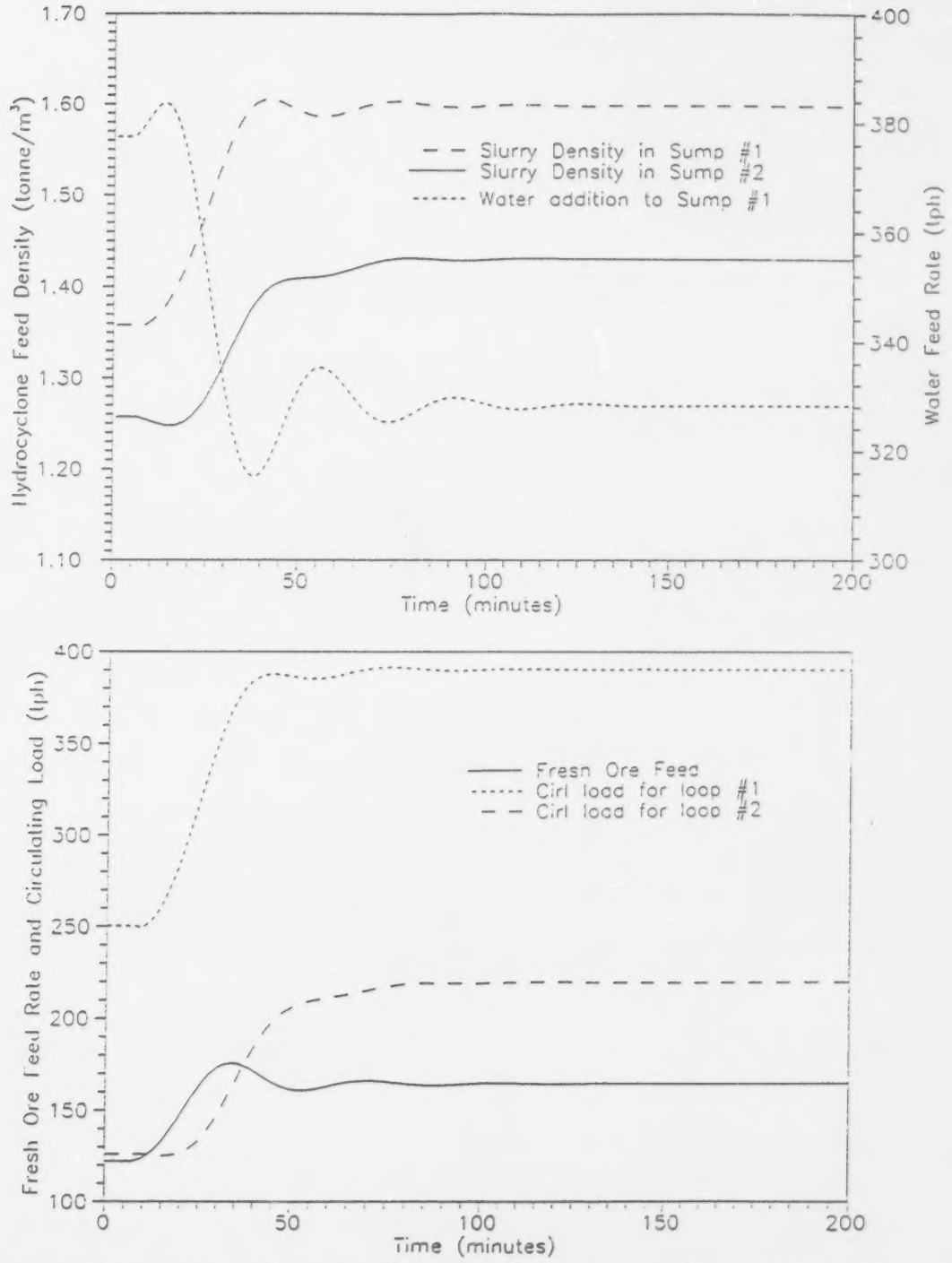

Figure 7.6: Closed Loop Response of the Slurry Densities and Circulating Loads to a Step Increase in the Fresh Ore Feed Density with $K_f = 1.5$, $\tau_f = 0.9$, $K_{s1} = 1.3$, $\tau_{I1} = 1.0$, $K_{s2} = 1.0$, $\tau_{I2} = 1.0$ and IAE=37.4

constants were chosen as $K_c = 1.7$ and $\tau_I = 0.9$. However these values resulted in an oscillatory behaviour. The reason for this can be seen from Figure. 6.17. The sump level response to a combined disturbance of disturbance of density and hardness exhibits an inverse response. In the closed loop situation, the sump water flow moves to 'compensate' accordingly for this kind of response. Consequently, high values of K_c for the sump level controller lead to an oscillatory kind of response in the overall control performance. In such a situation the solution is to back off on the level control in order to tighten up on the COS control and improve the circuit performance. By decreasing the sump level controller by 0.8, the COS control is greatly improved. Using K_c of 1.2 and τ_I equal to 3, the IAE value was reduced to a more acceptable value of 19.7. The closed loop responses are shown in Figures. 7.7 and 7.8. Perhaps a proportional only controller for the sump level would have been an alternative worth considering as suggested by Lynch (1977). But in that work he has used a variable speed pump. One could generalize saying that the control approach depends on the option available to the control engineer.

7.3.4 Controlling an Unusual Disturbance

In an attempt to analyze the behaviour of the controller to unusual disturbances, the response of the circuit was observed for a situation where there is a step input of 10 *tonnes/h* of water to the grinding mill #3. In a sense, this disturbance can be viewed as the extraneous water disturbance to the circuit discussed in Chapter 5. This disturbance was unique in the sense that there were no open loop tests to guide in fixing the initial controller constants nor were there any other indication of the kind of expected response. In view of this it was decided to assume initial values of $K_c = 1.7$ and $\tau_I = 0.9$, that is, the same value as for the hardness change. This followed from a reasoning that the controller setting for regulatory control should be able to handle

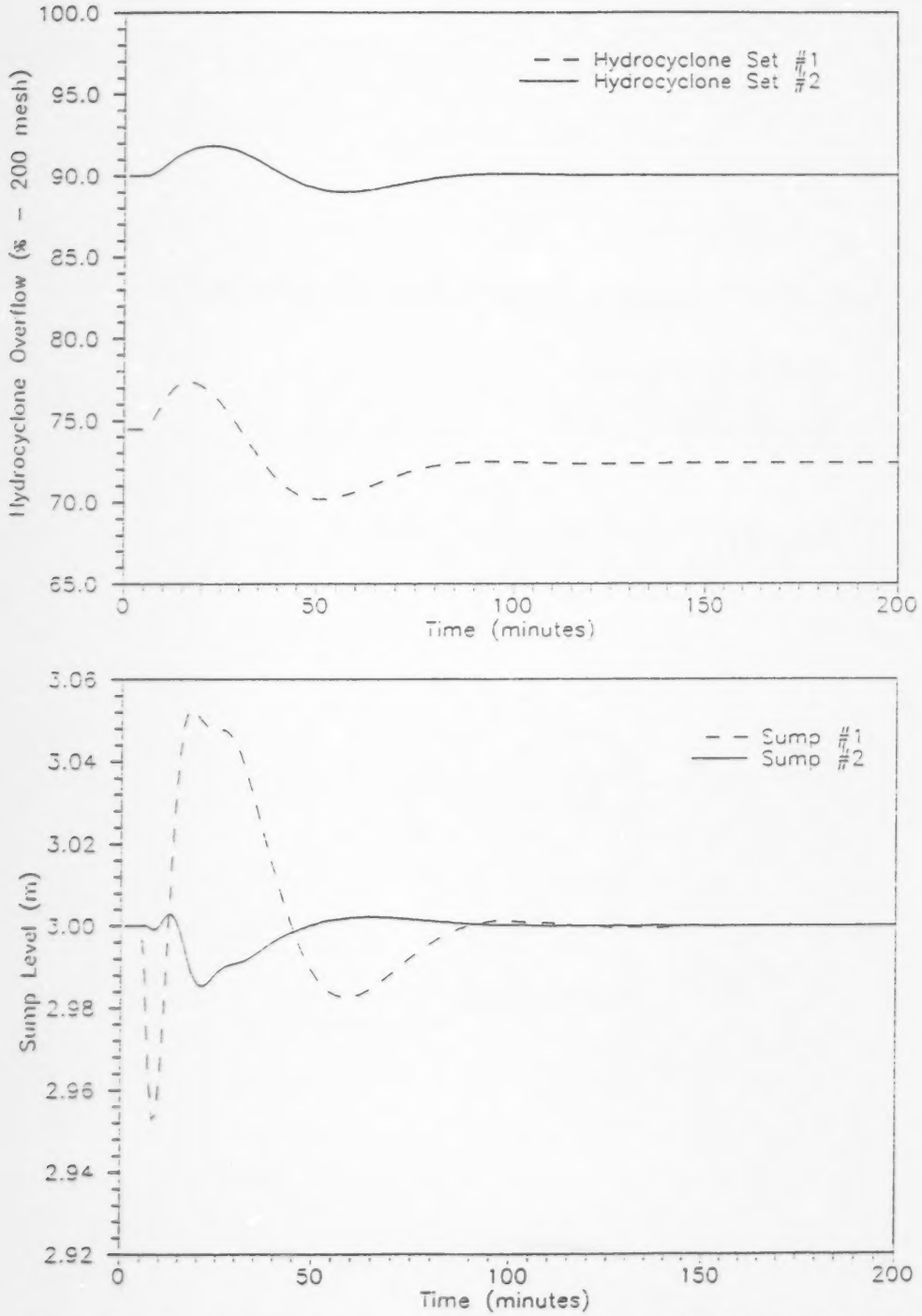

Figure 7.7: Closed Loop Response of the Hydrocyclone Overflows and Sump Levels to a Step Increase in the Fresh Ore Feed Density & Hardness with $K_f = 1.2$, $\tau_I = 3$, $K_{s1} = 0.5$, $\tau_{I1} = 1.0$, $K_{s2} = 1.0$, $\tau_{I2} = 1.0$ and IAE=19.7

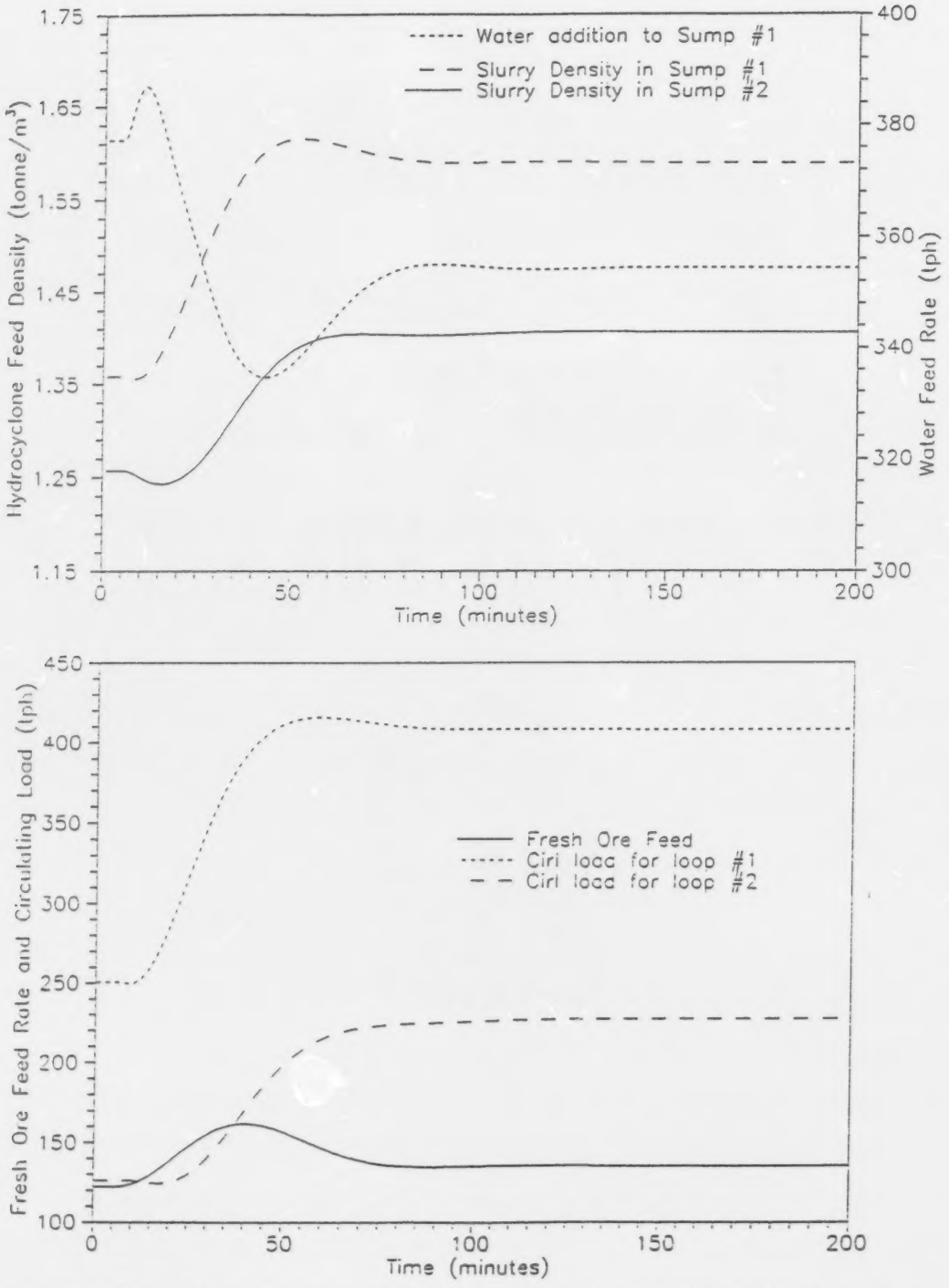
Water addition to Sump #1
Slurry Density in Sump #1
Slurry Density in Sump #2
Hydrocyclone Feed Density (tonne/m³)
Water Feed Rate (lph)
Time (minutes)
Fresh Ore Feed
Ciri load for loop #1
Ciri load for loop #2
Fresh Ore Feed Rate and Circulating Load (tph)
Time (minutes)

Figure 7.8: Closed Loop Response of the Slurry Densities and Circulating Loads to a Step Increase in the Fresh Ore Feed Density & Hardness with $K_f = 1.2$, $\tau_I = 3$, $K_{s1} = 0.5$, $\tau_{I1} = 1.0$, $K_{s2} = 1.0$, $\tau_{I2} = 1.0$ and IAE=19.7

as many 'disturbances' as possible. Consequently, the controller settings were left unchanged and the performance of the system simulated. Surprisingly, as shown in Figures. 7.9 and 7.10, the control was quite good with the COS settling in about 60 minutes. Similarly the sump levels quickly settle to their setpoint values and the whole circuit attains the new steady state in approximately 75 minutes. It must be noted that a similar disturbance could have been introduced to the second sump and appropriate control action could have been observed. In fact, if at all, the first and second sumps are the most likely places for such a disturbance to occur. However, the above situation, apart from demonstrating the satisfactory response of the controller to an 'unexpected' disturbance illustrates the utility of the simulator. Although this particular simulation did not add any new insight to controller design, it was useful in showing up the robustness of the controller being employed.

7.3.5 Servo Control

Servo control is often given secondary in some control studies because it is felt that in a typical plant, disturbance rejection is a more important function of a controller than set point tracking because of the higher frequency of load disturbances than changes in set points. However, it is useful to demonstrate the robustness of the controllers and to observe the response of the circuit to a change in the set point as on occasion it might be necessary to change the setpoint if warranted by changes in either upstream or downstream conditions. In these cases the changes to the setpoint are usually ramped in order to avoid sudden upsets in the circuits. At the outset it should be mentioned that Flintoff *et al.*(1985) and McDougall (1987) in their work have indicated that for the controller that was controlling COS using FOF some retuning of the 'regulatory' controller constants was required for satisfactory servo control. Figures. 7.11 and 7.12 show the response of the circuit variables for a 3% increase in the COS setpoint.

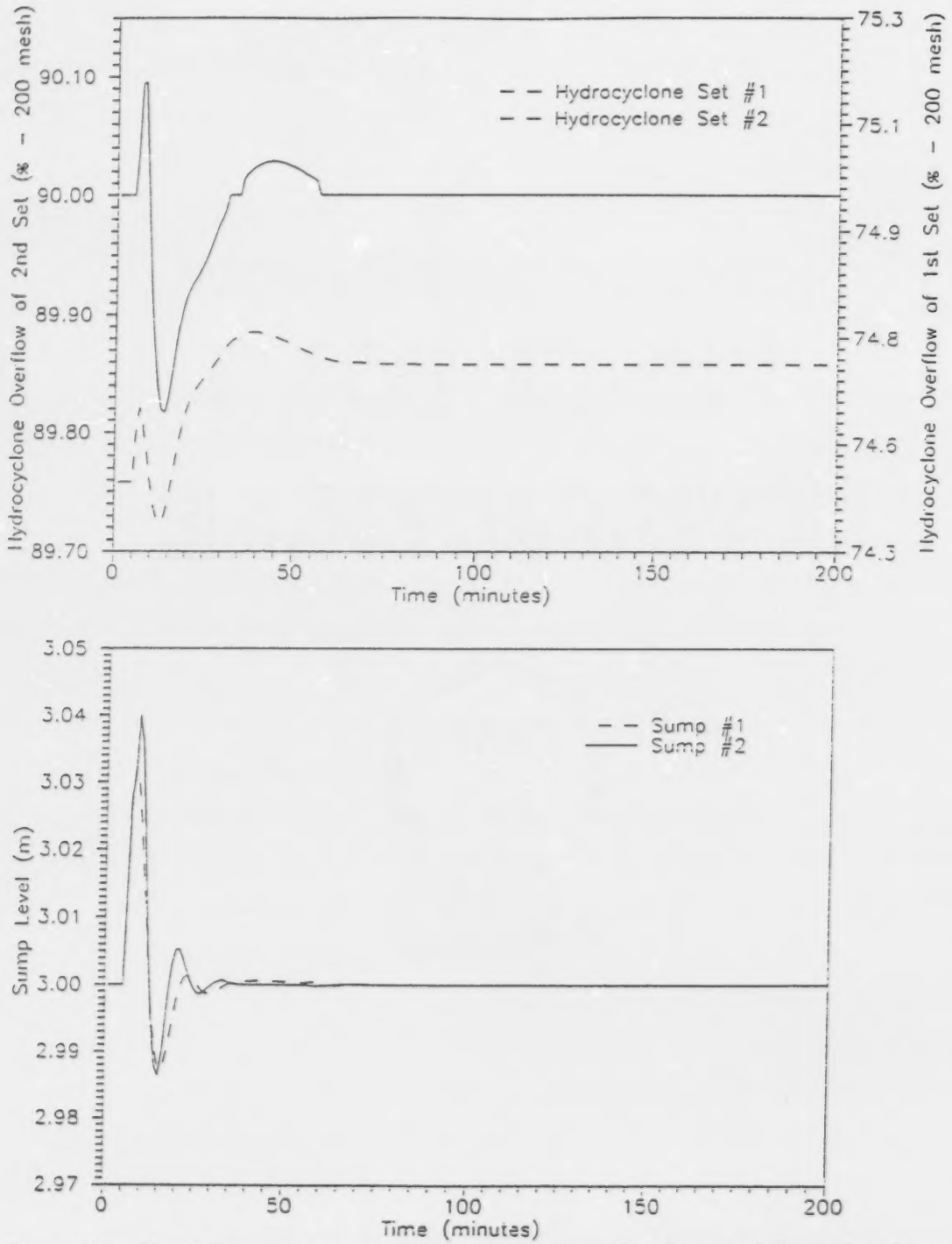

Figure 7.9: Closed Loop Response of the Hydrocyclone Overflows and Sump Levels to a 10 *tph* Step in Water Input to Ball Mill # 3 with $K_f = 1.7$, $\tau_I = 0.9, K_{s1} = 1.5, \tau_{I1} = 1.0, K_{s2} = 1.2, \tau_{I2} = 1.0$ and IAE=29.8

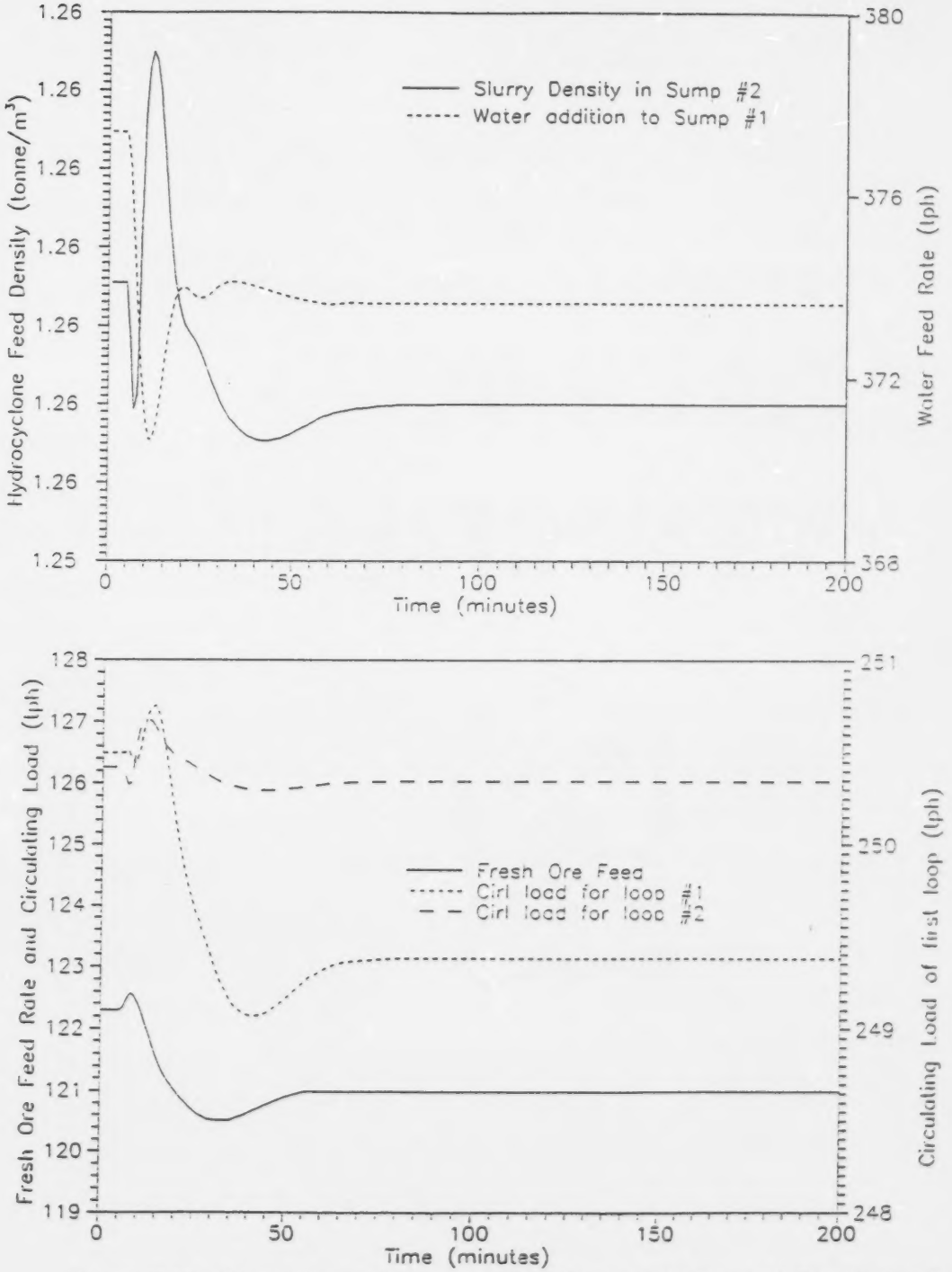
Slurry Density in Sump #2
Water addition to Sump #1
Hydrocyclone Feed Density (tonne/m³)
Water Feed Rate (tph)
Time (minutes)
Fresh Ore Feed
Cirl load for loop #1
Cirl load for loop #2
Fresh Ore Feed Rate and Circulating Load (tph)
Circulating Load of first loop (tph)
Time (minutes)

Figure 7.10: Closed Loop Response of the Slurry Densities and Circulating Loads to a 10 *tph* Step in Water Input to Ball Mill # 3 with $K_f = 1.7$, $\tau_I = 0.9, K_{s1} = 1.5, \tau_{I1} = 1.0, K_{s2} = 1.2, \tau_{I2} = 1.0$ and IAE=29.8

As with regulatory control it is quite easy to degrade the controller performance by demanding unrealistic changes. Set point changes need to be reasonable and enough time should be allowed for the controller to reach the new steady state. For this work a step change of ±3% in the COS set point was thought to be adequate. This change was however not ramped because the desire was to observe whether the controller could handle such a change when abruptly introduced. As observed by McDougall (1987) the controller performance with regulatory settings resulted in a slightly oscillatory performance and had a IAE of 80.7 for COS. Detuning the K_c values of the COS controller from 1.7 to 0.5 resulted in a better performance and the results are shown in Figures. 7.11 and 7.12 The circuit response to a -3% decrease in setponit is shown in Figures. 7.13 and 7.14. Further tuning of the constants brought the IAE to an acceptable 51.62.

Although some retuning of the regulatory controller settings was performed to improve the control performance, it should be mentioned that the controller can handle ±3% set point changes even without retuning. Consequently, it is felt that the controller should be tuned so that it performs good disturbance rejection, a more frequent occurrence, and can handle the occasional set point changes adequately.

7.4 Inferential Control of Grinding Circuits

It is common practice to use optimum grind size and ore recovery values obtained from representative laboratory work to design grinding circuit flow rates. This is because the relationships between particle size and upstream and downstream parameters are not understood well enough to permit on-line optimum grind size calculation. The principal reason for this lack of understanding is the frequent occurrence of changes in the characteristics of the ore entering the grinding circuit which dynamically affect

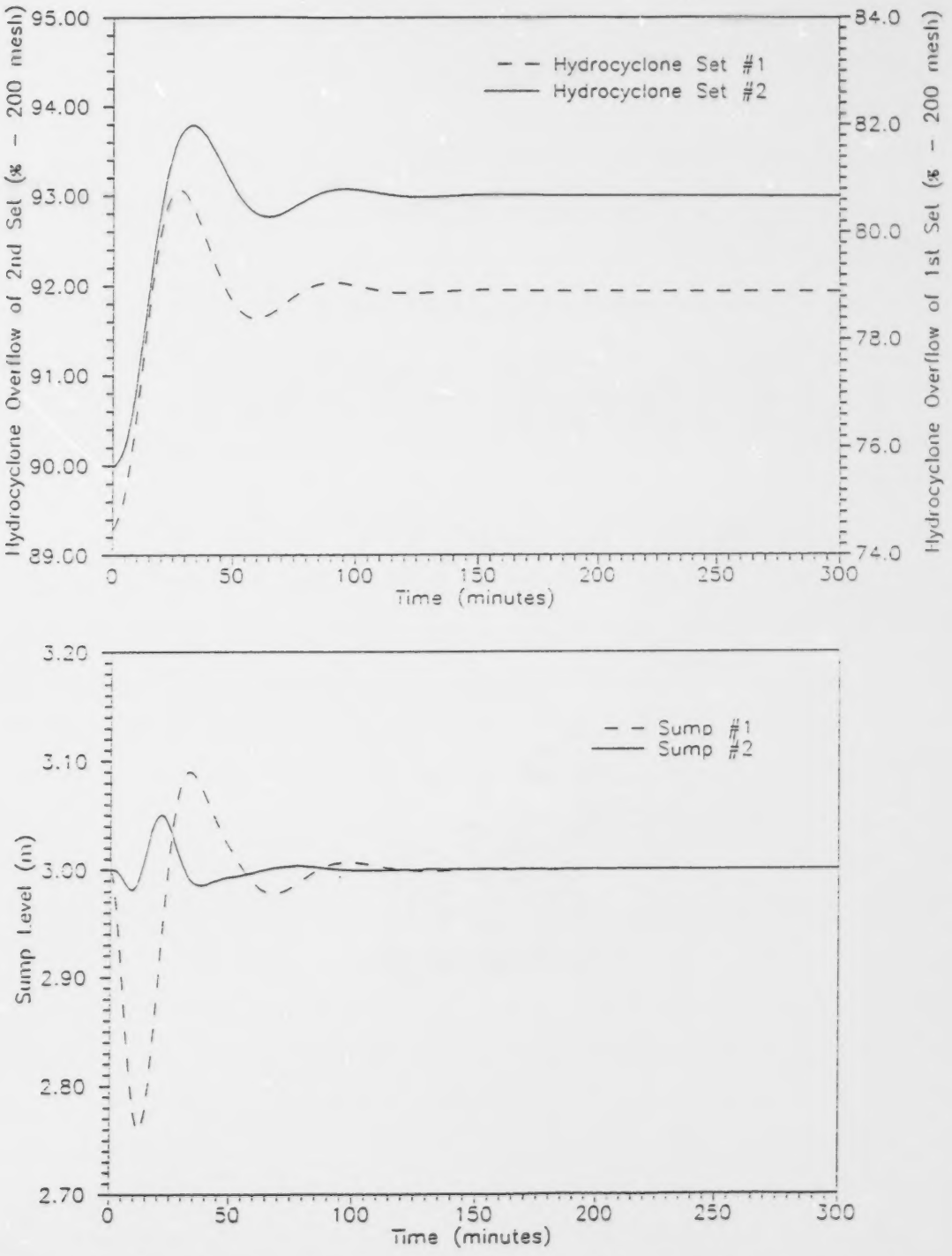

Figure 7.11: Closed Loop Response of the Hydrocyclone Overflows and Sump Levels for a +3% Change in the COS Setpoint with $K_f = 0.5$, $\tau_f = 0.9$, $K_{s1} = 1.5$, $\tau_{I1} = 1.0$, $K_{s2} = 1.2$, $\tau_{I2} = 1.0$ and IAE=77.3

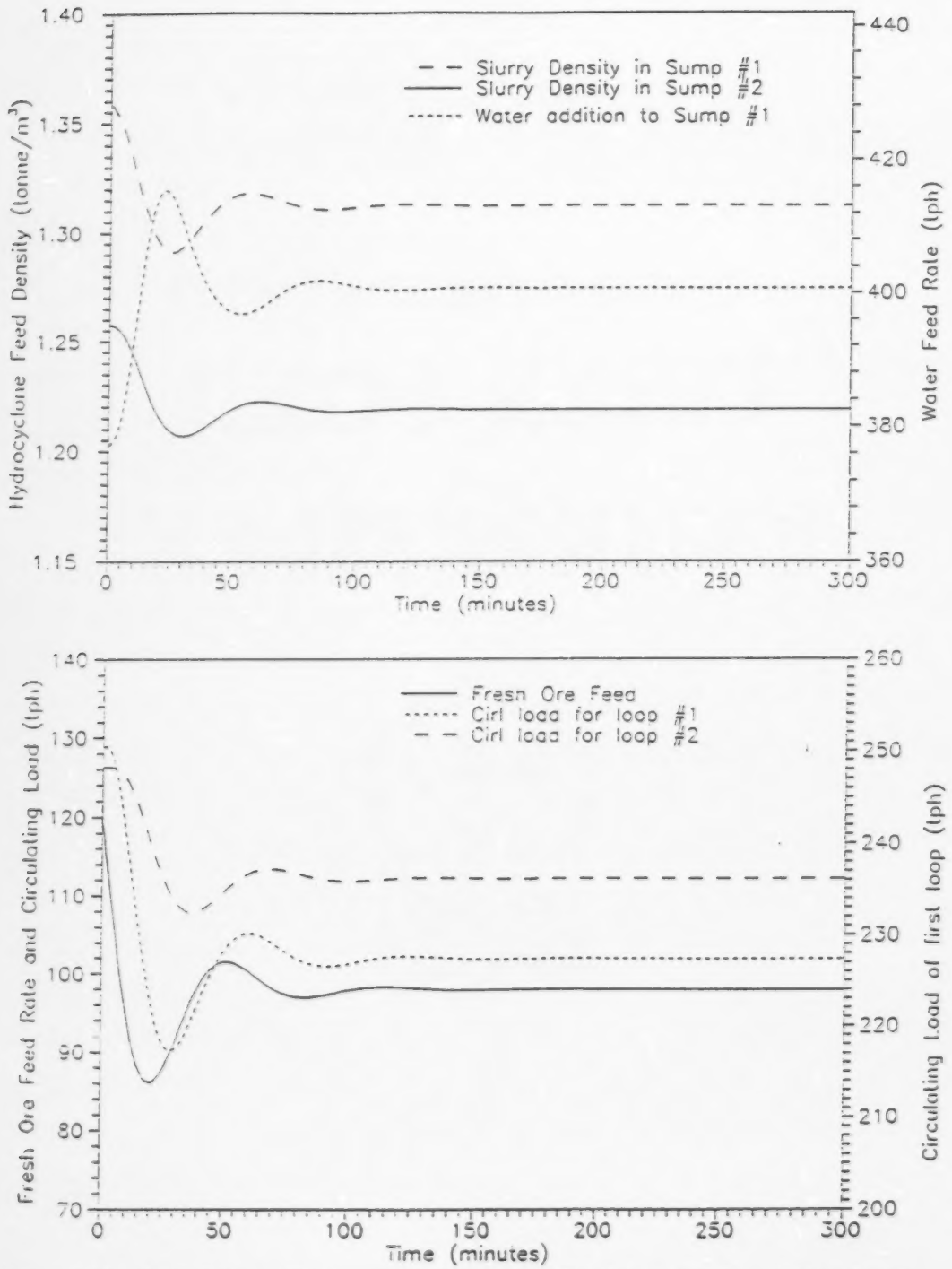
Slurry Density in Sump #1
Slurry Density in Sump #2
Water addition to Sump #1
Hydrocyclone Feed Density (tonne/m³)
Water Feed Rate (tph)
Time (minutes)
Fresh Ore Feed
Circ load for loop #1
Circ load for loop #2
Fresh Ore Feed Rate and Circulating Load (tph)
Circulating Load of first loop (tph)
Time (minutes)

Figure 7.12: Closed Loop Response of the Slurry Densities and Circulating Loads for a +3% Change in the COS Setpoint with $K_f = 0.5$, $\tau_I = 0.9$, $K_{s1} = 1.5$, $\tau_{I1} = 1.0$, $K_{s2} = 1.2$, $\tau_{I2} = 1.0$ and IAE=77.3

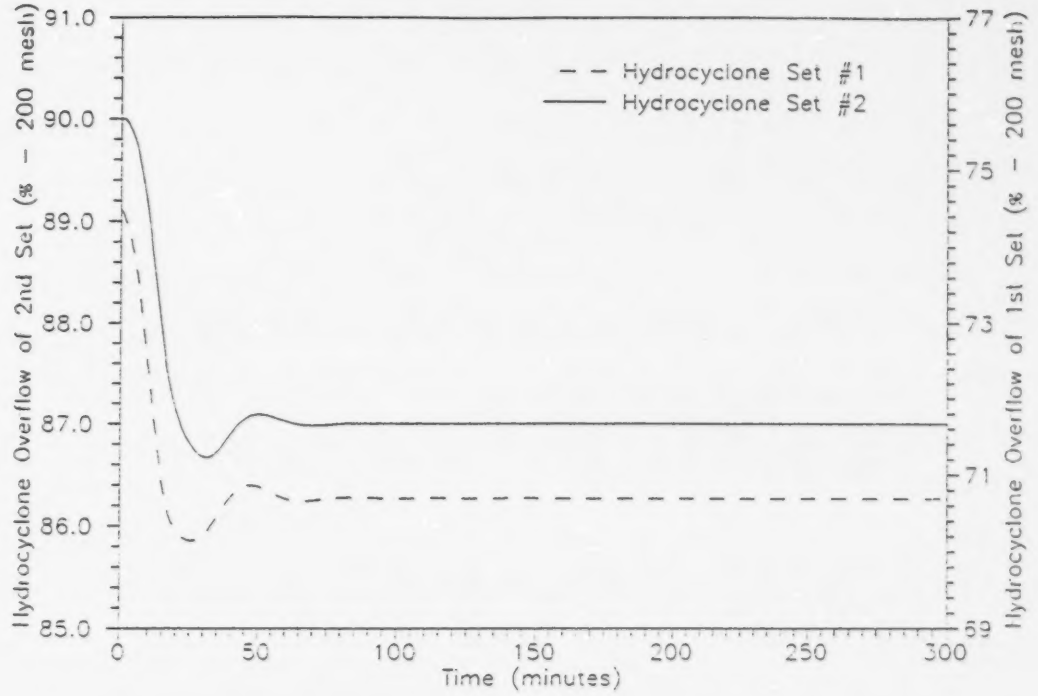

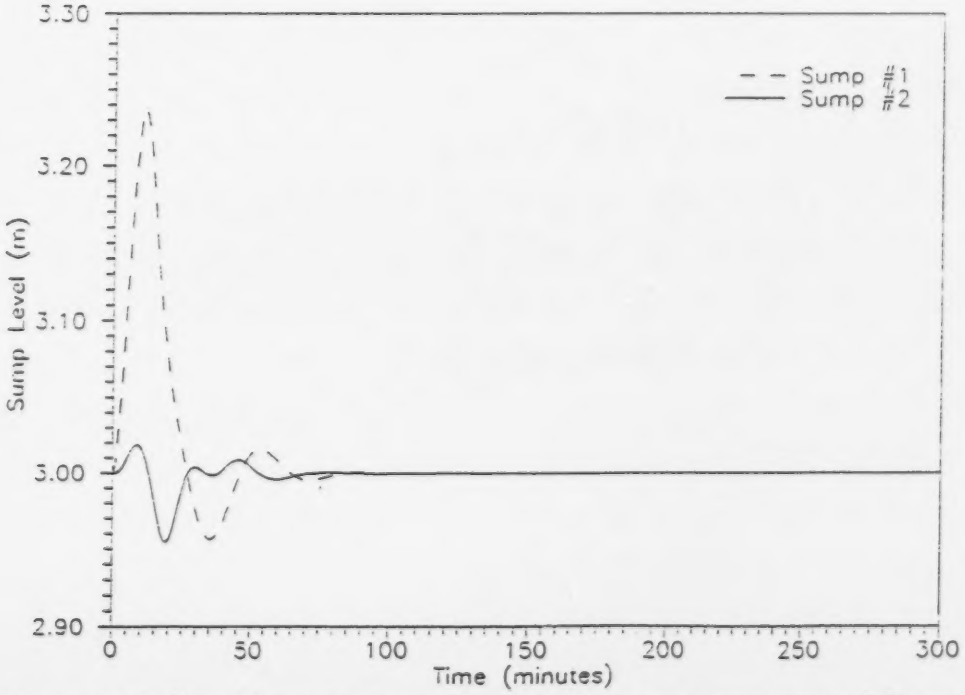

Figure 7.13: Closed Loop Response of the Hydrocyclone Overflows and Sump Levels for a -3% Change in the COS Setpoint with $K_f = 0.5$, $\tau_f = 0.9, K_{s1} = 1.0, \tau_{I1} = 1.0, K_{s2} = 1.0, \tau_{I2} = 1.0$ and IAE=51.6

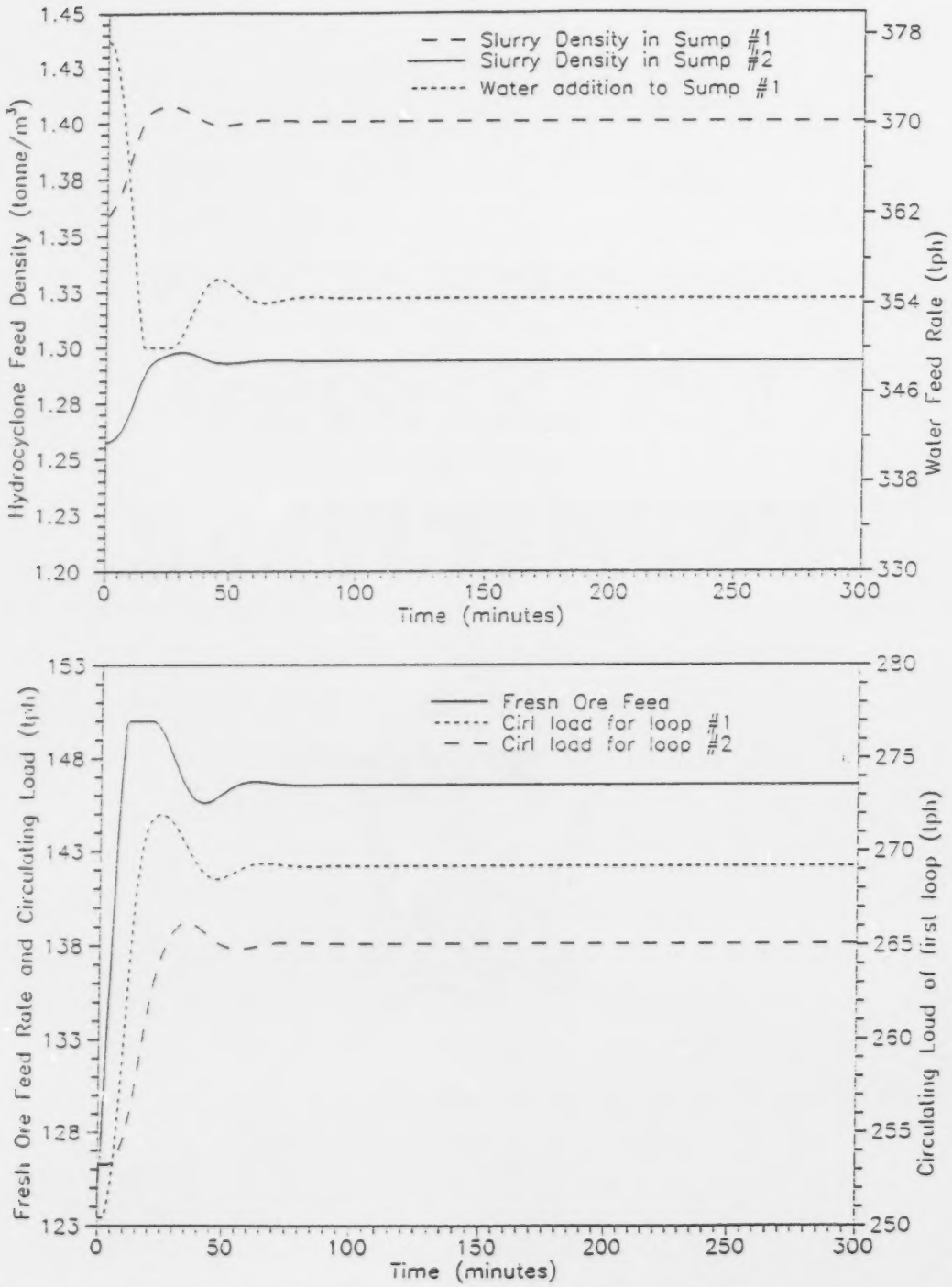
Slurry Density in Sump #1
Slurry Density in Sump #2
Water addition to Sump #1
Hydrocyclone Feed Density (tonne/m³)
Water Feed Rate (tph)
Time (minutes)
Fresh Ore Feed
Circ load for loop #1
Circ load for loop #2
Fresh Ore Feed Rate and Circulating Load (tph)
Circulating Load of first loop (tph)
Time (minutes)

Figure 7.14: Closed Loop Response of the Slurry Densities and Circulating Loads for a -3% Change in the COS Setpoint with $K_f = 0.5$, $\tau_I = 0.9, K_{s1} = 1.0, \tau_{I1} = 1.0, K_{s2} = 1.0, \tau_{I2} = 1.0$ and IAE=51.6

the circuit operation. It is now well accepted that the measurement of particle size of the grinding circuit product is key for any control strategy designed for efficient operation.

The particle size in slurries can be measured directly by a continuous on-line particle size monitor (PSM), or inferred from other circuit variables by means of a mathematical equation. Inferred particle size measurement systems unlike PSMs operate on the principle that changes in the operating conditions of a grinding circuit (such as hardness or size distribution of ore feed) result in a change of the product particle size and circulating load of the circuit. Consequently, if the mass flows of ore and water in the hydrocyclone feed stream (which influences hydrocyclone operation) along with other measurable variables are known, it is possible to infer the nature and magnitude of the resultant change in the product grind size. This method provides two additional benefits compared to alternative methods of on-line size analysis -

- data from the instrumentation used for inferring particle size provides significant information on the performance of the grinding circuit.

- problems associated with the sampling of high volume slurry streams are avoided along with their errors.

Inferred size calculation of the particle size in the hydrocyclone overflow stream is based on mass flow measurements of the feed streams to the hydrocyclones and the fresh ore feed rate using an expression of the form (Kawatra and Seitz, 1982):

$$\log(\%-200\,mesh) = k_1 - k_2 FOF + k_3 MFW - k_4 MFO$$

The water and ore rates, MFW and MFO are calculated directly from nuclear density gauges and magnetic flowmeters, signals and the constants k_1 to k_4 are found by regression analysis of experimental data. Once a reliable mathematical model of the classifier performance is established, the model can be used as an on-line sizing

instrument for use with the desired control strategy.

7.5 The Estimator Model for the Hemlo Circuit

To develop a valid estimator model for the classifier at the Hemlo grinding circuit, the dynamic simulator was used to obtain the response of the circuit to various disturbances. The observed variables were :

- fresh feed ore mass flow rate, *i.e.* FOF
- percent product passing 200 mesh in the hydrocyclone overflow stream, *i.e.* COS
- mass flow rate of solids to the hydrocyclone set # 2, *i.e.* MFO
- mass flow rate of water to the hydrocyclone set # 2, *i.e.* MFW
- total mass flow rate of water to the circuit, *i.e.* TW

A regression model of the form

$$\log(\% - 200\,mesh) = k_1 + k_2 FOF + k_3 MFO + k_4 MFW + k_5 TW$$

was thought to adequately model the circuit. The statistical software package, Minitab, available on the University of Alberta Amdahl 5870 computer was used to obtain a regression model.

Only a single input variable was disturbed for each test with the change in the other circuit variables being recorded after the circuit reached a new steady state. The circuit was subjected, in turn, to step changes of $\pm 10\%, \pm 5\%, \pm 10\%$ respectively in FOF, SWF1 and SWF2. The estimator model equation was :

$$\log(\% - 200\,mesh) = 4.64 - 0.00118 FOF$$

which predicts that the COS is inversely proportional to only the fresh ore rate. While the sign of the coefficient is correct, it is evident that assuming the overflow size to be a function of only the fresh ore feed rate would lead to erroneous results. Consequently this model was discarded and a better representation of the classification action was sought. In the second approach, simultaneous, smaller, disturbances were applied to the feed streams in a random fashion in order to simulate a more realistic situation. This method resulted in the following expression:

$$\log(\% - 200\,mesh) = 4.90 + 0.00108FOF - 0.00135MFO - 0.00044TW$$

Correlation between the variables was still quite high but this seemed to be a slightly better model. However the sign of the coefficient relating COS and FOF is not consistent with known operation of COS and FOF exhibiting an inversely proportional relationship *i.e.* the percent of the ore that is less than 200 mesh in size will decrease as the FOF is increased and vice versa. This could cause problems when attempting to control the product size in the case of a load disturbance. On substitution of the steady-state values into the expression, there was a prediction error of only about 1% which indicates that the expression provides a reasonably good estimation of the steady state conditions. The next step was to use the estimator and run close-loop simulations. The resulting simulations showed that the predicted values of COS were significantly different from the plant (simulator) values during the transient portion of the response but once the plant reaches its new steady state, the estimator's prediction is reliable. This behaviour of the regression model typifies the result of applying multiple linear regression to highly correlated data. Often, in such cases for a relationship of the form $\underline{Y} = \underline{A}\ \underline{X}$, the matrix A is so ill-conditioned that a new set of X values will alter $\underline{A}$ significantly. The only way to avoid such a problem is to obtain a good representative data set for regression. Consequently, it was decided to

obtain a better set of data for regression analysis. In view of the final objective of implementing such an estimator on a real plant, it was decided to include parameters which could be directly measured. Hence it was determined that circuit parameters like sump levels (SPLS), inlet pressure (PR) and hydrocyclone feed slurry density (CFD) should be monitored in addition to the input flow stream rates of ore and water. Since CFD was being measured it was felt that logging in MFO and MFW values was unnecessary. Factorial design of experiments, one of the well known statistical methods, was thought to be ideal in that it not only minimizes the amount of data that needs to be collected but also shows the significance of various input variables on output variables. Appendix C provides an introduction to designing a factorial experiment. A 2^4 factorial experiment was performed and the results were analyzed. Details of the run are also reported in Appendix C. The factors thought to influence the performance characteristics of the grinding circuit at Hemlo and subjected to a two level factorial experiment were :

- fresh ore feed rate *i.e.* FOF
- water feed to sump # 1 *i.e.* SWF1
- water feed to sump # 2 *i.e.* SWF2
- fresh ore feed hardness *i.e.* HRD

After making due assumptions, it was concluded that while individually all four factors were significant to the hydrocyclone product stream, some interaction effects like combined effects of fresh ore feed rate and water to sump # 2, combined effects of water flow rates to both sumps etc. were not significant to the product size. The estimator model using the data generated by the factorial experiment was found to

be:

$$\log(\%-200mesh) = 3.78 - 0.0074SPL2 - 1.33CFD + 0.00145FOF$$

$$-0.000763SWF1 - 0.000569SWF2$$

Once again the model predicted FOF and COS to be directly proportional. The steady state prediction shows an error of 0.8% which shows that the steady state estimation is good. As was done in the Type I feedback control systems design case, the first starting point for designing the controllers for the estimator model is to examine the open loop responses of all the circuit variables in the regression equation. It should be mentioned that CFD here describes the density of the slurry feed to hydrocyclone set #2. From Figures. 6.11 and 6.12 one can see the responses of the COS, sump level and CFD to a step change in hardness. While the COS decreases steadily to a new steady state, both, the slurry level in sump #2 and the corresponding slurry density show a non - minimum phase response immediately after the disturbance occurs. In a closed loop situation with the simulator, a similar situation would drive the controller to reduce the FOF while the water flows will be altered to keep the levels constant. However, with the estimator model the situation will be different. An increase in the hardness will first manifest itself as an increase in the slurry level in sump #1 as the circulating load in the first loop increases. Since the level in sump #1 is not a factor in the regression equation, it will not show up in the estimator. However, the increased circulating load in the first loop will mean that the overflow from the first hydrocyclone decreases. As a consequence, both, the level in sump #2 and slurry feed density in sump #2 decrease. This phenomenon appears in the estimator equation as a net increase in the right hand side. At the same time the sump level controllers will try to 'compensate' for changes in circulating load by decreasing the water flow to sump #1 and increasing the flow to sump #2. While

this change in water rate the sump #1 will not be immediately felt in the latter part of the circuit *i.e.* the second loop, the increase in flow of water to sump #2 will further decrease the CFD thereby increasing the COS even further. The result of all this will be that while the actual COS will reduce as a result of the increase in hardness, the estimator will predict an initial increase in the COS. This prediction by the estimator will drive the control action so as to reduce the COS *i.e.* increase the FOF. Therefore due to the erroneous prediction by the estimator, the circuit will begin to increase the flow of fresh ore with an increased hardness ! This 'inverse' response will continue till the increase in the circulating load in the first loop reaches the sump in the second loop at which time the COS will steadily decrease as SL2 and CFD increase, and SWF2 decreases. However by this time the circuit is virtually 'out of control' and although a controller with a small gain can ultimately take the circuit to steady state, the control is not very robust and in case of large disturbance, cannot be controlled.

This analysis shows that development of a reliable regression type simulator does not happen to be a trivial task. Due to the presence of a sumps and the mills which act as a capacitor, the effects upstream are not relayed to the COS until significant amount of time has elapsed. The key to developing an estimator model for such systems would seem to suggest a method wherein the transient behaviour of the circuit is also taken into consideration. While using time delay compensation techniques maybe a possibility, it must be remembered that this inverse effect is prevalent for a considerable amount of time and therefore such a scheme could lead to degraded controller performance. Other viable solutions could be the use of self tuning controllers, adaptive controllers or controllers based on pole placement techniques. However such methods are complicated and time consuming. Among the easier techniques that

might be considered is the use of an estimator based on a regression equation generated by a multiple linear regression package and continuously updated. This would then include the transient effects as well as take care of the steady state conditions.

Chapter 8

Conclusions and Recommendations

8.1 Conclusions

With the realization that the mineral industry is still interested in a general purpose dynamic grinding circuit simulator, this work, in continuation of previous efforts at the University of Alberta, was directed to developing a dynamic simulator that could simulate the operation of an existing plant so that it could be employed to design an appropriate control strategy. At every stage of the development, this simulator has been structured so that the users can easily develop their own simulator by including the appropriate combinations of the various modules available. The current version of the simulator will operate on any IBM PC or XT using the DOS 3.2 operating system and the MS FORTRAN compiler.

Following the DYFLO2 programming approach, the simulator structure is highly modular and allows for as much expansion as desired. An interactive front end allows the user to construct the data file with minimum effort and use of COMMON BLOCKS facilitates passing of information from one subroutine to another. Other features include a choice of open loop, closed loop simulations and options

to recover results of every simulation. As well, the DYFLO2 subroutines have been modified and used as a framework to design a separate control block that offers the user a choice of control schemes for each run.

The simulator has been tested for its reliability by simulating the Hemlo grinding circuit. First, the open loop characteristics were demonstrated by the simulator and subsequently tested to perform closed loop simulations with an appropriate control strategy. The open loop simulations reveal some interactions between the circuit variables though the response was uniformly linear. As has been demonstrated by the results presented in Chapter 7, the Type I control strategy using the fresh ore feed rate to control the percent overflow and sump water addition rates to control sump levels was found to perform regulatory control quite well. Simple PI feedback control algorithm was adopted and both the hydrocyclone sets were fed by fixed speed pumps.

Realizing that the Plitt model for hydrocyclone required a lot of data about a circuit before it could predict the circuit's product stream size distribution, an attempt was made to design an 'estimator' that could predict the product size from the measurements of input and other measureable output variables of the circuit. Factorial design was adopted to collect a representative set of data that could be used to develop a model by regression. Though the prediction of the product stream (COS) by this estimator was good at steady states, its performance during the transients was poor. Due to the high correlation between the circuit variables, developing of such an estimator capable of good prediction during the transient behaviour of the circuit is not an easy task. It is felt that till such time that a reliable general purpose estimator is not developed, the Plitt model is the most reliable model for predictions of the classification action of a hydrocyclone.

8.2 Suggestions for Future Work

In spite of including as many features as possible, it is recognized that the level of complexity is limited only by the user's imagination. It should be however kept in mind that increased complexity could result in the simulator becoming less flexible, less portable and accessible to only the trained expert. As well, cost and the time incurred for each run would increase. Despite these concerns, it is felt that the future researcher could look more closely at the following areas.

Modelling

A close inspection at the models described in Chapter 3 will reveal that the present method of pre-calculating the net friction factor from plant studies makes the simulator 'site-specific'. As referred in refcch:chap2, a method to dynamically calculate the friction head starting from the first principles should be incorporated in the simulator. This model should be able to handle both start-up and steady state situations.

A method to determine the Plitt hydrocyclone model constants on-line or alternately derive it from the Lynch-Rao constants should be considered. This capability will provide the user the choice of using either model for predicting hydrocyclone performance.

Finally, an alternate method to assign breakage and selection functions to individual mills should be established such that these functions are generated automatically by the simulator. This would perhaps imply inclusion of other functional forms besides the form currently implemented.

Simulation

In order to make such simulators really powerful and all purpose, it is necessary to design a grinding circuit simulator similar to the one developed in this work with a real time operating system. Such a package would mean that the simulator can be used both as an automatic controller of an actual grinding circuit as well as optimize and design grinding circuits off-line.

Similarly, inclusion of a plotting package to the simulator that creates trend plots of the grinding circuit controlled and manipulated variable would enhance the value of the simulator. This feature, apart from simplifying the plotting of simulation results, would also help the control engineer in controller tuning.

Control Strategies

Only continuous classical control has been implemented and evaluated. Inclusion of discrete control options would make the simulator more versatile. As well, advanced control algorithms like adaptive or other optimal controllers would give the user a wider choice of control options. Making the simulator capable of handling plant interactions and non-linearities would also be welcome.

Finally, to make the simulator represent the true behaviour of a grinding circuit, consideration should be given to including sensor element dynamics and measurement noise.

References

Adel,G.T. and K.V.S. Sastry. Design aspects of a mineral processing simulation package. In *Proc. 17th APCOM*, pages 681–692. SME/AIME Publication, 1982.

Apling, A.C., D Montaldo, and P.A. Young. Hydrocyclone model in an ore grinding context. In *Intl. Conf. on Hydrocyclones, BHRA Fluid Engineering*, pages 113–125, 1980.

Austin, L.G. A review introduction to the mathematical description of grinding as a rate process. *Powder Tech.*, 5:1–17, 1972.

Austin, L.G., R.R. Klimpel, and P.T. Luckie. Process engineering of size reduction. ball milling. *SME/AIME New York*, pages 388–407, 1984.

Bascur, O.A. and J.A. Herbst. Dynamic simulators for training personnel in the control of grinding/ floatation systems. In *Proc. IFAC Symp. on Automation for Mineral Resource Development*, pages 315–324, 1985.

Bloor, M.I.G. On axially symmetric flow models for hydrocyclones. In *3rd Intl. Conf. on Hydrocyclones, BHRA Fluid Engineering*, pages 83–90, 1987.

Bloor, M.I.G. and D.B. Ingham. The influence of vorticity on the efficiency of the hydrocyclone. In *2nd Intl. Conf. on Hydrocyclones, BHRA Fluid Engineering*, pages 41–50, 1984.

Bloor, M.I.G., D.B. Ingham, and S.D. Laverack. An analysis of boundary layer effects

in a hydrocyclone. In *Intl. Conf. on Hydrocyclones, BHRA Fluid Engineering*, pages 49–60, 1980.

Bradburn, R.G., B.C. Flintoff, and R.A. Walker. Practical approach to digital control of a grinding circuit at Brenda Mines Ltd. *SME/AIME Trans.*, 262:140–147, 1977.

Bradley, D. *The Hydrocyclone*. Pergamon Press, London, 1965.

Bradley, D. and D.J. Pulling. Flow patterns in the hydraulic cyclone and their interpretation in terms of performance. *Trans. Inst. Chem. Eng.*, 37:34–45, 1959.

Braun, T. and M. Bohnet. Influence of feed solids concentration on the performance of hydrocyclones. *Chem. Eng. and Tech.*, 13:15–20, 1990.

Deister, R.D. Buick concentrator process control development. *SME/AIME Trans.*, 280:50–55, 1986.

Duggins, R.K. and P.C.W. Frith. Turbulence effects in hydrocyclones. In *3rd Intl. Conf. on Hydrocyclones, BHRA Fluid Engineering*, pages 75–82, 1987.

Fahlstrom, P.H. Studies of the hydrocyclone as a classifier. In *Proc. 6th Intl. Min. Proc. Congr.*, pages 87–114, 1963.

Finlayson, R. M. and D.G. Hulbert. The simulation of the behaviour of individual minerals in a closed grinding circuit. In *Proc. 3rd IFAC Sym. on Automation in Mining Mineral and Metal Proc.*, pages 323–332, 1980.

Flintoff, B. C., L.R. Plitt, and A.A. Turak. Cyclone modelling: A review of present technology. *CIM Bulletin*, 80(905):39–50, 1987.

Flintoff, B.C., W.Y. Wong, and R.K. Wood. Dynamic simulation of grinding circuit control. *ISA Trans.*, 25(1):11–22, 1985.

Ford, M.A. and R.P. King. The simulation of ore dressing plants. *Intl. J Min. Proc.*, 12:285–304, 1984.

Fournier, R.D. and H.W. Smith. Experimental prameter identification for a dynamic model of a continuous rod mill. *CIM Bulletin*, 65:79–82, 1972.

Franks, R.G.E. DYFLO update. In *Proc. Summer Computer Simulation Conf.*, pages 507–513, 1982.

Gary, A.G. and F Maria. Alternate to standard friction factor equation. *Oil and Gas J.*, pages 120–127, April 1985.

Herbst, J.A. and J.F. Alba. An approach to adaptive optimal control of mineral processing operations. In *Preprint 15th Intl. Min. Proc. Congr.*, volume 3, pages 75–87, 1985.

Herbst, J.A. and O.A. Bascur. Mineral processing control in the 1980's - realities and dreams. In J.A. Herbst, editor, *Control '84, Mineral/Metallurgy Processing*, pages 197–215. SME/AIME, 1984.

Herbst, J.A. and D.W. Fuerstenau. Scale-up procedures for continuous grinding mill design using population balance models. *Intl. J. Min. Proc.*, pages 1–31, 1980.

Herbst, J.A. and A.L. Mular. Modelling and simulation of mineral processing unit operations. In A. Weiss, editor, *Computer Methods for the 80's in the Mineral Industry*, pages 823–840. SME/AIME, 1979.

Herbst, J.A. and K. Rajamani. Control of grinding circuits. In A. Weiss, editor, *Computer Methods for the 80's in the Mineral Industry*, pages 770–786. SME/AIME, 1979.

Herbst, J.A. and K. Rajamani. Modelling and simulation of mineral processing unit operations. In A. Weiss, editor, *Computer Methods for the 80's in the Mineral*

Industry, pages 823–840. SME/AIME, 1979.

Herbst, J.A., K. Rajamani, and Pate W.T. Identification of ore hardness disturbances in a grinding circuit using a Kalman filter. In *Proc. 3rd IFAC Symp. on Automation in Mining, Mineral and Metal Proc.*, pages 333–348, 1980.

Hinde, A.L., P.J.D. Lloyd, J.G. Mackay, and R.P. King. The use of stochastic modelling techniques to describe the dynamics of s gold milling circuit. In *Proc. 2nd IFAC Symp. on Automation in Mining, Mineral and Metal Proc.*, pages 565–575, 1977.

Holland-Batt, A.B. A bulk model for separation in hydrocyclones. *Trans. Inst. Min. Metall. (Section C)*, 91:c21–c25, 1982.

Hsieh, K.T. and K Rajamani. Phenomenological model of the hydrocyclone : Model development and verification for single-phase flow. *Intl. J. Min. Proc.*, 22:223–237, 1988.

Hulbert, D.G. The state of art in the control of milling circuits. In *Proc. 6th IFAC Sym. on Automation. Mining, Mineral and Metal. Proc.*, pages 1–10, 1989.

Hulbert, D.G., J. Koudstaal, M. Braae, and G.J. Gossman. Multivariable control of a industrial grinding circuit. In *Proc. 3rd IFAC Symp. on Automation in Mining Mineral and Metal Proc.*, pages 311–322, 1980.

Kawatra, S. and R. Seitz. An analysis of wet grinding circuit control using inferential particle size measurement. In *Preprint 82-18, SME-AIME Annual Meeting, Dallas, TX*, pages 1962–1964. SME/AIME, 1982.

Kawatra, S.K. and T.C. Eisele. Rheological effects in grinding circuits. *Intl. J. Min. Proc.*, 22:251–259, 1988.

Kawatra, S.K., T.C. Eisele, D.X. Zang, and M.T Rusesky. Temperature effect on

grinding circuit performance. *Min. and Met. Proc.*, pages 85–87, 1989.

Kawatra, S.K. and R.A. Seitz. Calculating the particle size distribution in a hydrocyclone overflow product for simulation purposes. *Min. and Metal Proc.*, 2:152–154, 1985.

Kelsall, D.F. A further study of the hydraulic cyclone. *Chem. Eng. Sci.*, 2:254–273, 1953.

Kelsall, D.F., P.S.B. Stewart, and K.J. Reid. Confirmation of a dynamic model of closed circuit grinding. *Trans. Inst. Min. and Metall.*, 77:C120–C127, 1968.

Klimpel, R.R. The influence of a chemical dispersant on the sizing performance of a 24-inch hydrocyclone. *Powder Tech.*, 31:255–262, 1982.

Laguitton, D. *SPOC Manuals, CANMET Report SP85-1*, 1984.

Laguitton, D, R.F. Pilgrim, and F.X. Seguin. Steady state simulation of comminution circuits. In *Proc. Summer Computer Simulation Conf.*, pages 811–816, 1983.

Lanthier, R., D. Hoduin, and A. Pomerleau. Internal model control of grinding circuits : an evaluation by simulation. In *Proc. 6th IFAC Symp. on Automation in Mining, Mineral and Metal Proc.*, pages 93–102, 1989.

Larsen, C.R. and R. Tessier. Golden Giant Mine mill process description and operating highlights. In *Proc. 18th Annual Meeting of the Candian Mineral Processors*, pages 108–123, 1986.

Lee, J.E. Slurry pumping at the Inco Metals Company (Ontario Div. *Can. Min.*, 99(3):14–16, 1978.

Lynch, A.J. *Mineral Crushing and Grinding Circuits - Their Simulation, Optimization, Design and Control.* Elsevier Scientific Publishing Company, 1977.

Niemi, A.J. Dynamic models of ore dressing processes, their steady state counterparts and use for control. In *Proc. 4th IFAC Symp. on Automation in Mining, Mineral and Metal Proc.*, pages 15–24, 1983.

Plitt, L.R. An analysis of solid-solid separation in classifiers. *CIM Bulletin*, 64(708):42–47, 1971.

Plitt, L.R. A mathematical model of the hydrocyclone classifier. *CIM Bulletin*, 69(776):114–123, 1976.

Plitt, L.R., P. Conil, and A. Broussand. An improved method of calculating the water split in hydrocyclones. *Min. Eng.*, 3:533–535, 1990.

Plitt, L.R., B.C. Flintoff, and T.J. Stuffco. Roping in hydrocyclones. In *3rd Intl. Conf. on Hydrocyclones, BHRA Fluid Engineering*, pages 21–34, 1987.

Rajamani, K. Self tuning control of a ball mill grinding circuit. *Instrumentation in Mining Metallurgy Industry*, 12:153–159, 1985.

Rajamani, K. and L.B. Hales. Developments in adaptive control and its potential in the minerals industry. *Min.and Met. Proc.*, pages 18–24, 1987.

Rajamani, K. and J.A. Herbst. Optimal control of a ball mill grinding circuit - Part i and ii. *Chem. Eng. Sci.*, 46(3):861–879, 1991.

Rhodes, N., K.A. Pericleous, and S.N. Drake. The prediction of hydrocyclone performance with a mathematical model. In *3rd Intl. Conf.on Hydrocyclones, BHRA Fluid Engineering*, pages 51–58, 1987.

Richardson, J.M. The application of general purpose process simulators in the mining industry. In *Proc. Summer Computer Simulation Conf.*, 1983.

Rietma, K. Performance and design of hydrocyclones - parts i to iv. *Chem. Eng. Sci.*, 15:298–325, 1961.

Lynch, A.J. and T.C. Rao. The operating characteristics of hydrocyclone classifiers. *Ind. J. Tech.*, 6:106–114, 1968.

Lynch, A.J. and T.C. Rao. Modelling and scale-up of hydrocyclone classifiers. In *Proc. 11th Intl. Min. Proc. Congr.*, pages 245–270, 1975.

McDougall, G.B. *Dynamic Simulation of the Control Behavior of Mineral Grinding Circuits.* M.Sc., University of Alberta, 1987.

McDougall, G.B., B.C. Flintoff, and R.K. Wood. Dynamic simulation for the analysis of grinding circuit control. In *Proc. Summer Computer Simulation Conf.*, pages 880–885, 1986.

Medronho, R.A. and L. Svarovsky. Tests to verify hydrocyclone scale-up procedure. In *2nd Intl. Conf. on Hydrocyclones, BHRA Fluid Engineering*, pages 1–14, 1984.

Napier-Munn, T.J. Influence of medium-viscosity on density separation of minerals in cyclones. In *2nd Intl. Conf. on Hydrocyclones, BHRA Fluid Engineering*, pages 63–82, 1980.

Napier-Munn, T.J. and Lynch A.J. The modelling and computer simulation of mineral treatment processes - current status and future trends. *Min. Eng.*, 5(2):143–167, 1992.

Neale, A.J. *Simulation and Control of a Rod Mill-Ball Mill Grinding Cicuit.* M.Sc., University of Alberta, 1987.

Niemi, A., P. Heinonen, S.L. Jamsa, H. Melama, T. Iivarinen, and U. Paakkien. Experiences in multivariable control of sulphide ore grinding in the Vuonos concentrator. In *Proc. XIV Intl. Min. Proc. Congr.*, volume 3, pages 5.1–5.12, 1982.

Romberg, T.M. and W.S.V. Jacobs. Identification of a mineral processing plant from normal operating data. In *Proc. 3rd IFAC Symp. on Automation in Mining, Mineral and Metal Processing*, pages 275–282, 1980.

Rosenbrock, H.H. *Computer Aided Control System Design.* Academic Press, London, 1975.

Sastry, K.V.S. and G.T. Adel. A survey of computer simulation software for mineral processing systems. In J.A. Herbst, editor, *Control '84, Mineral/Metallurgy Processing*, pages 121–130. SME/AIME, 1984.

Smith, H.W. and D. Guerin. Dynamic modelling, simulation and control of a grinding circuit. *CIM Bulletin*, 73(821):133–138, 1980.

Stephanopoulos, G. *Chemical Process Control.* Prentice-Hall Inc., 1984.

Stewart, P.S.B. The control of wet grinding circuits. *Aust. Chem. Proc. Eng.*, pages 22–33, 1970.

Stewart, P.S.B. and K.R. Weller. Hold-up and residence time characteristics of full scale grinding circuits. In *3rd Iranian Congr. Chem. Eng.*, 1977.

Svarovsky, L. *Hydrocyclones.* Holt, Rinehart and Winston, 1984.

Svarovsky, L. and B.S. Marasinghe. Performance of hydocyclones at high feed solids concentrations. In *Intl. Conf.on Hydrocyclones, BHRA Fluid Engineering*, pages 127–142, 1980.

Ulsoy, A.G. and K.V.S. Sastry. Principal developments in the automatic control of mineral processing systems. *CIM Bulletin*, 74(836):43–53, 1981.

Vien, A., C.R. Fragomeni, D.and Larsen, and D.G. Fisher. MOCCA. A grinding circuit control application. In *Preprint SME/AIME Annual Meeting*, pages 1–10, 1991.

Wong, W.Y. *Control of a Grinding Circuit.* M.Eng., University of Alberta, 1984.

Wood, R.K. Modelling and control of crushing and grinding circuits. In *Procc. 30th Annual ISA Conf.*, pages 647(1)–647(15), 1975.

Wood, R.K. and B.C. Flintoff. Dynamic process simulation :CSSL vs. Process simulation language. In *Proc. Summer Computer Simulation Conf.*, pages 492–497, 1982.

Appendix A

DATA STRUCTURE

There are currently four common blocks being used in the simulator. These blocks have the following form in the source code :

```
COMMON/CHAR1/TITLE,TITLE1,TITLE2
COMMON/CINT/T,DT,JS,JN,DXA(500),XA(500),IO,JS4
COMMON/CNTRL/ICNTRL,ZR1,RNG1,AXN1,SP1,PB1,PRT1,OI1,
                    DI1,ZR2,RNG2,AXN2,SP2,PB2,RPT2,OI2,
                    DI2,ZR3,RNG3,AXN3,SP3,PB3,RPT3,OI3,
                    DI3,SGAIN(4)
COMMON/DATA1/NCIRC,NCOMP,NSTRM,NSIZE,NOMILL,NCYCL,NSUMP,
                    SUMP(2,65),RMILL(6,40,3),PLUG(20,45,10),
                    DATA(4,20),STREAM(30,45),EQUIP(4,30)
```

While the first three common blocks are concise and self-explanatory, the fourth block, which carries information specific to the particular circuit being simulated is comprehensive and big, requiring further elaboration. The common block CINT includes information relevant to the DYFLO subroutines such as the value of the independent variable T, the incremental step size DT, order of integration *etc.*The CHAR1 common block holds the character string TITLE which is a variable used to carry the simulation title while the CNTRL common block holds the required control

parameters for closed loop simulation. The most important common block is the DATA1 block which supplies information to all the process model subroutines. The first seven variables are integer variables that are used in the simulator at various points to control the program flow. Briefly they are as follows :

NCIRC is a flag to define circuit configuration as being either reverse closed, standard closed or open circuit. The present circuit being simulated does not have other configurations and hence NCIRC = 1.

NCOMP indicates the number of solid components in the fresh ore feed. At present the simulator is designed to handle a maximum of 2. It should be noted that expanding it to handle three or more components, although not very difficult, is non-trivial and time consuming.

NSTRM gives the number of streams being monitored through the simulation. This is of great help in debugging in the initial stages and provides a good starting point to make and observe changes. The present simulator has NSTRM = 30.

NSIZE is used to indicate the number of size classes being monitored by the simulator. In its present form the simulator, NSIZE can handle upto 20 size class data.

NOMILL indicates the number of mills in the circuit. Although the circuit simulated in this work has only 3 mills, future developments might necessitate the use of alternate configuration in which case the value of NOMILL may be significant.

NCYCL is used to indicate the number of hydrocyclone sets present in the circuit. This parameter is very useful in setting up the data file. The NCYCL has a value equal to 2 in the current simulator.

NSUMP gives the number of sumps in the circuit. There is an assumption that a pump is associated with each sump. Again this parameter is very useful when building the data file.

The remaining variables are 1, 2 or 3 dimensional arrays employed to hold information pertaining either to a particular process model or to the streams in the circuit.

SUMP(I,J) carries vital information regarding the sump/pump models used in the simulator. The array is designed thus:

I = Sump number

J = attribute index

$1 \leq J \leq 39 \rightarrow$ Size distribution of solids in the sump

$J = 40 \rightarrow$ Sump outflow model

$41 \leq J \leq 46 \rightarrow$ Stream macro properties

as

$J = 41 \rightarrow$ Solids holdup in sump

$J = 42 \rightarrow$ Water holdup in sump

$J = 43 \rightarrow$ Volumetric holdup of slurry in sump

$J = 44 \rightarrow$ Mass percent of slurry in sump

$J = 45 \rightarrow$ Height of slurry in sump

$J = 46 \rightarrow$ Cyclone feed density

$51 \leq J \leq 53 \rightarrow$ Fixed speed pump coefficients

$J = 54 \rightarrow$ Friction factor of pipe to hydrocyclones

$J = 55 \rightarrow$ Sump cross section area

$J = 56 \rightarrow$ Sump height

$J = 57 \rightarrow$ Flag to indicate sump overflow

$58 \leq J \leq 60 \rightarrow$ Variable speed pump coefficients

J = 61 → Steady state sump level

J = 62 → Steady state flow rate to sump

J = 65 → Proportional gain controller constant

RMILL(I,J,K) is a large array which retains all the information needed by the mill model. It is set up thus :

K → Grinding mill number

$1 \leq J \leq 20$ → Breakage elements

I = 1 → Component # 1

I = 2 → Component # 2

$3 \leq I \leq 5$ → Volume holdup in the three mixers

I = 6 → Particulars of mill volume, number of mixers etc.

PLUG (I,J,K) contains stream information as it is held up in the CONSDEL and VARIDEL subroutines. The arrangement is as:

$1 \leq K \leq 10$ → Number of calls to the delay routines

$1 \leq J \leq 40$ → Stream size distribution of the two components

$41 \leq J \leq 45$ → Macro properties of stream

$1 \leq I \leq 20$ → Maximum number of cells available in any buffer

DATA(I,J) is another array with information required throughout the circuit. The set-up is as follows:

$I = 1, 1 \leq J \leq 14$ → Characteristic size classes

I = 1, J = 19 → Percentage of solids in feed stream to a mill # 1

$I = 2\&3, 1 \leq J \leq 6$ → Hydrocyclone number and corresponding dimensions

I = 3, J = 20 → Density of water

$I = 4, J = 1, 2$ → Densities of the solid feed components

I = 4, J = 10 → Disturbance flag = 0 for no disturbance; = 1 for disturbance

$I = 4, 11 \leq J \leq 20$ → Flags to direct flow in DISTRB subroutine

STREAM(I,J) holds the micro and macro properties of each stream within the circuit. The array is designed as follows :

I→ Stream number

$1 \leq J \leq 40 \rightarrow$ Size distribution of the two feed stream solids components

$41 \leq J \leq 45 \rightarrow$ Stream macro properties

$J = 41 \rightarrow$ Stream solids mass flow rate

$J = 42 \rightarrow$ Stream water mass flow rate

$J = 43 \rightarrow$ Stream slurry volumetric flow rate

$J = 44 \rightarrow$ Stream solids mass percent

$J = 45 \rightarrow$ Stream solids volume percent

EQUIP(I,J) has all the data required to define the hydrocyclone model parameters defined in equations(.). It is arranged as:

$I = 2\&3$ $1 \leq J \leq 30 \rightarrow$ Plitt hydrocyclone model constants

Appendix B

DYFLO Utilities

A short description of the DYFLO subroutines included in this simulator is given below. These subroutines are as given by Franks (1982) with suitable modifications.

Subroutine PRNTF

Purpose→ Print values of specified circuit variables at a specified frequency and to test for end of simulation run.

Use → PRNTF(PRI, FNR, NF)

Parameters :

PRI	= print interval
FNR	= termination time
NF	= finish index (NF = 1, not finished)

Subroutine INTG

Purpose → Dependent variable general subroutine. This subroutine is capable of performing first order Euler integration, and second and fourth order Runge-Kutta integration.

Use → INTG(X, DX)

Parameters :

X	= dependent variable

DX = independent variable

Subroutine INTI

Purpose → Integration control subroutine. This routine integrates the independent variable.

Use → INTI(TD, DTD, IOD)

Parameters :

TD = independent variable name

DTD = integration step size

IOD = integration method

- IOD = 1 ⇒ first order Euler
- IOD = 2 ⇒ second order Runge-Kutta
- IOD = 4 ⇒ fourth order Runge-Kutta

Subroutine CONTR1

Purpose → Proprotional (P) only controller subroutine.

Use → CONTR1(VI, CO, ZR, FSRDG, SP, AXN, PB, OI)

Parametes :

VI = output signal

CO = controller output

ZR = zero reading

FSRDG = full scale reading

SP = setpoint

AXN = controller action (+1 ⇒ direct, -1 ⇒ reverse)

PB = proportional band

OI = bias

Note The bias OI must be initialized before calling this routine. It is calculated as :

OI = steady state value of output in % of full scale reading.

Subroutine CONTR2

Purpose → Proprotional plus integral (PI) controller subroutine.

Use → CONTR2(VI, CO, ZR, FSRDG, SP, AXN, PB, RPT, OI)

Parametes :

VI = output signal

CO = controller output

ZR = zero reading

FSRDG = full scale reading

SP = setpoint

AXN = controller action (+1 ⇒ direct, -1 ⇒ reverse)

PB = proportional band

RPT = reset rate, repeats per unit time

OI = bias

Note The integral action (OI) must be initialized before the first call is made to this routine. The integral action is defined as :

OI = steady state value of controller output.

Subroutine CONTR3

Purpose → Proprotional plus integral plus derivative (PID) controller subroutine.

Use →

CONTR1(VI,CO,ZR,FSRDG,SP,AXN,PB,RPT,RT,RA,OI,DI,ODI,DODI)

Parametes :

VI = output signal

CO	= controller output
ZR	= zero reading
FSRDG	= full scale reading
SP	= setpoint
AXN	= controller action (+1 ⇒ direct, -1 ⇒ reverse)
PB	= proportional band
RPT	= reset time, repeats per unit time
RT	= rate time
RA	= rate amplitude
OI	= bias
DI	= derivative of integral action
ODI	= output of deivative action
DODI	= derivative of derivative action

Note Both the integral action (OI) and the derivative action (ODI) must be initialized before the first call to this routine. These two variables are calculated as follows:

OI = steady state output value in % of full scale reading

ODI = 1.0 / RA - 1.0

Subroutine FUN1

Purpose → Linear function subroutine Y vs X.

Use → FUN1(A, N, X, Y)

Parameters:

A	= input variable
N	= total number of coordinate points
X	= independent variable array
Y	= dependent variable array

Subroutine FUN2

Purpose → Two dimension function generator

Use → FUN2(A, B, N, M, X, Y, Z)

Parameters:

A	= X value
B	= Z value
N	= total number of coordinate points
M	= total number of coordinate points in groups
X	= independent variable array
Y	= dependent variable array
Z	= array of Z values

Subroutine CONV

Purpose → Wegstein convergence

Use → CONV(X, Y, NR, NCON)

Parameters:

X	= trial value
Y	= calculated value
NR	= routine call index
NCON	= convergence index

Appendix C

The Factorial Design of Experiments

C.1 Introduction

This is a statistical method under the area of analysis of variance. This choice of treatment design leads to a logical partitioning of treatment sum of squares into additive components with corresponding tests of hypotheses. A factor is a kind of treatment, and in factorial experiments any factor will supply several treatments. For example, if diet is a factor in an experiment then several diets will be used. The term level refers to the several treatments within a factor. Hence each diet composition is a level. Factorial experiment is one in which the set of treatments consists of all possible combinations of the levels of several factors. However, often factorial experiments are performed with each factor taken at only two levels. The resulting design is called a 2^k factorial design and it is common to refer to the two levels of each factor as the low and high levels and to denote them by 0 and 1 respectively. It must be mentioned that for the 2^k factorial experiments case there exist some computational shortcut. Unfortunately, adopting these shortcuts precludes any insight into whether the effects produced by variations in a factor are linear or non-linear. A 2^k factorial experiment requires 2^k experimental conditions. As their numbers tend to be large, it is convenient to represent the experimental conditions by means of a special notation

and list them in a standard order. The notation for treatment combination generalizes directly with each treatment combination being denoted by the lower case letters corresponding to the high-level factors of the combination. For instance, a 2^6 design has the six factors A,B,C,D,E,F and abdf denotes the combination with A,B,D and F at high levels and C and E at low levels. To find the standard order for treatment combinations, begin with (1) i.e. a case where all the factors are at the low level, introduce the factors in alphabetical order, and as each is listed for the first time, combine it (in order) with all combinations listed previously. For instance, the standard order for the 2^4 design is (1),a,b,ab,c,ac,bc,abc,d,ad,bd,abd, cd,acd,bcd,abcd. Again for a 2^2 case if A and B are the only factors then each factor will have a main effect and an interaction effect given by A, B and AB. In this case the treatment combinations as per the standard order will be (1),a,b,ab. Any non trivial linear combination of treatment totals is called an effect contrast. Hence the A, B and AB contrasts will be defined by

$$[A] = ab + a - b - (1)$$

$$[B] = ab + b - a - (1)$$

$$[AB] = ab - a - b + (1)$$

and the sums of squares are given by

$$SSK = \frac{[K]^2}{4n}$$

where K = A , B or AB and n = number of replicates.

While each average effect is given by dividing the corresponding contrast by 2n, each average interaction effect is equal to the interaction contrast divided by 2n.

While this is easy for a 2^2 case, it becomes non trivial as k goes on increasing. To find the average effects and the sum of squares in the 2^k design, it is necessary to find effect contrasts.

To find any effect contrast, expand the expression

$$(a \pm 1)(b \pm 1) \cdots (l \pm 1)$$

algebraically, using a minus sign in a parenthesis if the appropriate factor is included in the effect and a plus sign otherwise (the assumption being that the k factors are A,B,...,L). When the computation is completed replace 1 by (1).

Having found the effect contrasts, the average effects are found by the relation

$$K = \frac{[K]}{2^{k-1}n}$$

for K = A,B,AB,C,...,AB $\cdots$ L and the corresponding sum of squares are given by

$$SSK = \frac{[K]^2}{2^k n}$$

For instance, in a 2^7 design the interaction average corresponding to A,B,C,D,E and F is

$$ABDEF = \frac{[ABDEF]}{2^6 n}$$

and the corresponding sum of squares is

$$SSABDEF = \frac{[ABDEF]^2}{2^7 n}$$

C.2 A Single Observation Per treatment Combination in the 2^k design

Although there are only two levels for each factors in a 2^k factorial design for large k, there are quite a number of treatment combinations, the exact number being 2^k. Therefore, it is sometimes desirable to employ a 2^k design without replication. Now, in the case of a 2^k factorial experiment there are many higher-order interactions. Should one of these be null, then its mean square can be taken as an estimate of σ^2. More generally, if a number of higher order interactions are presumed to be null, then σ^2 is estimated by the average of their mean squares,

and it is this average that is taken as MSE when computing the F statistics for the remaining effects. As an illustration of the method, consider a 2^5 design and suppose all interactions containing four or more factors to possess zero effects. Then it is possible to test the main effects for A,B,C,D and E and the interaction effects for AB,AC,AD,AE,BC,BD,BE,CD,CE,DE,ABC,ABD,ABE,ACD,ACE, ADE,BCD,BCE,BDE and CDE. The error sum of squares is taken as the sum of the sums of squares of the fourth- and fifth-order interaction sums of squares namely,

$$SSE = SSABCD + SSABCE + SSABDE + SSACDE + SSBCDE + SSABCDE$$

Each sum of squares possess a single degree of freedom so that SSE is equivalently equal to the sum of the mean squares. MSE is taken as the average of the fourth and fifth order interaction sums of squares i.e. MSE = SSE / 6. The number of higher-order interactions that are taken to be null (in this case six) is the number of degrees of freedom associated with SSE. As always, there is a risk in making an a priori assumption that certain interactions possess zero effects. Indeed, if MSE is an average of interaction mean squares and should one or more of the interactions be significant, then MSE will overestimate σ^2. Since the F statistics associate with the lower-order effects each possess MSE in the denominator, these statistics will be reduced, and significant lower order effects might not be detected.

C.3 A Factorial Design for the Hemlo Grinding Circuit

A 2^4 factorial experiment was performed on the output variables of the Hemlo grinding circuit to determine the significance of each of the input variables. Table C.1 lists the factors considered to affect the output variables. Each of the input variable was altered as illustrated in Table C.2. The sign '-' means that the steady state value of the variable was considered. The left most column shows the factors considered for that run with the lower case letters being the same as listed in Table C.1. The

steady state values of all the output variables were recorded for each 'experimental' run. The resulting matrix of output variables was the analyzed for its variance. A matrix consisting of both the input and output variables was used as the coefficient matrix to generate the regression equation for the estimator. The results show a high degree of correlation existing between the input and ouput variables.

Table C.1: Identification of Factors for the Hemlo Circuit

Input Variables	Factor	Magnitude of step	Output Variables
FOF	A	10%	COS
SWF1	B	5%	SPL1
SWF2	C	10%	SPL2
HRD	D	50%	CFD
			PR

Table C.2: Order followed in changing the input variables

Combination	FOF	SWF1	SWF2	HRD
S.S. Values	-	-	-	-
a	10%	-	-	-
b	-	5%	-	-
ab	10%	5%	-	-
c	-	-	10%	-
ac	10%	-	10%	-
bc	-	5%	10%	-
abc	10%	5%	10%	-
d	-	-	-	50%
ad	10%	-	-	50%
bd	-	5%	-	50%
abd	10%	5%	-	50%
cd	-	-	10%	50%
acd	10%	-	10%	50%
bcd	-	5%	10%	50%
abcd	10%	5%	10%	50%

Tables. C.3 to C.7 are tables summarizing the ANOVA in the output variables using the Yates' method for a single observation case. This implies an assumption that the 3rd level and 4th level interactions are zero *i.e.* [ABC], [ABD], [ACD], [BCD], and [ABCD] contribute to only the error. For $F_{(.05),1,5} = 6.61$ and $F_{(.01),1,5} = 16.26$, the results shown on the ANOVA tables can be summarized thus:

a) *Influence of the input variables on COS*

Only the combined effects of ore feed rate and water flow rate to the second sump *i.e.* [AC] and the combined effects of water feed to the two sumps *i.e.* [BC] found to be not significant.

b) *Influence of the input variables on SPL1*

All factors except the effect of SWF2 [C], combined effects of FOF and SWF2 *i.e.* [AC], combined effects of water feed to the two sumps *i.e.* [BC] and the combined effects of SWF2 and HRD *i.e.* [CD] are significant.

c) *Influence of the input variables on SPL2*

All factors except the combined effects of FOF and SWF1 significant at .05 level. At .01 significance level, only combined effects of FOF and SWF1 *i.e.* [AB], combined effects of SWF1 and SWF2 *i.e.* [BC], combined effects of FOH and HRD *i.e.* [AD], and the combined effects of SWF2 and HRD *i.e.* [CD] are not significant.

d) *Influence of the input variables on CFD*

The combined effects of FOF and SWF1 *i.e.* [AB], combined effects of FOF and HRD *i.e.* [AD], combined effects of FOF and SWF2 *i.e.* [AC], combined effects of SWF1 and SWF2 ([BC]) and the combined effects of SWF2 and HRD ([CD]) are not significant.

e) *Influence of the input variables on PR*

Except the combined effects of FOF and SWF2 *i.e.* [AC], combined effects of SWF1 and SWF2 ([BC]) and the combined effects of SWF2 and HRD *i.e.* [CD], all factors are significant.

Table C.3: ANOVA table for the Cyclone Overflow Stream (COS)

Source of Variation	Sum of Squares	Degrees of Freedom	Mean Square	F-Statistic (Calc.)	F-Statistic (Tab.)
A	7.694	1	7.694	126131	All
B	8.484	1	8.484	139081	factors
C	0.039	1	0.039	645	except
D	84.47	1	84.47	1384754	AC & BC
AB	1.23E-3	1	1.23E-3	20.1	are
AC	1.86E-5	1	1.86E-5	0.344	significant
AD	0.059	1	0.059	967.2	at
BC	2.23E-5	1	2.23E-5	0.366	both
BD	0.221	1	0.221	36223	significance
CD	1.87E-3	1	1.87E-3	30.62	levels
Error	3.05E-4	5	6.10E-5	-	

Table C.4: ANOVA table for the Sump #1 Level (SMPL1)

Source of Variation	Sum of Squares	Degrees of Freedom	Mean Square	F-Statistic (Calc.)	F-Statistic (Tab.)
A	0.334	1	0.334	250981	All
B	0.016	1	0.016	117787	factors
C	2.25E-8	1	2.25E-8	0.169	except C,
D	0.465	1	0.465	3506534	AC, BC
AB	3.00E-6	1	3.00E-6	22.6	and CD are
AC	1.00E-10	1	1.00E-10	7.53E-4	significant
AD	1.15E-5	1	1.15E-5	86.63	at
BC	3.00E-7	1	3.00E-7	2.260	both
BD	2.84E-5	1	2.84E-5	213.94	significance
CD	3.00E-7	1	3.00E-7	2.26	levels
Error	6.64E-7	5	1.33E-7	-	

Table C.5: ANOVA table for the Sump #2 Level (SMPL2)

Source of Variation	Sum of Squares	Degrees of Freedom	Mean Square	F-Statistic (Calc.)	F-Statistic (Tab.)
A	0.363	1	0.363	100221	All
B	1.14E-3	1	1.14E-3	3144.8	factors
C	1.41E-5	1	1.41E-5	38.79	except AB
D	0.965	1	0.965	2662068	at .05 level
AB	1.56E-6	1	1.56E-6	4.31	and AB, AC, BC
AC	6.25E-6	1	6.25E-6	17.24	& CD significant
AD	5.63E-7	1	5.63E-7	15.53	at
BC	5.63E-7	1	5.63E-7	15.53	both
BD	8.56E-5	1	8.56E-5	236.14	significance
CD	5.63E-7	1	5.63E-7	15.53	levels
Error	1.81E-6	5	3.63E-7	-	

Table C.6: ANOVA table for the Cyclone Feed Density (CFD)

Source of Variation	Sum of Squares	Degrees of Freedom	Mean Square	F-Statistic (Calc.)	F-Statistic (Tab.)
A	1.16E-3	1	1.16E-3	7706.7	All
B	1.06E-3	1	1.06E-3	7040.0	factors
C	9.00E-6	1	9.00E-6	60.00	except AB,
D	8.41E-4	1	8.41E-4	5606.7	AC, AD,
AB	0.0	1	0.0	0.0	BC & CD
AC	2.50E-7	1	2.50E-7	1.67	significant
AD	2.50E-7	1	2.50E-7	1.67	at
BC	0.0	1	0.0	0.0	both
BD	4.00E-6	1	4.00E-6	23.67	significance
CD	2.50E-7	1	2.50E-7	1.67	levels
Error	7.50E-7	5	1.50E-7	-	

Table C.7: ANOVA table for the Pressure at Cyclone Inlet (PR)

Source of Variation	Sum of Squares	Degrees of Freedom	Mean Square	F-Statistic (Calc.)	F-Statistic (Tab.)
A	55.69	1	55.69	2121523	All
B	4.48	1	4.48	170666	factors
C	4.73E-3	1	4.73E-3	1801.9	except
D	104.8	1	104.8	3992761	AC, BC
AB	5.06E-4	1	5.06E-4	19.3	& CD
AC	5.62E-5	1	5.62E-5	2.14	significant
AD	2.76E-3	1	2.76E-3	105.14	at
BC	5.63E-5	1	5.63E-5	2.14	both
BD	4.56E-3	1	4.56E-3	173.71	significance
CD	5.63E-5	1	5.63E-5	2.14	levels
Error	1.30E-4	5	2.630E-5	-	

END

09/02/93

FIN